ABSTRACT

FOSTER, JR., HOWARD ALLEN. Opto-electronic Technique For Error Fault Detection In Textile Joining Applications. (Under the direction of Hans Hallen.)

The purpose of this research has been to develop an opto-electronic method for detecting error faults in textile joining applications. The application of this study would be in on-line determination of skipped stitches in seam sewing operations. The research begins with a selection of materials that covers a range of textile materials commonly used, and then determining several physical parameters based upon industry standards. The next portion of the research is to determine the proper wavelength of light to use for the opto-electronics, using near infrared and visible spectrophotometric techniques for acceptable light reflection levels for qualitative analysis. This study then focuses on using NIR wavelength light at 1550nm, using an InGaAsP laser diode module with optics and corresponding Germanium photodiode detector with a wavelength-matched interference filter, to monitor a stitch line passed by the test apparatus to determine the presence of skipped stitches, or stitches where the top thread and looper thread do not properly catch and hold in the sewing of a seam. Due to the spot size of the manufactured laser diode module, a ½" basting stitch, commonly used to temporarily attach fabric pieces, is selected as the best stitch type to use to verify the hypothesis. After determining the ideal positions of the laser diode and photodiode assemblies using geometric optics arguments and extensive position-related intensity measurements, the assembly is mounted onto a linear slide table, and fabric samples, sewn with the ½" basting stitch to simulate a seam, are aligned and tested for variations in light levels based on the presence of a stitch or a space. It is then shown that this method for detecting skipped stitches is a viable alternative to the current visual inspection performed by factory employees.

OPTO-ELECTRONIC TECHNIQUE FOR ERROR FAULT DETECTION IN TEXTILE JOINING APPLICATIONS

by
Howard Allen Foster, Jr.

A thesis submitted to the Graduate Faculty of
North Carolina State University
in partial fulfillment of the
requirements for the Degree of
Master of Science

Physics

Raleigh

2002

APPROVED BY:

Hans Hallen
Chair of Advisory Committee

Michael Paesler

Christopher R. Gould

Dedication

I'd like to dedicate this research to all my family and friends whose unwavering love and support have uplifted, enlightened and amazed me for a number of years. There are too many of you to name, but each of you know that I write of you.

I'd also like to specifically dedicate this research to several people:

- To Kevin and Mike, the better two-thirds of the Three Physics Stooges triumvirate (No, we're not in a band.);
- To Gwen, the love for which I've looked a long time (Go Team Mosquito!);
- To Elizabeth, the friend of a lifetime (well, 1/3 of it so far);
- To Jenny, the best graduate office administrator ever cited in a body of work;
- To my professors who have been so very patient with this work; and, of course,
- To my mother and father whose love of learning inspired my sister and myself to excel not only in our educational careers, but also in every aspect of our lives. Thanks Mom and Dad!

Biography

Howard Allen Foster, Jr. was born on May 14, 1971 in Raleigh, the mighty capital of North Carolina. However, he spent the better part of his life growing up in the foothills of western NC, in small Forest City.

After graduating with honors from East Rutherford High School and Isothermal Community College, he returned to Raleigh to educate himself at the finest school in the South: North Carolina State University. His chosen path: applied physics.

Much of his life was spent working with his hands (and his back) with his father, who gave him a love of the contact of work and an insatiable curiosity of what makes things work. Not satisfied to merely function as a part of a process, Howard has striven to learn all the ins and outs of every occupation he has held. To that end, Howard has maintained not only the educational sense that comes from his text books, but also the common sense bestowed upon him by members of his family who saw fit to make him into the well rounded man that he is today.

Howard enjoys reading nearly all printed material, which makes him the somewhat irritating “master of all things trivial” that his friends claim him to be. He also has a fantastic sense of humor, enjoys long walks on the beach, listening to the night rain on a tent fly or on a tin roof, and modestly talking about himself in third person.

Acknowledgements

There are a number of sources worthy of acknowledgement for the work contained herein. First, the original sponsors of this work were the National Textile Center, a federally funded consortium of six major US universities which strive to keep the US textile industry at the forefront through support of research in developing technologies.

Next, to Dr. Timothy Clapp and Dr. Kimberly Titus, of the NCSU College of Textiles, the originators of this research and selectors of Howard Foster as the student worthy of the research. Their support and aide throughout the process was founded on the desire to not only further the US textile industry, but also to assist in the education and advancement of all the students under their tutelage.

Finally, to Dr. Hans Hallen, of the Physics Department at NCSU, the committee chair for this graduate work, without whose guidance, patience, and supreme abilities as an educator, this body of work would not have been completed.

Table Of Contents

List Of Tables

List Of Figures

1. Introduction

Inspection of sewn seams has long been a method of quality control in the textile industry. The inspection is carried out in one or more of the following ways: an employee is required to visually inspect the seam of a garment as it is being sewn, extra employees are hired whose job is to visually inspect each garment as it comes from the sewing section of a factory, or there is an automated tactile process which measures a variable in the sewing process such as sewing thread tension. The time and man power requirements of the first two methods are costly, and this cost is eventually passed on to the consumer. The third is a rapidly developing technology, but also must contend with the argument that any time the material, fabric or thread, comes in contact with another object, there is a higher potential of material failure due to the wear and tear caused by the added contact. The development of a non-tactile, non-destructive system for inspection during the sewing process, such as an opto-electronic, or vision, system, could provide immediate feedback of sticth defects to the sewing machine operator, free employees for more production lines, and reduce the cost of products for the consumer.

This research focuses on the development of such an opto-electronic system for the inspection of sewn seams. The following sections define the problem, review research of the use of opto-electronic inspection systems in the textile industry to increase quality in production, and which could possibly be adapted to skipped stitch detection, and, review research on opto-electronic skipped stitch detectors already in use in the textile industry.

1.1 Defining The "Skipped Stitch"

This research is based upon a new idea to determine a joining error caused by a skipped stitch. A stitch is made of two entirely separate threads, a top thread and a bobbin thread. The top thread is visible from the top or outside of the seam, while the interlocking bobbin thread is visible from the bottom side of the seam. A stitch is fromed when the top needle and the looper needle, the top thread and the bobbin threads' respective needle names, pass one another on the underside of the seam during the sewing process. Timing is crucial for this operation such that the threads cross one another and pull tight via only the friction between them to form a strong bonding stitch. End knots are used to keep the threads from pulling apart from one another and ruining a seam.

Several factors may cause a skipped, or dropped, stitch. Broken threads are the culprits most of the time. Machine timing being slightly off, or mis-calibration of the sewing machine for the type of seam, mainly number of layers, are other major causes. Minor reasons may include broken needles, oil or dirt on the needles or threads, and fabric misfeeds. While many of these problems would cause an obvious seam problem, mainly the complete stoppage of the sewing process, as machinery and understanding of the working and formation of stitches advance, the number of "catastrophic" failures decreases. What is left are the minor faults or skipped stitches where the sewing process continues. The seam is finished because the threads realign and begin forming a proper stitch again. An example of this is seen below in Figure1-1.

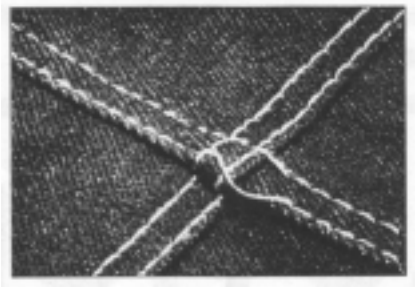

Figure 1-1 Image Of A Skipped Stitch [36]

This research is focused upon those failures which are not immediately obvious in the sewing process, but may be picked up later in the inspection process, or, worse, further downline after washing when the material cannot be salvaged for reuse. As an example of the type of failure this study is based upon, see Figure 1-2, below.

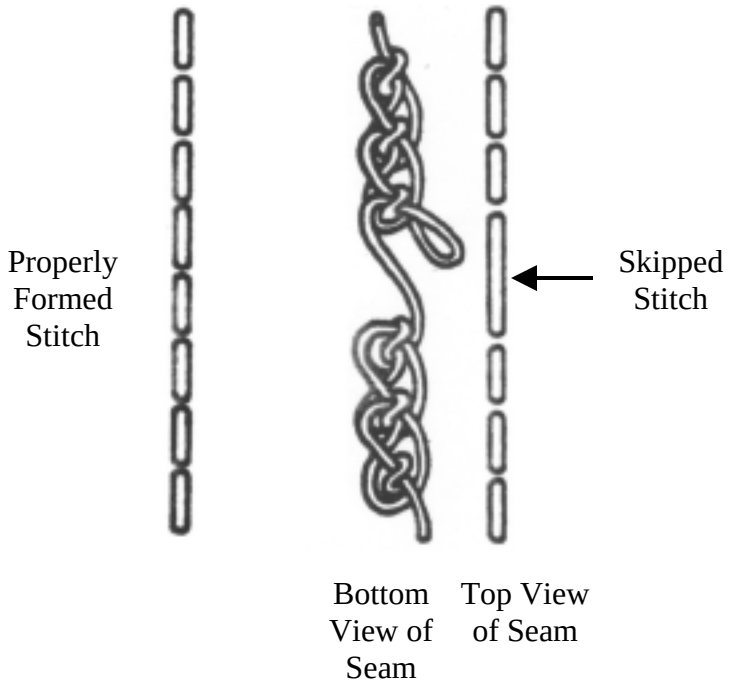

Figure 1-2 Examples Of Properly Formed Stitches (Left) And A Skipped Stitch (Right) [2]

In Figure 1-2, the stitchline on the left shows a properly formed stitch as viewed from the top of the seam. Note the regular pattern of stitches. The stitchline to the right shows the top and bottom of a skipped stitch. On the bottom of the seam, the looper thread has not been properly caught by the top thread and as the top needle ascended it pulled the top thread back out. When the top thread is not caught on the underside of the seam, the regular pattern seen in the stitchline on the left of the figure is broken by what the industry calls a "skipped stitch," as pointed out in the righthand stitchline.

Given the view of the properly formed stitch, we hypothesize that a repeated pattern could be discerned from the regular formation of seams by monitoring the amount of light reflected back from the stitch line using a non-tactile, optical detection system. When this pattern is broken, by a skipped stitch, the system could alert the worker to halt the sewing process and remove the faulty seam. By placing the system on the sewing machine in such a position that it has a clear view of the seam just after it has been sewn, defects can be found immiediately. The sewing threads could then be removed and the fabric pieces resewed with minimal waste of time, effort and more importantly, material. Such an optical test system is the point of this research.

1.2 Opto-electronic Sensing Devices In The Textile Industry

Opto-electronic sensing devices are widely used by many industries, including the textile industry. Usage of these devices in the textile industry include detection of faults such as holes [17, 20], slubs [11], uneven dyeing [31], stains [21, 27], broken threads [8, 28, 30], mising threads [15], and misoriented threads [20]; count of warp and weft yarns [23, 41]; post-dyeing and –washing shrinkage [32]; parameter measurements such as

length and width [33], thickness [25, 29, 33], roughness [14], yarn orientation [19, 22], warp/weft density [18], crimp [34] and surface characterization [1, 7]; pattern characterization and recognition [22]; and uses in final garment production [2, 4, 5, 16, 36]. As the reader will note, the majority of these reports deal with the opto-electronic detection of defects for woven fabrics, or webs, for defects in the manufacture of the material. The research of interest to this study deals with the testing of finished products which would be passed on to the consumer. Two areas of interest studied here are in garment production. Specifially, the study of seams of garments to detect two types of possible faults: number of layers in the seam and skipped or missed stitches.

1.2.1 Determining The Number Of Layers In A Seam Using Opto-electronics Combined With Tactile Devices

The number of layers in a seam depends on the type of seam the sewer wishes to produce. Occasionally, the edge of a layer in a seam does not get fed correctly and the stitch holding the edge is near enough to that edge that under some stress, such as washing, the seam may fall apart. There are products available that detect and correct the position of the edge before being sewn. Two examples of this type of device are made by AMF Reece [36]. The devices are actually folders, much like the ones used in most seaming machines, however, these have fiber optic sensors that determine the position of the edges in the folder and then, using splined wheels, control the position of the edges within the folder so that the final seam has edges which are correctly placed. However, these are tactile devices that in touching the fabric may do some damage to the fabric, especially the splined wheels. Thus, methods are needed to detect the position of the

edge of the layer either on the way to being sewn or after being sewn without physical contact with the fabric.

1.2.2 Determining The Number Of Layers In A Seam Using Opto-electronic Devices

Due to positioning of the sewing machine and the operator, it would be easier to position a sensor on the fabric after the stitching has taken place. Here a sensor may find a fault and alert the operator so the piece may be repaired or removed from the production line saving the manufacturer time and money. This is where opto-electronic sensors would be useful, due to their relatively small size and cost. Using some form of light to pass through the fabric, detection of the number of layers in the seam may be possible. Various research has been published on the principal of light transmission and its application to fabrics. Mostly, the research is done to determine the density of a single-layer, or a still or running web [3, 18]. These authors' research focused mainly on the determination of the density of a single layer to aid in quality control measurements, and material classification for producer to consumer sales, rather than number of layers for final production items.

A more promising direction is the use of laser triangularization to determine the thickness of the fabric [25, 29]. This method uses reflected light from the surface of the fabric. Light is initially shone onto a reflective surface and received by a photosensitive detector. When a piece of fabric is put over the reflective surface the position of the reflected light on the detector is changed due to the difference in height. In this manner the thickness of the fabric can be gauged. The authors posit that this may be extendible

to determine the number of layers in a seam, but again their research focuses on the quality control measurement issues, rather than in-line detection systems.

Another possible method is the use of reflected light and charge-coupled device (CCD) cameras or fiber optic arrays to detect position or intensity of singular, or arrays of, reflected pinpoint light beams [9]. By studying the pattern of the reflected light Liu, et. al. were able to tell the thickness of a material by the curvature and change in reflected patterns. Similar work was done by Toba and Sawaji [20] to use the speckle patterns produced by diffracted light off of the surface of a web to determine if there were irregularities in the material. There are several interesting studies outside of the textile industry also done on the pattern of reflected light off of surfaces to determine surface features [6, 10, 26]. Possibly two or more of these methods may be combined to give a reliable and repeatable reading of the number of layers in a seam.

Redefining the application of these methods could be used to aid in the detection of skipped stitches, the focus of this study. Specifically, the seam could be analyzed to determine if the edges of the seams are placed correctly to hold under stress or if the number of layers are correct in the seam indicating that the seam could potentially pull apart under some stress. Unfortunately, these methods could not be easily applied in the on-line inspection of skipped stitches as they would merely indicate an area where a seam is weak and a skipped or weak stitch <u>could</u> cause a problem when the seam is stressed. Thus, a visual inspection would still be needed for skipped stitches or the seam would need to be stressed in some fashion to prove it would “hold together” compliant with some standard. To this end, more research has been done for the optical detection of skipped stitches.

1.2.3 Opto-electronic Detection Of Skipped Stitches

The second area of interest where the development of opto-electronic sensing devices may be useful is in detecting skipped stitches. There have been many studies of skipped or missed stitch detection in sewing of seams and decorative stitching. In fact, there are several patents issued for skipped stitch detectors [5, 16]. To date, these detectors have been mainly based on tactile sensing of top thread or bobbin thread tension going into the stitch [4, 12]. If the tension on the sensor drops below a certain value, the detector alerts the operator through visual or audible alarms. There are also many tension devices used in monitoring multiple threads in tufting and weaving [24, 28, 30] which may be adaptable to detecting skipped stitches. While these detectors function reasonably well, the problem still exits of having the detector coming in contact with the thread possibly causing damage which may cause the seam to fail or a visual defect in the decorative stitching reducing consumer appeal.

One promising system was developed and patented by Bellio [2] in 1993 for Draper Labs, Inc. His method involved passing the thread through an optical detector between the take-up lever and the needle. An enlarged view of the sensor is seen below in Figure 1-3.

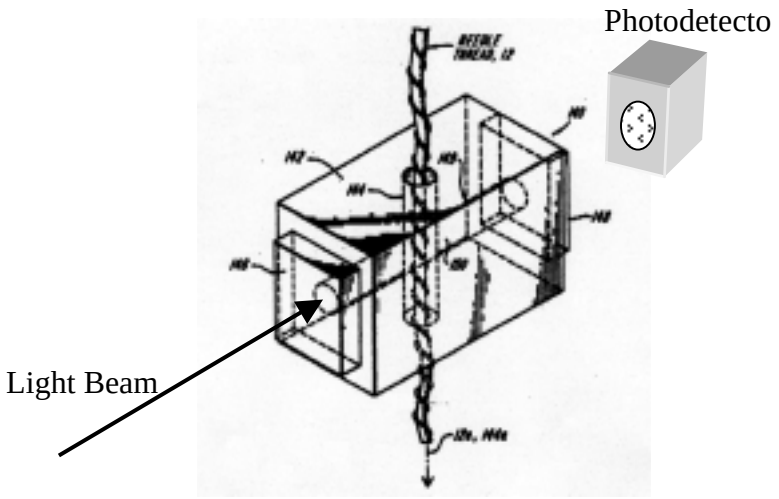

Figure 1-3 Draper Labs Needle Thread Motion Sensor [2]

An LED is used to project a beam of light down the channel perpindicular to the thread channel, which is then received by a photodetector. Variations in the absorption and transmission of the received beam are registered as thread movement through the thread channel. These movements are correlated with a timing system attached to the sewing machine's shaft, which controls the motion of the sewing needle, to show that a stitch was properly formed. If the shaft timing and the thread motion do not match up, either due to thread breakage or misformed stitches, an alarm can be rung to alert the sewer of the defect.

Another system, developed by Porat and Alagha [13], detected skipped stitches by placing an optical fiber and lens arrangement inside a 401 chainstitch sewing machine, a common stitch type used in garment production, to detect for the proper formation of the underside of the stitch, as seen in Figure 1-4, below. When a stitch is properly formed, a "triangle" is formed consisting of the needle thread loop, looper, and looper thread. When a beam of light is focused on a particular spot of the polished stainless steel looper,

the light is diffracted by the presence of the needle thread loop in a properly formed stitch. Thus, an absence of the “break” in the beams’ intensity implies that a stitch was not properly formed.

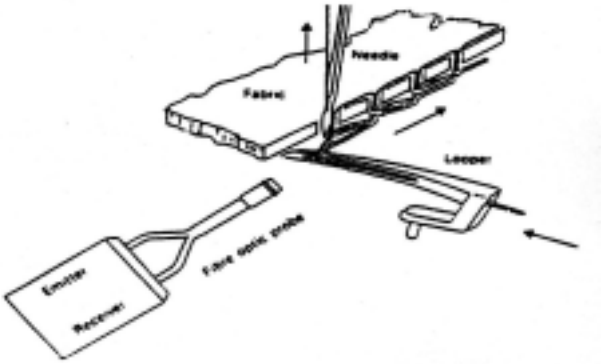

Figure 1-4 Porat And Alagha’s Optical Miss Stitch Detection System [13]

This system is not, however applicable to all types of stitches as not all form the required triangle below the surface of the fabric. Also, not all sewing machine interiors can accommodate even the smallest fiber optic probe, due to their surrounding structure (such as special tables), positioning of the worker, and small body size of the machine.

2. Introduction Of Test Materials

The material chosen for this study was an important factor, so many preliminary tests were done to determine the material, fabric as well as stitch thread, to use. This led to the selection of the equipment used, the arrangement of the equipment, and the method of testing for skipped stitches. These initial tests include a general survey of the textile industry for commonly used materials, determination of several American Society of Testing and Methodology (ASTM) standard physical parameters, and near infrared and visible spectrophotometric analysis.

2.1 Initial Fabrics

Two of the most widely used materials in the textile industry are cotton twill, or denim, and woven nylons, commonly used in the airbags of motor vehicle safety devices. The denim and nylon materials were also chosen for the initial testing because of their ready availability, sturdy construction, and well documented properties.

2.1.1 Denim Fabrics

The denim fabrics were divided into ten distinct categories according to variations in coloration of warp thread, the longer thread running parallel to a fabric rolls' edge, or selvage edge, and weft thread, the thread which traverses the fabric. The color variation was chosen to aid in the selection of the wavelength of light most suitable for a wide variety of textile fabric colors. Table 2-1a below shows the classification of the denim fabrics.

Table 2-1a Denim Fabric Identification Table

Fabric #	Identifying Name	Distinguishing Feature (warp thread color, weft thread color)
1	White	white, white
2	Tan	tan, tan
3	Beige	beige, white
4	dark green	green, white
5	blue #1	blue, white (brightest blue)
6	blue #2	blue, white (medium blue)
7	blue #3	blue, white (dull blue)
8	black #1	gray, white
9	black #2	black, white
10	black #3	black, black

2.1.2 Airbag Fabrics

The three airbag fabrics were similarly categorized, but according to their weave tightness rather than color, as all the fabrics were pure white, or undyed. Similar to the color range the weave variation was chosen to aid in the selection of the wavelength of light used for this study. Table 2-1b below shows the classification of the airbag fabrics.

Table 2-1b Airbag Fabric Identification Table

Fabric #	Identifying Name	Distinguishing Feature (weave tightness)
11	Airbag #1	loose weave
12	Airbag #2	medium weave
13	Airbag #3	tight weave

A more complete manufacturer's description can be found in the Appendix, Table A-1.

2.1.3 Stitch Thread Material

The thread chosen for the stitching was also an important consideration. The thread preferred was of a type commonly used in the textile industry for garment manufacturing. It is made up of a polyester core about which two cotton threads are twined. This makes for a robust and inexpensive thread for which the color variation is only limited by the dyes available in the textile industry. Eight colors were selected for this study for further examination of the effect of color in the detection of skipped stitches. The colors were black, light blue, green, orange, purple, red, tan, and white.

2.2 Physical Parameters Of Initial Fabrics

There are a number of important characteristics used to define a fabric in the textile industry. These characteristics are often referred to as the physical parameters of the fabric. Five of these parameters that were determined for the various fabrics used in this study are fabric weight, average yarn count, average yarn crimp ratio, average yarn take-up ratio, and the average diameter of the threads that make up the fabric. The American Society of Testing and Methodology (ASTM) has defined a number of methods for determination of the physical parameters of materials ranging over all the current industries in the US allowing a standard method of determining and reporting these parameters. Respectively, the ASTM Test Method Designation for the above listed parameters are: D3776, D3775, D3883 (both crimp and take-up), and D204 [38, 37, 39, 40]. The fabrics were prepared and conditioned according to these standards and the standard for conditioning (atmospheric, humidity, and temperature), D1776 [35]. The

following is a description of the test methods. The tabulated results can be seen in the Appendix, Table A-2.

2.2.1 Environmental Conditioning

Before any testing was done on the samples, they were prepared for size and shape and then conditioned via the standard ASTM 1776. This standard outlines that the samples be in the test area for a minimum of 24 hours. The "test area" is described as an environmentally controlled lab setting of atmospheric pressure, temperature, and relative humidity. For this study, the variables were equivalent to exterior atmospheric pressure, and approximately 68ºF and 40% relative humidity.

2.2.2 Fabric Weight

To determine the weight per unit area of a fabric, a 6" x 6" square is cut from each fabric and weighed on a sensitive scale. The measurements are then converted to give ounces per square yard and grams per square meter, for comparison in English and SI units. The results for the average weight of the 13 fabrics of this study are seen in Table A-2.

2.2.3 Yarn Count

The average yarn count of a fabric is determined by counting the number of warp or fill yarns per inch using some sort of magnification device. For this study a video microscope was used to examine a sample cut from the fabrics. A small scale was used in the frame of the picture to help determine the lengths counted over. For the average

values, the fabric count is sampled in five random locations, for both warp and fill yarns, at least one inch away from any cut edge, to avoid miscalculation due to stretching from cutting the fabric samples. Figure 2-1, below, shows images from the video microscope for fabrics #1, 3, 11, and 13. This figure shows the view of four fabrics with a millimeter scale in each view for counting threads. Additional images found in the Appendix Figure A-21, show more examples of fronts and the backs of two of the fabrics. The results for yarn count are seen in Table A-2.

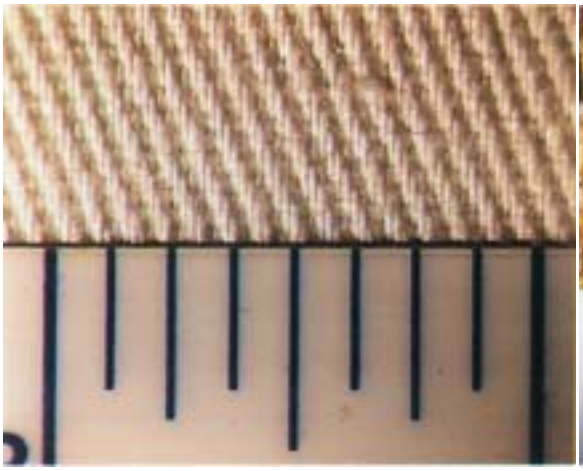

(a) Fabric #1, White Denim,
Front Side,
Warp Perpendicular to
Millimeter Scale

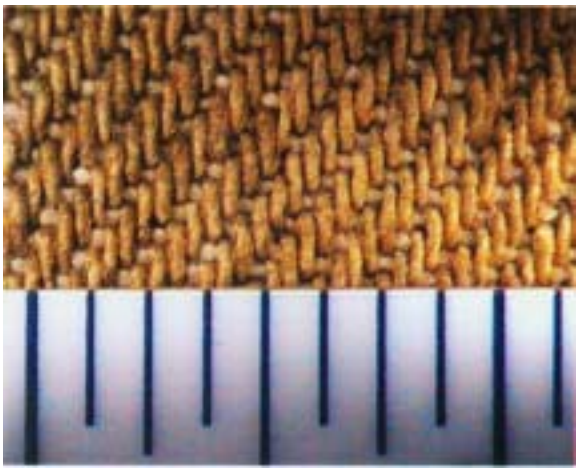

(b) Fabric #3, Beige Denim,
Front Side,
Warp Perpendicular to
Millimeter Scale

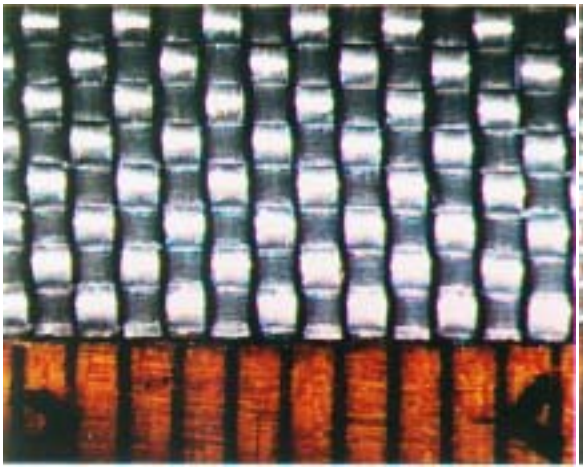

(c) Fabric #11, Loose Weave
Nylon, Front Side,
Warp Perpendicular to
Millimeter Scale

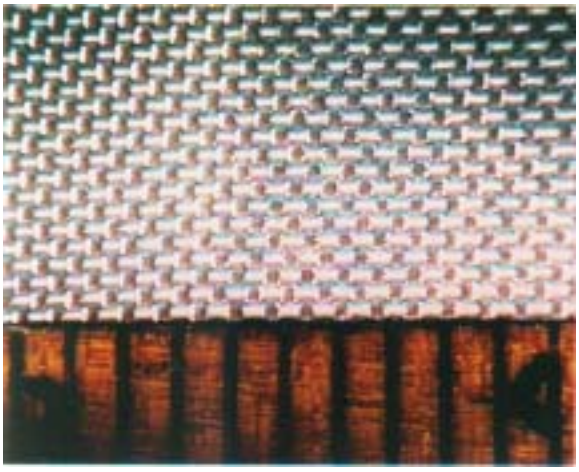

(d) Fabric #13, Tight Weave
Nylon, Front Side,
Warp Perpendicular to
Millimeter Scale

Figure 2-1 Example Images Of Test Fabrics For Yarn Counts

2.2.4 Yarn Crimp Ratio And Yarn Take-up Ratio

The average yarn crimp ratio and the average yarn take-up ratio are related quantities with subtle differences. Yarn crimp is defined as the "undulations or waviness in a yarn due to interactions with other yarns" [39], and is reported as a percent based on the in-fabric distance. Yarn take-up is defined as the "additional length of yarn used to make a given length of fabric" [39], and is reported as a percent based on the out-of-fabric distance. The test method for both of these parameters is as follows:

1. Determine a set length in the fabric of both the warp and fill yarns at least 1" away from any cut edge, this will be the in-fabric length;
2. Mark or carefully cut the yarns at this length and unravel the fabric to at least 1" from a cut edge;
3. Remove 10 successive yarns from the fabric;
4. Using a specific tension for all the samples, measure and average the out-of-fabric lengths of the samples; and,

5. Determine the yarn crimp and yarn take-up ratios using the following equations:

$$C = 100 * (Y - F)/F \qquad \textbf{Eq. 2-1}$$

$$T = 100 * (Y - F)/Y \qquad \textbf{Eq. 2-2}$$

Where: C = yarn crimp [%]

T = yarn take-up [%]

F = in-fabric length

Y = out-of-fabric length under a specific tension

This study followed the method outlined above with the following conditions:

- A dye was used to cut all the samples a specific length of 9 3/8”
- Tension was applied to each sample by attaching a 14.662 g mass to one end of the yarn, holding for five seconds and then measuring the length of the sample by holding it up to a ruler in a vertical position (no relaxation)

The values were averaged and tabulated in Table A-2.

2.2.5 Yarn Diameter

The average yarn diameter for the warp and fill yarns was calculated by cutting small samples from the unraveled yarns used for the crimp and take-up ratios and looking at them under a microscope at 10X magnification. Five samples of both warp and fill yarn from each fabric were made and the values were averaged. In general the yarn samples are held on the microscope slide using mineral oil to create a seal between the slide and the cover glass, as outlined by ASTM Standard D204 [40]. After a few trials

with the cotton samples, however, it was determined that even in a short amount of time the yarns absorbed enough oil to make a significant difference in the size of the yarns and thus application of the oil was abandoned and all the samples were re-measured dry. A listing of the measurements are found in Table A-2.

Eight final stitch threads were chosen to use as test samples. The average yarn diameter of the threads was also measured as stated above and are reported in Table A-2.

2.3 Near Infrared Wavelength Spectrophotometric Analysis

To determine the best wavelength of light to use in this study, a technique known as spectrophotometric analysis was employed to gauge the test materials' light reflection/absorption/transmission qualities. Near infrared wavelength light, 1100-2500 nanometers, was selected for the primary analysis because longer wavelength light is generally more reflected than absorbed, and is less likely to be affected by color and coatings applied to materials. Thus, by selecting a longer wavelength light source, more light would be reflected back to a detector, carrying more information about the surface of the sample. To begin with, three comparative analyses were done for the test fabrics in different orientations to show that, since the test material is similarly woven fabrics, the wavelength chosen is independent of number of material layers, material orientation; minimally dependent on the material type; and strongly dependent upon the color variation of the test fabrics.

2.3.1 NIR Wavelength Spectrophotometer Equipment

The NIRSystems NIR Spectrophotometer (NSAS) is a common device used in the textile industry to measure the dye content and molecular makeup of a material by comparing the absorption at set wavelengths to known standards for wavelength absorption of concentrations of chemical bonds such as OH, CH, and NH. When the concentration of these constituent molecules is high, more light is absorbed at those wavelengths. The results from the analysis by the NIRSystems device is reported in absorbance units ("au"), derived from the equation:

log (intensity of reference / intensity of sample) = absorbance unit **Eq. 2-3**

Where the device establishes a baseline reference intensity by running a test with no sample present, and compares the intensity of the sample to this reference for standardization. Since light intensity does not drop linearly when absorbed by greater numbers of constituent molecules, a logarithmic function is used to clarify the results. As an example, if a sample absorbs 90% of the source light, and transmits 10%, the relative absorbance is:

log (100% / 10%) = log (10) = 1au **Eq. 2-4**

Or, if the sample transmits only 1%:

log (100% / 1%) = log (100) = 2au **Eq. 2-5**

Thus, we can see a trend that as more constituent molecules are present, the higher the absorbance unit.

Transmission through a sample is, however, unreliable due to difficulties such as particle size difference in a sample material, suspended solids in liquids or slurries, source lamp intensity, and gain settings on the detector. So, many spectrophotometric systems use reflected rather than transmitted intensities, while still using the relative absorbance. This reflected intensity does not change the nature of the functions used to describe the results, as seen here:

log (intensity of reference / intensity of sample) = absorbance unit **Eq. 2-6**

Here, the device uses a white Coors ceramic calibration block to set a baseline reflective reference intensity, and compares the reflected intensity of the sample to this reference for standardization. Given that the data tabulated is in absorbance units, it is more helpful to see the data in terms of reflectance. Thus, the data is converted to percent reflectance via:

log (1 / reflectance) = absorbance $\Rightarrow$

reflectance = 10^(-absorbance) **Eq. 2-7**

The test device is situated as seen in Figure 2-2. The incident beam is directed perpendicularly to the surface of the sample, and diffused light reflected from the surface

is collected by photosensitive electronics at a 45° angle to the surface of the sample to minimize the measurement of specular reflection, or glare.

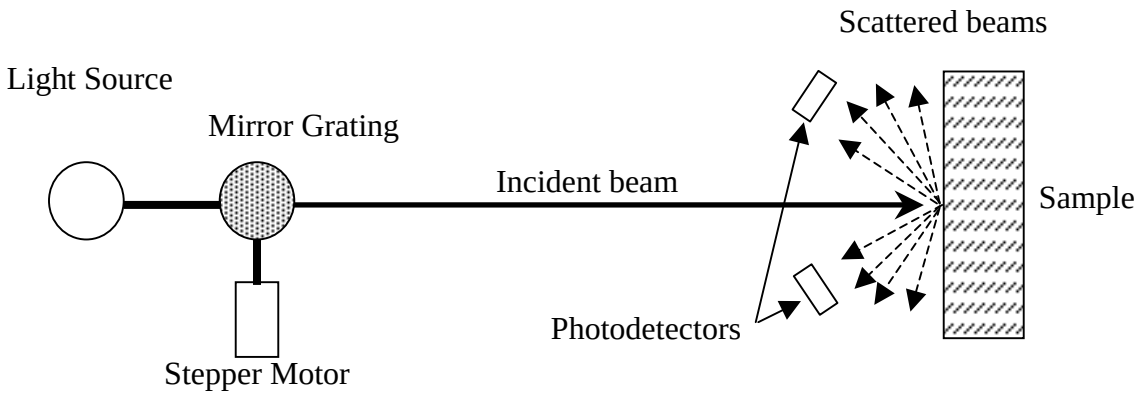

Figure 2-2 NIR Wavelength NSAS Spectrophotometer Test Device

The system includes a sample holder to standardize the sample area that is analyzed. The sample holder holds a sample which is 7 7/8 inches long by 1 3/8 inches wide and 1/4 inch thick. The holder is a metal frame with glass panels to contain a liquid for analysis, or to maintain the position of a material to keep the surface flat. The holder is loaded into a motor driven assembly and moved in a single plane such that approximately 75% of the total area of the sample is scanned. Thirty two scans per specimen are made and averaged together for the final measurement. To reduce error due to scattered, reflected light in reflectivity data, a paperboard, black card is inserted behind the material to absorb light transmitted through the material, keeping it from reflecting off the back wall of the holder or the interior of the system behind the holder.

The device scans the sample by splitting the source light into 100 separate wavelengths in the NIR range of 1100-2500nm, at intervals of 14nm. The light source for the device is a high quality tungsten halogen lamp. Splitting the light into the separate wavelengths is accomplished through a concave mirror with a finely etched grating on the surface, which is moved through a predetermined arc. The concavity of the mirror causes the light to be refocused as a point, and the arc of motion gives the correct wavelength at the sampling position at maximum intensity. The motion of the mirror is handled by a stepper motor – encoder system which is controlled by an internal processor. The system also has an internal wavelength standard which produces sharp absorption peaks at well known positions throughout the spectrum. Software run on the processor locates these peaks and uses them to keep the wavelength scale constantly calibrated and control the encoder/motor/mirror grating for exact positioning such that a known wavelength is incident on the sample. This ensures that the reflection data collected from the sample is at a calibrated, known wavelength.

As an example of the data output by the spectrometer, see Figure 2-3, below. This graph shows the data for cotton and nylon 6 in the form of the logarithm of one over the reflectance versus time. This is equivalent to the absorbance of the light at distinct wavelengths by the sample. The graph shows distinct points where the material absorbs light due to the molecular bonds of the material. Cotton, or natural cellulose, has a molecular formula of $[C_6H_{10}O_5]_n$, where the n indicates the repeating sequence. This material has sharp absorption peaks at 1490, 1930, and 2100nm corresponding to the molecular bonds that absorb at those wavelengths. Nylon, a man-made material produced through repeatable chemical process, has the molecular formula $[C_6H_{13}NO_2]_n$.

For nylon, the repeat of this sequence relates to the number identifying it. For example, nylon 6 has six repeated sequences with a nitrogen-oxygen bond as the link. Nylon 6,6 has two sets of repeating six sequences to differentiate it. Looking to Figure 2-3, we can see the absorption peaks related to the molecular bonds of this material at 1720, 2050, and 2300nm.

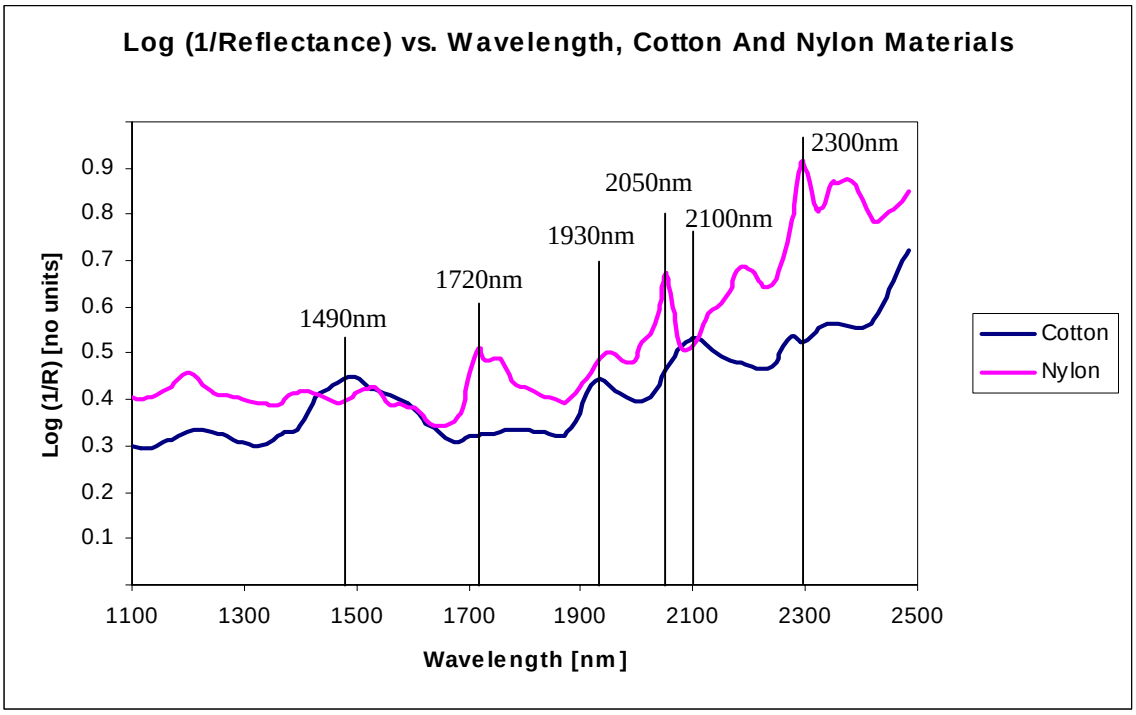

Figure 2-3 Representative Data From The NIR Spectrophotometer For Cotton And Nylon

2.3.2 Fabric Preparation And Orientation Distinctions

To help determine the reliability of a wavelength selection based on the data provided through spectrophotometric testing, a number of analyses of data taken by the NSAS system was completed. These analyses mainly involved the orientation of the test

fabrics in the system. The goal behind this portion of the research was three-fold. First, to determine if the amount of layers of the material had a bearing on the total reflectance of the test fabrics, an analyses was done for each fabric using different number of layers. Second, to help eliminate the possibility of data variation, and hence, final system reliability, due to the weaving pattern, the test fabrics orientation was slightly changed from data set to data set. Though slight physically, the weave pattern shifts were distinctly significant. Third, to examine differences caused by varying colorations of the warp and weft threads, the range of the test fabrics colors was evaluated and compared. Together, this research will ensure a wavelength which is reliable for practically every type of fabric.

The fabric rolls were again environmentally conditioned via ASTM D1776. Then the fabrics were cut into strips 7 7/8 x 1 3/8 inches (hereafter referred to as "samples") to fit into the sample holder. To begin with, 40 samples were cut from each of the first three fabrics. These were cut such that 20 samples had the warp thread on the long side and 20 samples with the weft thread on the long side. In other words, effort was taken such that the samples were cut such that the warp threads or weft threads were basically parallel to the long or short side of the sample.

From the forty samples cut thusly, two other comparisons also made were to evaluate the difference between the data for 1, 2, 3, or 4 layers of fabric, which may affect the amount of absorption since seams consist of more than one layer, and, the difference in front and back of the sample to emphasize the variation due to coloration variation of the threads and the weave pattern.

In summary, the first three fabrics had data sets taken each for the following orientations: 1, 2, 3, and 4 layers; warp thread on long side or weft thread on long side; and, front or back toward the incident beam. Permutations of these orientations were made such that a sample orientation may read "warp on long side, 4 layers, front toward detector," or "weft on long side, 2 layers, back toward detector." Twenty such scans were made for each orientation and an average was made for each set giving a total of 320 scans for each of the first three fabrics. After the first three fabrics were completed, their data was compared for significant deviation between scanning a sample 20 times and scanning the sample 10 times. Since the NSAS system scans each sample 32 times and averages the results, the deviation was minimal and the remaining 10 fabrics had 10 samples each cut from the original fabric, in the same manner and size as described above.

The NSAS system allows the data to be saved to a file which can be converted to text and analyzed elsewhere (such as any PC), so a file nomenclature system was developed as seen in Figure 2-4, below.

C:\NIRS\$\#_f \alpha_1 \alpha_2 \#_2 \alpha$ where : $\#_f$: test fabric number

α_1 : war**p** or wef**t** on long side of sample

α_2 : **f**ront or **b**ack toward detector

$\#_2$: number of layers

α : letter designating scan number

Figure 2-4 NIR Wavelength Spectroscopy Data File Name Format

As an example, a data file might be named “3pf4t” indicating that it represents fabric number three, with the warp thread on the long side of the sample, the front of the fabric toward the scanner, four layers thick, and scan number twenty of the series. Another example would be “8tb1c” indicating that it represents fabric number eight, with the weft thread on the long side of the sample, the back of the fabric toward the scanner, one layer thick, and scan number three of the series.

Lastly, the denim fabrics have a weave pattern that leads to what is known as “ribbing.” These are the ridges that form a regular pattern seen on most denims and many other fabrics due to the method and style of the weave. The ribbing can be seen in the following figure:

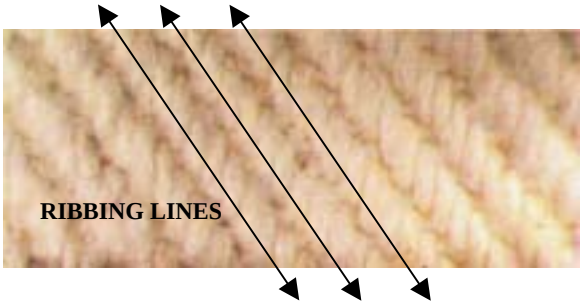

Figure 2-5 Example of Denim “Ribs” Due To Weave Style

Here, the ribbing can be seen as the pronounced lines on the surface of the fabric angled from left to right. The airbag fabrics do not have this pronounced ribbing due to a different style of weaving, and were thus excluded from this part of the study.

To demonstrate any variation due to the ribbing, 10 samples each were cut from fabrics #1, 3, 4, 5, and 8. These fabrics were chosen from the test fabrics to cover the

range of coloration varieties, and give variation in the ribbing orientation, either due to weave tightness or yarn diameters. The fabrics were cut into the same 7 7/8 x 1 3/8 inch pattern, taking great care to ensure that the ribbing was turned both parallel and perpendicular to the long cut edge. Due to the different tightness of the weaves and different yarn diameters of the samples, this translated to orienting the warp threads 45° – 80° off the long cut edge.

These "ribbing" samples were then placed into the NSAS system for analysis as the other samples described above. An additional file nomenclature was developed for these samples, as seen in Figure 2-6:

C:\NIRS\ribbing\$\#_f \alpha_1 \alpha_2$ where : $\#_f$: fabric sample number

α_1 : ribbing turned **h**orizontal or **v**ertical (in relation to the cut edge)

α_2 : **f**ront or **b**ack toward detector

Figure 2-6 NIR Wavelength Spectroscopy Data File Name Format For Ribbing Orientations

As an example a file may have been named "1hf" for fabric number 1, ribbing turned horizontal to the scanning path, and front turned toward the scanner. The data sets from these samples were then compared to the initial samples where the determining factor was the warp thread being oriented parallel or perpendicular to the long cut edge.

The final comparison of data sets for the NIR spectrophotometric data was made for color variation across all the samples. This was done to help determine the effect of

the samples' colors on the amount of light reflected from the surface and to aide in determining the appropriate wavelength of light to use to minimize this effect.

2.3.3 NIR Wavelength Spectroscopy Data Analysis

To begin the analysis of the NIR spectroscopy data, the data was grouped according to the following table:

Table 2-2 Test Fabric Grouping For Comparison Of NIR Spectroscopy Data

	Comparison Made	Held Constant Across Data Set
Fabric #1-13	Multiple layers	Warp or Weft Thread On Long Side & Front or Back Toward Scanner
Fabric #1-13	Warp vs. Weft Thread On Long Side & Front vs. Back Toward Scanner	Three Layers
Fabric #1, 3, 4, 5, 8	Ribbing Turned Horizontal vs. Vertical & Front vs. Back Toward Scanner	Three Layers
Fabric #1-13	Color variations	Three Layers, Warp on Long side, and Front Toward Scanner

2.3.3.1 Multiple Layer Comparison

Table 2-2 shows that for the initial analysis, the 13 fabrics' data sets were compared first for deviation caused by the number of layers, with the warp or weft thread on the long side and front or back toward the scanner held constant. Thus, as can be seen in the Appendix in Figure A-1, for fabric #1, there are four graphs, representing the Reflectance vs. Wavelength of the samples for the different arrangements. These arrangements are "Multiple Layers, Warp On Long Side, Front Toward Scanner," and, "Multiple Layers, Warp On Long Side, Back Toward Scanner." Similar graphs seen are for the "Weft On Long Side" cases. Appendix Figures A-2 through A-13 are similar graphs for each of the test fabrics, the figure number corresponding to the fabric number.

These graphs repeatedly show that the variation in reflectance due to the number of layers is decidedly minimal. As an example, see Figure 2-7 below, where the reflectance data for four fabrics, #1, 5, 10, and 12, are shown. Here we see that the number of layers has very little effect in the reflectivity across the entire NIR spectrum.

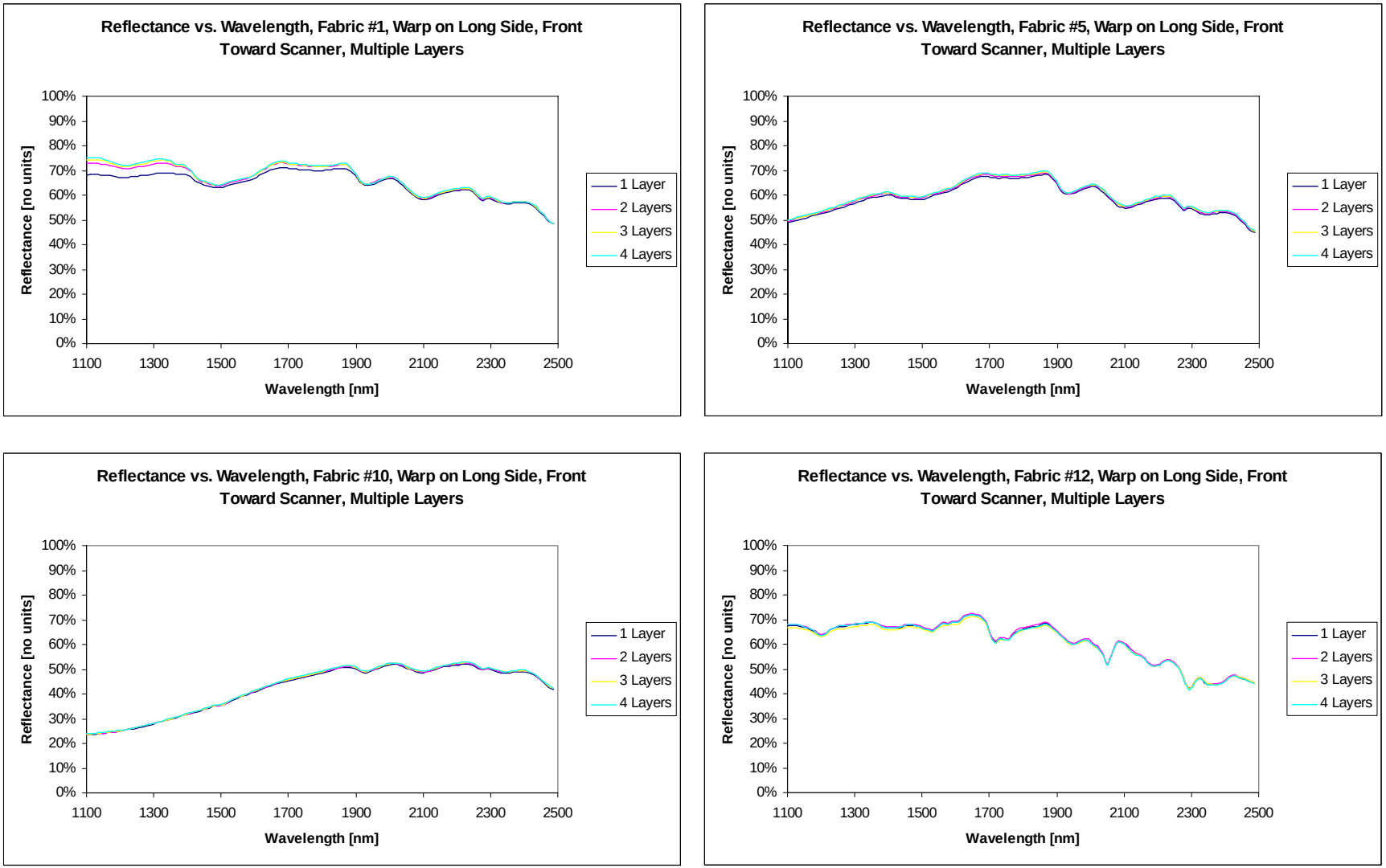

Figure 2-7 Multiple Layer Comparisons For Fabrics #1, 5, 10, And 12

Note that for fabric #1, and also #2 which can be seen in Figure A-2, the lower wavelengths do show some differentiation in the percent reflectance, due to the number of layers affecting the total amount of light reflected. To aid in the reflectivity study using the NSAS system, a stiff paperboard card is inserted behind the material. The card is black to absorb light that transmits through the material, reducing reflections from the back of the carrier device and from the interior of the system behind the carrier, as the carrier is a double paned-glass holder. This affects the amount of light reflected as shown in the graphs as more light is reflected back to the detectors as more layers are added. With one layer, much of the light that transmits through the first layer, through holes in the material and through the yarns themselves, is absorbed by the black absorbing background. Adding another layer causes some of this primary transmitted light to be reflected back through the first layer off of the second layer. These two reflected light wave sets interfere with one another, mainly constructively, to produce a higher reflective value. However, as in the first layer, a portion of the light is also transmitted through the second layer and absorbed by the black background. Additional layers repeat this process. As the wavelength of light increases, the reflectivity data for multiple layers tends to come together more. This is due to the wavelength of light being more evenly absorbed/reflected/transmitted in the material and off of the black background for any number of layers.

However, this is not the case for the remainder of fabrics, leading to the conclusion that this condition is mainly in relation to the color of the samples. Fabrics #1 and 2 are both light colored fabrics (white on white and tan on tan), and the remainder of the fabrics are of a darker nature. The darker color fabrics absorb more of the light near

the visible end of the spectrum represented, allowing less light through to be absorbed by the background, except when more layers are added. For any number of layers, it can be seen that the amount of light reflected back from the darker fabrics is nearly the same throughout the NIR spectrum.

This confirms the supposition that the effect of layers on the reflectance is minimal. The remainder of the data analysis is then streamlined such that only three layers of samples are placed in the holder at any one time. Three layers is chosen mainly due to the size of the NSAS system sample holder. As described above, the sample holder is approximately 7 7/8 inches long by 1 3/8 inches wide and 1/4 inch thick. The interior of the chamber requires some thickness (~1/8 inch) of material to hold the sample in place with out allowing the surface to undulate. Three layers was determined to be the optimal number for the fabrics used in this research.

2.3.3.2 Warp Thread vs. Weft Thread On Long Side Comparison

The second analysis was again across all 13 test fabrics' data sets, this time comparing the warp and weft thread orientation as well as front vs. back of the samples. Figure 2-8, below, shows the data for four of the fabrics, #2, 6, 9, and 13. Additionally, in the Appendix, Figures A-14 through -17 show graphs of sample arrangements of "Warp vs. Weft on Long Side, Front vs. Back," for each test fabric with three layers used. Both warp and weft on the long side and front and back toward the scanner are shown on these graphs since the two do not have conflicting cross references.

Figure 2-8 Comparison Of Warp vs. Weft On Long Side And Front vs. Back For Fabrics #2, 6, 9, And 13, Three Layers

Fabrics #1, 2, and 11-13 show almost no deviation between warp and weft orientation and front or back orientation. The other samples show relatively little difference between warp and weft orientation, but marked difference between the front and back of the samples. This is due to the color variations between the warp and weft threads rather than any orientation causes. Note that test fabrics #1, 2, and 11-13 have warp and weft threads of the same color; white or tan. The remainder of the test fabrics have slightly different colors to completely different colors, such as fabric #3 (beige on white) and #9 (black on white). Thus, the data lines for #1, 2, and 11-13 are very close together, whereas the remainder of the test fabrics show the front and back data lines slightly to greatly separated, but their respective warp and weft orientation data lines close together.

There are two conclusions one can draw from this analysis. First, the orientation of the warp and weft thread has no bearing on the reflectance at these wavelengths. On the scale of the wavelength of light used, 1100-2500 nm, the fabric surface appears relatively flat, and yet rough due to it's makeup. The size of the threads that make up the fabrics, ~0.1 to 1.0 mm in diameter, leads to the conclusion that there is a scattered reflection of the light at the surface of the fabric. With diffuse scattering, the light impinging on the surface is randomly reflected off such that no constructive/destructive interference patterns are set up leading to a pattern in the reflected light, as shown in Figure 2-9, below.

Second, the reflectance level based on the orientation of front or back of a fabric is highly dependant upon the color of the threads which constitute the fabric, but independent of surface presented. This again confirms the original supposition that the

color of the sample is the greatest contributor to difference in percent of light reflected from the surface of the fabric.

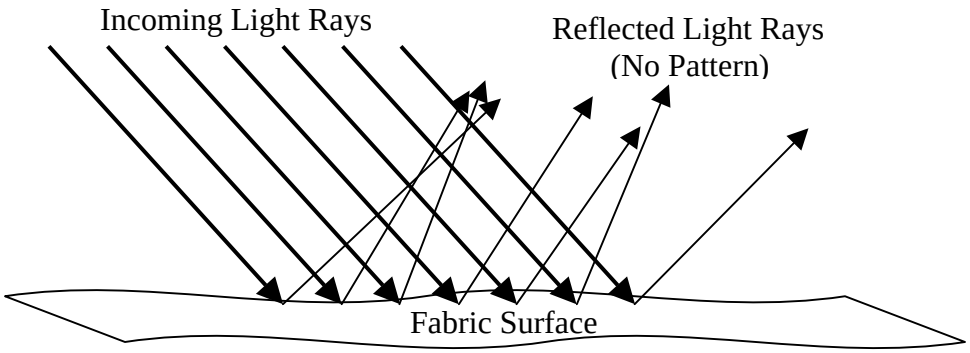

Figure 2-9 Diffuse Scattering From Fabric Surface

2.3.3.3 Ribbing Turned Horizontal vs. Vertical Comparison

The third comparative analysis that was done with the NIR spectrophotometric data is the ribbing orientation. As stated above, the ribbing on the material is caused by the method of weaving and the size of the yarns that make up the fabric, as shown above in Figure 2-5. To cover the range of materials' properties and colorations, fabrics 1, 3, 4, 5, and 8 were chosen. Also, as above, the nylon materials are not studied here since their weave patterns do not lead to ribbing structures on the surface. The graphs for fabrics #1, 3, 4, and 5 can be seen in Figure 2-10, below. The graphed data for fabric #8 for these orientations can be seen in the Appendix, Figure A-18. For completeness, the analysis included the orientation of front and back of the sample, as the ribbing is evident from both sides of the fabric. Thus, the graphs are of the arrangements "Horizontal vs. Vertical Ribbing, Front vs. Back" for the 5 selected test fabrics, each with three layers as above.

As with the warp vs. weft and front vs. back orientations of the prior comparisons, the data shows that the reflectance for the horizontal and vertical ribbings are nearly identical, while there is a distinct variation between front and back data sets. The first part goes back to the geometric optics argument above that the fabrics diffusely reflects the light striking upon its surface. The second part again shows that the color difference of the surface presented to the system is of more importance than the actual surface itself.

Figure 2-10 Comparison Of Horizontal vs. Vertical Ribbing And Front vs. Back For Fabrics #1, 3, 4, 5, Three Layers

2.3.3.4 Color Comparison Across All Test Fabrics

The final analysis of the NIR spectrophotometric data was a comparison across all the test fabrics to evaluate optimal wavelength ranges to use for any color of fabric. The graph for this analysis can be seen in Figure 2-11, below. For this comparison, the data sets of "three layer, warp on long side, front toward scanner" for all 13 test fabrics were used.

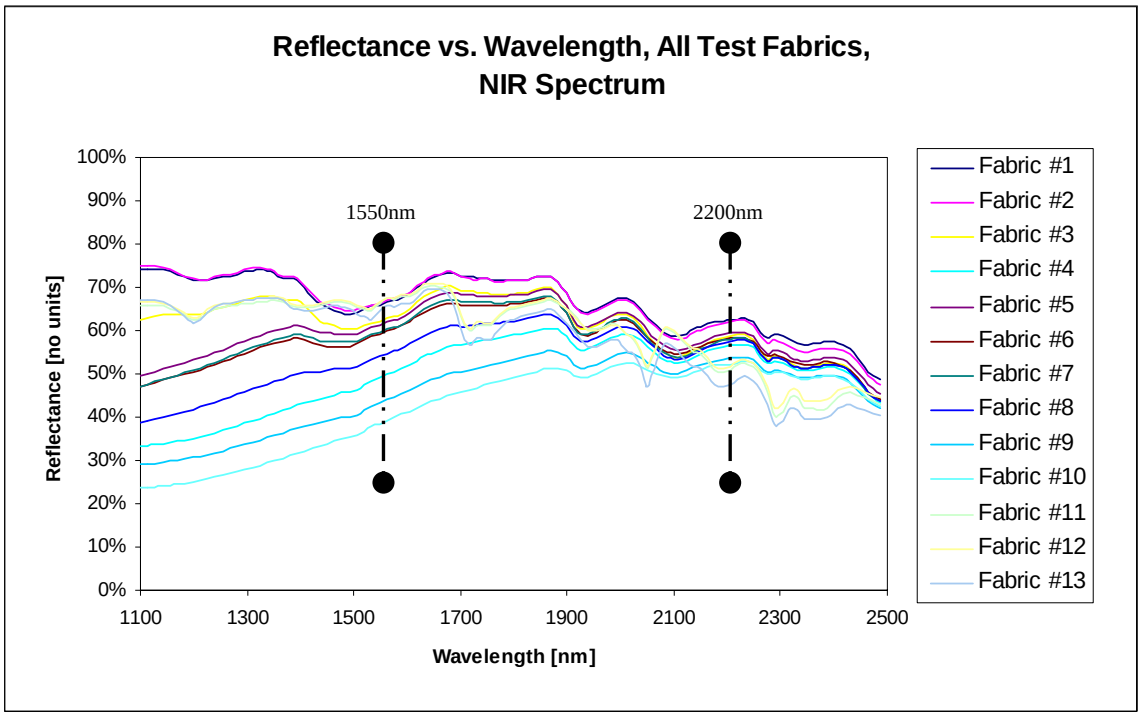

Figure 2-11 Color Comparison For Fabrics #1-13, Near Infrared Spectrum, 1100-2500nm

Calculating the difference between the highest and lowest reflectance data revealed several things. First, the largest spread of reflectance percentages, 51.2% between highest and lowest reflectance, occurs at the shortest wavelength, 1100nm. This

is to be expected as this wavelength is closest to the visible spectrum and so colors have a large part in the reflectance properties of a material. On the other end of the test spectrum, at 2486nm wavelength, far from the visible spectrum, the data shows that the reflectance of different colors and materials becomes nearly identical, with a difference of only 8.3%.

Second, the data again shows that the difference in material and weave are not extremely important factors. Fabrics #1-10 are all cotton denim samples, while fabrics #11-13 are nylon-based material, natural versus man-made fibers. The denim fabrics have a dull luster compared to the nylon fabrics. The denim fabrics have varying yarn diameters averaging 0.407mm for the warp threads and 0.455mm for the weft threads. The nylon fabrics also vary, averaging 0.843mm and 0.770mm, respectively. The denim fabrics are woven nearly identically, while the three nylon fabrics have differing a weave tightness among themselves as well as compared to the denim samples. Yet with all these differences among the materials, their properties and their finished assembly, the data shows that all the reflectivities fall within reasonable amounts of separation. The only significant factor involved in the reflectance of light comes down to the color of the material.

2.3.3.5 Determination Of Suitable Wavelengths For Research Use

Finally, groupings of the data around specific wavelengths of light help to determine the wavelength that should be used to complete this research. Upon completing a survey of the opto-electronic transmission devices being used throughout the world, it was determined that there were only a few viable wavelengths that stood

further investigation. The manufacture of NIR lasers is extremely difficult and quickly becomes expensive as the wavelength increases. However, there are two mass produced wavelengths which are very commonly used in the telecommunications industry. Mainly used in the transmission of data across fiber optic lines due to their high reflectivity in the medium, the wavelengths of 1550nm and 2200nm are readily available for purchase and are fairly inexpensive.

Comparing the data taken by the NIR spectrophotometric system, as seen in Figure 2-11, above, the average reflectance for all the test fabrics and the difference between the upper and lower reflective percentages for all the fabrics at those wavelengths showed promise in their use for this research, as shown in Table 2-3.

Table 2-3 Difference In % Reflectance For Fabrics #1-13 At 1550nm And 2200nm

Wavelength [nm]	Average % Reflectance	Maximum % Reflectance, Test Fabric #	Minimum % Reflectance, Test Fabric #	% Reflectance Difference
1550	58.22	66.53, #12	38.53, #10	28.00
2200	55.93	62.38, #1	47.34, #13	15.04

Evaluating these data at the lower wavelength once again confirms that the coloration of the material is the largest factor in amount of reflectivity. For both wavelengths selected, the two maximum reflectances are by the whitest samples. In fact, closer examination of the graph reveals that the five lightest colored samples (#1, 2, 11, 12, and 13) are nearly the same at the 1550nm wavelength, averaging 65% reflectance, while the darker fabrics score progressively lower based upon their color. At the 2200nm wavelength, the colors are only slightly involved, and the material itself becomes the dominating factor. Here,

the highest and lowest reflecting fabrics, #1 and #13, are only separated by approximately 15%. Fabric #1 is the white denim and #13 is a white nylon.

However, an interesting trend is seen as the wavelength increases. The denim fabrics' percent reflectances become closer together with a slight decrease, while the airbag fabrics range stays nearly the same but shows a significant decreasing trend. This is indicative of the material itself rather than color or weave variation, but also lends credence to the argument of color being less important as wavelength continues to increase. The denim material is a naturally occurring cellulose-based fiber (cotton), while the airbag material is a man-made product, consisting mainly of nylon, produced through repeatable chemical reactions. So, we may conclude that as the wavelength increases, the color has less effect on the reflectance and the materials' molecular composition comes into play. We can also conclude that natural cellulose's molecules reflect more light at the higher wavelength than the molecules of the nylon material, until around 2500nm, where the reflectances once again converge. Conversely, this says that at higher wavelengths, cotton molecules absorb less light than the nylon molecules.

To get an overall analysis of the NIR spectra comparisons at the selected wavelengths, see Figure 2-12a and -12b, below.

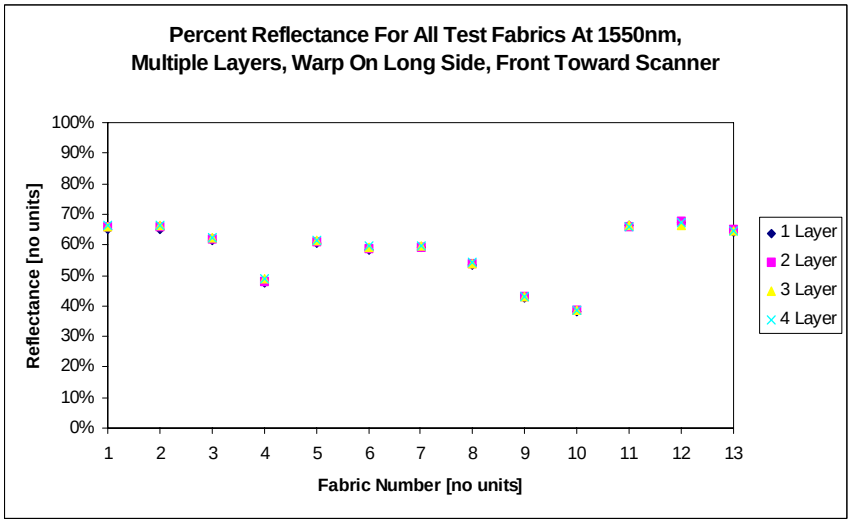

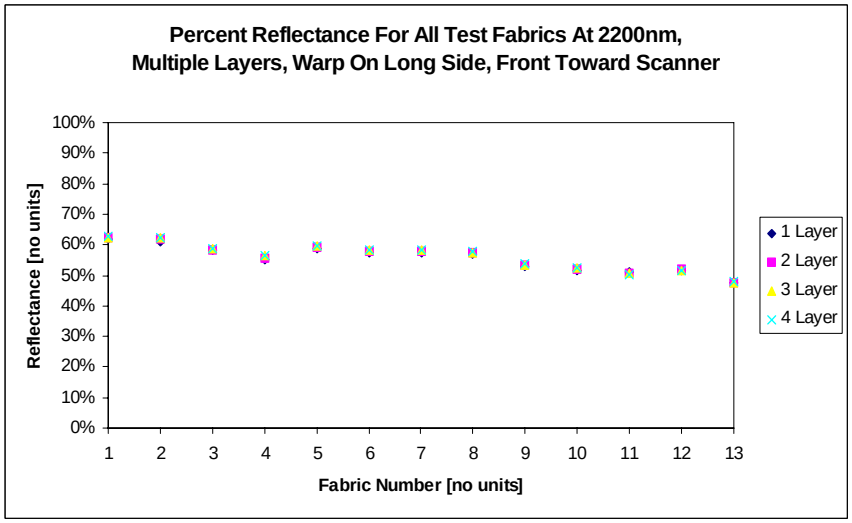

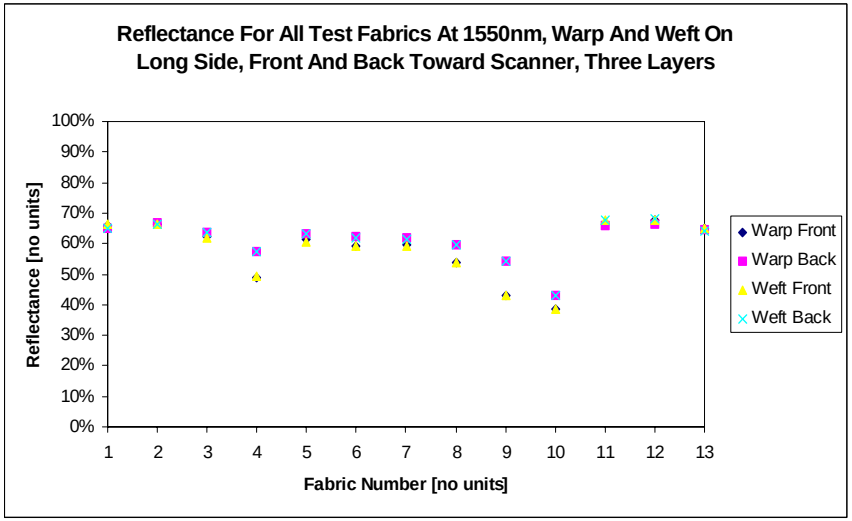

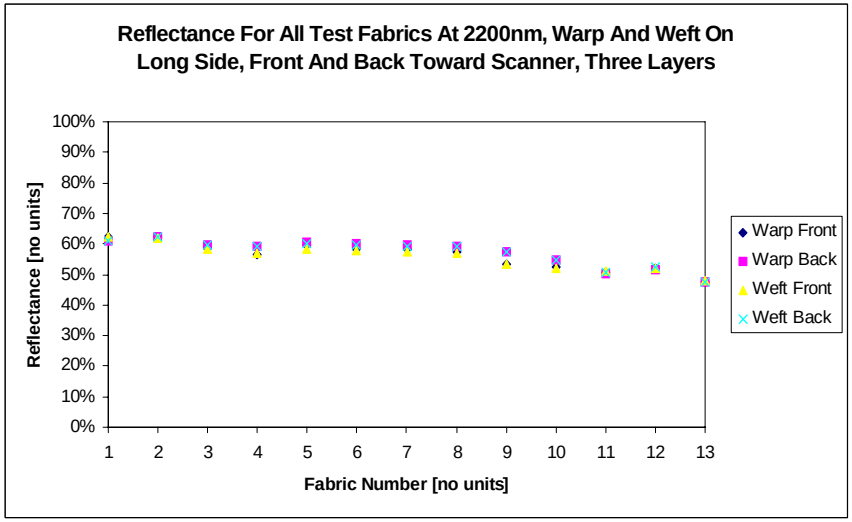

Figure 2-12a Comparison Data For All Test Fabrics At 1550nm And 2200nm

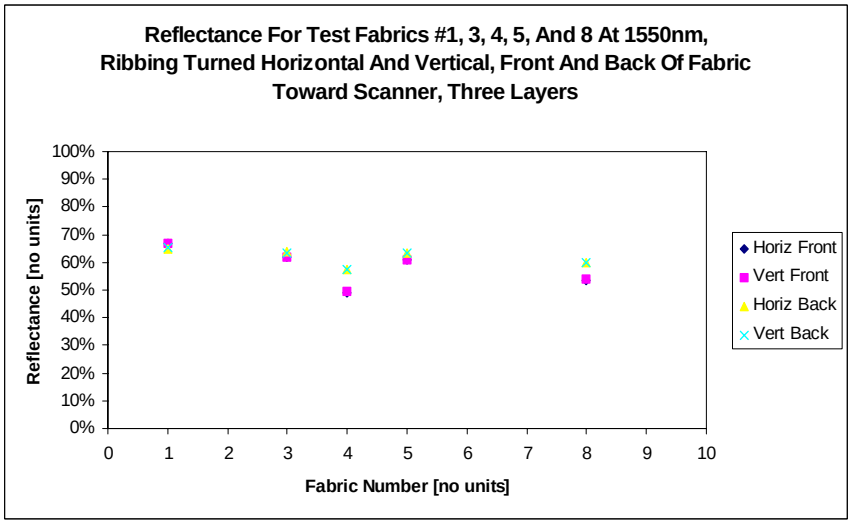

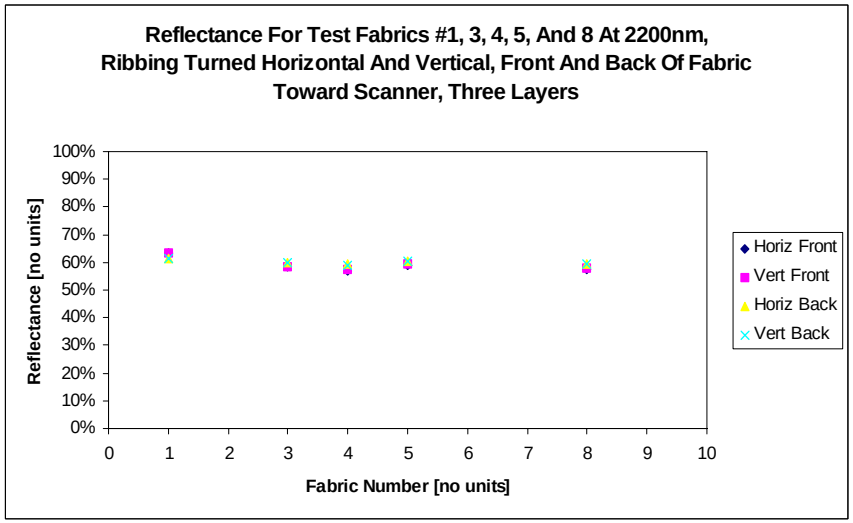

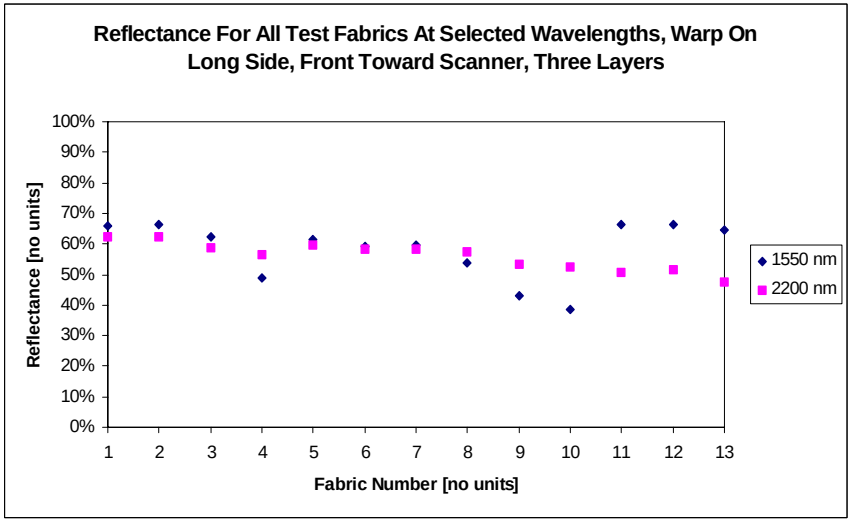

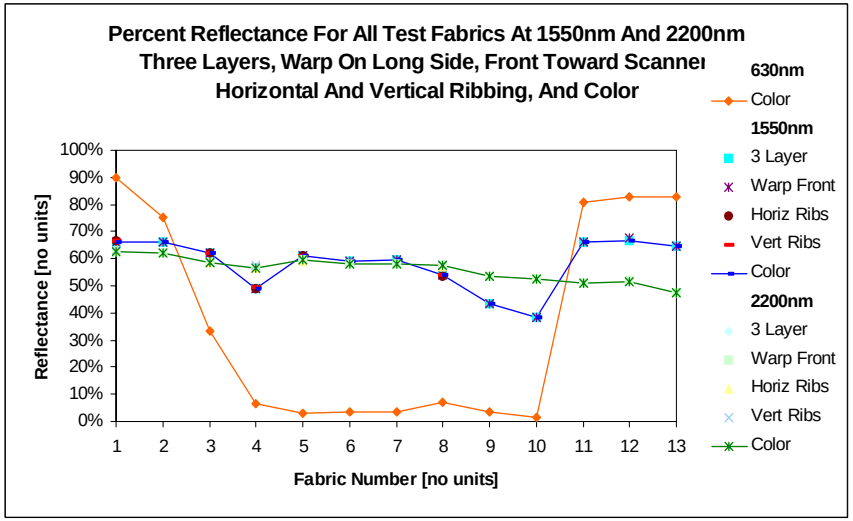

Figure 2-12b Comparison Data For All Test Fabrics At 1550nm And 2200nm

Figures 2-12a and -12b show the reflectance data for the comparisons made earlier across all or part of the test fabrics at the two selected wavelengths, 1550nm and 2200nm. The top graphs in Figure 2-12a show the reflectance for all fabrics with the warp threads on the long side of the sample for multiple layers. These graphs show that for all the materials at both the selected wavelengths the reflected light is nearly the same intensity for any number of layers, as indicated by all the corresponding points overlaying one another.

The bottom two graphs of Figure 2-12a correspond to the earlier comparison for warp and weft threads on the long side of the sample and front and back of the samples. As before, we see that the lower wavelengths' data shows no difference between warp and weft at all, and only a difference between front and back of the samples when there is a significant color difference between the warp and weft threads. Recall that the warp thread is mainly visible from the front of the fabric and the weft from the back, giving rise to different reflection levels front to back due to their color differences, such as in #4 (green and white) and #9 (black and white). At the higher wavelength, as shown in the bottom right graph of the figure, these differences almost disappear except in the case of #9 where there is only a slight difference between reflected light from the front and back of the sample.

The third comparison made initially was to determine any difference made by ribbing caused by the weaving. Samples were cut from fabrics #1, 3, 4, 5, and 8 with the ribbing oriented along the long side (vertically) or the short side (horizontally) of the sample. As with the bottom graphs of Figure 2-12a, the ribbing comparison graphs, seen as the top graphs in Figure 2-12b, show no significant difference for ribbing orientation at

either wavelength, but do show differences front to back at the lower wavelength (specifically, fabrics #4 and #8, again due to different color warp and weft threads) which virtually disappears at the higher wavelength.

Finally a comparison was made for reflectance versus color of the samples at the selected wavelengths, which can be seen in the graph in the lower left hand corner of Figure 2-12b. The reflected percentages for the 1550nm wavelength show variation according to the color of the sample. As the color darkens in the denim samples (#1 through 10), the percentage decreases from a high 66.36% for fabric #2 (a tan color) to a low 38.53%, for #10 (the black on black color). This is a range of approximately 28%, but still has significant reflection for the darker samples. For the nylon samples at the 1550nm range the reflection is high, 64.5% or better.

The reflected percentages versus color for the 2200nm wavelength range show more similar levels for all samples, regardless of color or material. The samples for the denim do show a slight decreasing trend according to color with the highest for the white sample, #1, at 62.50%, and the lowest for the black sample, #10, at 52.29%, a difference of only approximately 10%. The nylon samples reflect only slightly less at this wavelength averaging right at 50%.

Overall, the 2200nm wavelength appears to be the more ideal range of light sources due to the more consistent level of reflection for any material at any color. In fact, looking over all the comparisons together, as in the bottom right graph in Figure 2-12b, we see that the 2200nm wavelength of light is reflected consistently above 47% for all conditions of the samples. This includes different numbers of layers, orientations of yarns and weave patterns, front and back of samples, and colors. However, we cannot

rule out the use of the 1550nm wavelength at it shows a solid reflectance percentage above 38% for all the above conditions as well. Color more than anything else is the main variant for the 1550nm range, with the lowest being the black colored fabric, which is naturally more absorbent of light when color is a consideration, and the highest being the undyed nylon sample, which naturally reflects more light at all wavelengths.

This series of comparisons for the reflectance of the materials leads ultimately to the selection of a device producing a wavelength usable for many types of materials. The two wavelengths chosen to focus upon are readily available in the telecommunications industry, with the cost of the devices being the only remaining factor. A 2200nm wavelength device would be the ideal for this implementation, but it's overriding cost is an inhibiting factor. Prices ranged from $1000-2000 U.S. for laser diodes with this range of wavelengths, while the 1550nm devices were well under $1000 U.S. This cost difference can be mainly attributed to the industry's ability to produce stable, steady laser diodes in these wavelengths, as stated at the beginning of this section.

In conclusion, weighing the factors of cost versus response for the two device ranges led the study toward selecting a device with a 1550nm wavelength range. While the 2200nm wavelength had more consistent values for the materials and colors tested, the 1550nm source would show discernable reflection percentages for all types of fabrics while also keeping the cost down for a final production unit.

2.4 Visible Wavelength Spectrophotometric Analysis

Although the main focus of this study was for a device using near infrared wavelength laser light for implementation, for completeness, the study here includes spectrophotometric analysis in the visible wavelengths, 400 – 700nm. This will aide to clarify the need to use a wavelength of light that is not affected by color. To this end a device used widely in the textile industry to measure the dye content of a sample was employed for measurements of the 13 test fabrics.

2.4.1 Visible Wavelength Spectrophotometer Equipment

The Macbeth Spectralight system is a spectrometer much like the NSAS NIR system described in §2.3, except this device measures light intensities in the visible range rather than the NIR range. The Macbeth system is used to measure the dye content of a sample by illuminating the sample with three types of light, and measuring the reflected light for comparative analysis. A baseline is established by using a Coors ceramic standard, the same as the NSAS system.

The three light types are supplied by a single source and are classified as “north sky daylight,” which is the scattered blue light found in a clear sky; “fluorescent,” which approximates the lighting conditions found in a laboratory or office with fluorescent lighting; and, “full sunlight,” or the entire visible spectrum with no emphasis on any particular range. The Macbeth system then reports the reflected intensities of the visible wavelengths between 400 and 700nm, in 20nm increments, or 16 total wavelengths. By a proprietary calculation, the Macbeth system also uses this data to extrapolate the relative luminosity, red/green mixture, and yellow/blue mixture of light which the sample

reflects. This type of system is commonly used in the textile industry to assure standards of dye concentrations in materials.

The test device is situated as seen in Figure 2-13. The incident beam is directed at a sample held at 45° to vertical, and the reflected light is collected by photosensitive electronics nearly parallel to the incident beam, allowing the collection of a 10° cone of light (the solid angle from the observers eye). This arrangement is used to minimize the specular reflection off of the surface of the material.

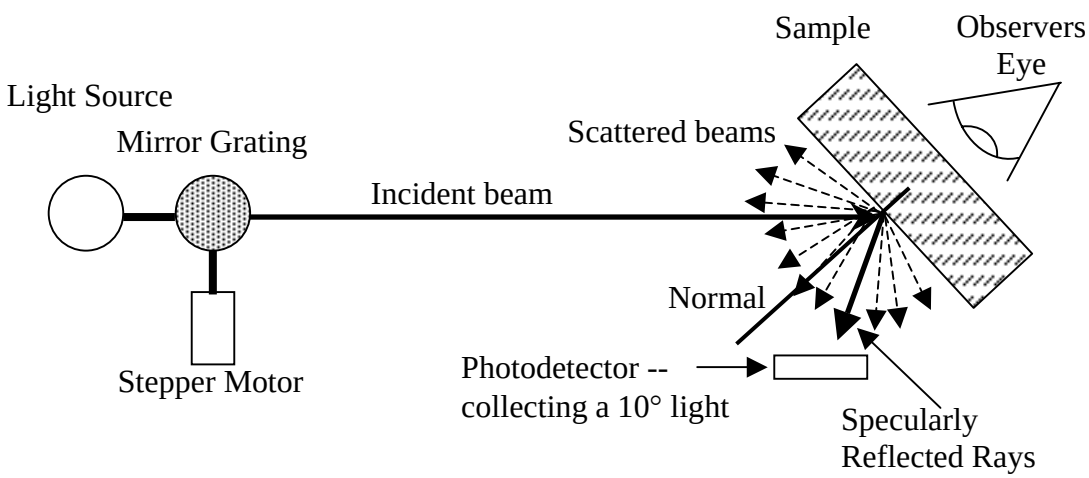

Figure 2-13 Visible Wavelength Macbeth Spectralight Test Device

The system holds the sample in place by clamping it over a cutout hole in the devices body, such that the surface area scanned by the device is ~0.8in^2. Exterior light is also blocked from entering by the clamp. The system scans the sample by splitting the source light into 16 wavelengths in the visible range of 400-700nm, using a concave mirror with a finely etched grating on the surface, which is moved through a predetermined arc. The concavity of the mirror causes the light to be refocused as a point,

and the arc of motion gives the correct wavelength at the sampling position at maximum intensity. The motion of the mirror is handled by a stepper motor – encoder system which is controlled by an internal processor.

The system scans the sample three times for the three light types described above and then averages the values and reports the percentage of reflected light at 16 wavelengths, as well as using proprietary calculations for the remainder of the data and reporting them based on industry standards of shade and color. First, the luminosity of the sample is reported as "L*." These values are scaled such that zero is black and 100 is white. Next, the concentration of red/green is reported as a value labeled "a*" between –20 and +20, where –20 is all red and +20 is all green. There is also a value, "b*," given for the concentration of yellow/blue on a –20 to +20 scale, where –20 is all yellow and +20 is all blue. For these three categories, there are three sets of data, one for each type of light. From this data, analysts in the textile industry rate a sample according to the reported dye content of a material.

2.4.2 Fabric Preparation And Orientation Distinctions

The fabric samples were environmentally conditioned via ASTM D1776 for atmosphere, humidity, and temperature. Then, the samples were grouped by color and type into three layers of thickness, with the front of the fabrics toward the scanner. No further testing was done to measure the effect of different number of layers, front or back of a sample, or ribbing orientation for the visible spectrum analysis, since these were determined not to affect the readings in the NIR analysis. The only pertinent characteristics are color and material.

2.4.3 Visible Wavelength Spectroscopy Data Analysis

The portion of the data collected by the Macbeth Spectralight system useful for this study is the percent reflectance at set wavelengths, the same as with the NIR spectroscopy data. A graph of the data can be seen in Figure 2-14. The remainder of the data is not necessary for this study, but for completeness is included in the Appendix, Tables A-3a, -3b, and -3c.

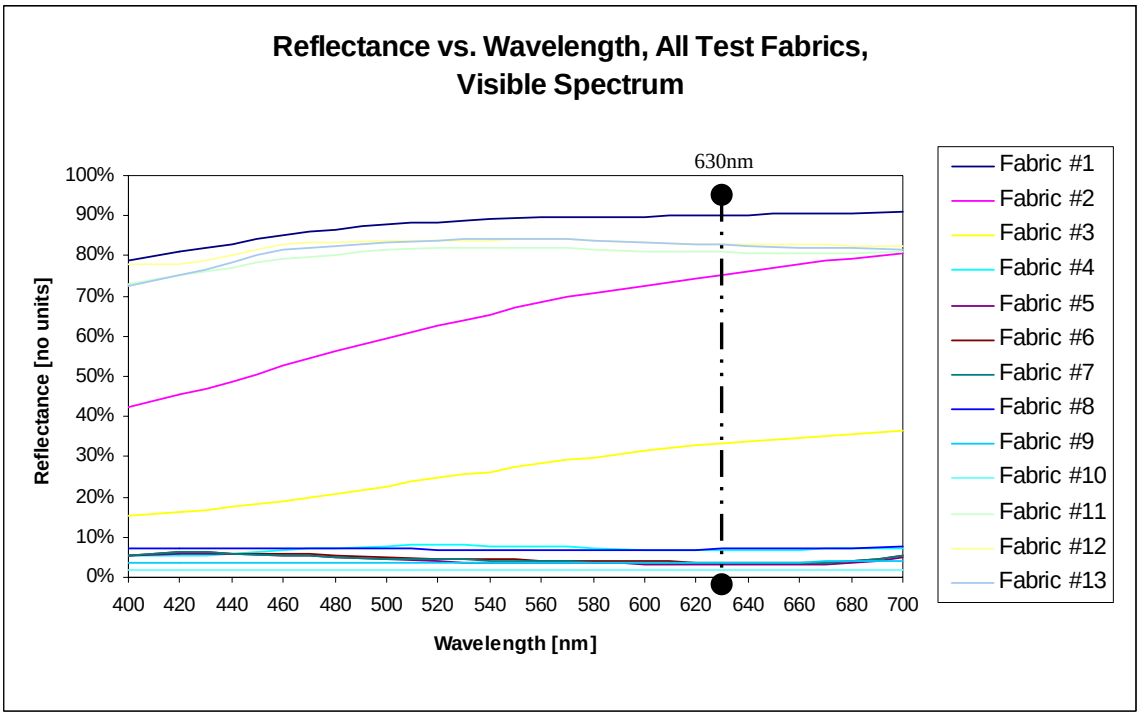

Figure 2-14 Color Comparison For Fabrics #1-13, Visible Spectrum, 400-700nm

2.4.3.1 Color Comparison Across All Test Fabrics

The graph presented in Figure 2-14 is a comparison of the percent reflectance vs. wavelength for all 13 samples in the visible wavelength range, 400-700nm. Examining this, it is observed that once again, the color of the material is the strongest factor in the

amount of light reflected. The lighter colored fabrics, #1, 11, 12, and 13 are all well above 70% across all wavelengths. This is because they are the whitest samples, and therefore should reflect all wavelengths nearly the same, as white light is merely the combination of all colors. Also of note in this graph is the grouping of the darker fabrics, #4 – 10, at less than 10% reflectance values. This is also expected due to the darker fabrics absorbing all wavelengths nearly the same, and only reflecting wavelengths close to their true color.

2.4.3.2 Color Comparison Of Test Fabrics Grouped By Color

A more demonstrative set of graphs follow in Figure 2-15. Here, the fabric samples are grouped according to color and their percent reflectance can more clearly be seen. The first graph, in the top left corner, shows the four whitest fabrics, #1, 11, 12, and 13, to be nearly identical in their percent reflectance. The only discerning factor of these materials is their physical makeup. The cotton fabric, #1, clearly reflects more light, while the three nylon fabrics, reflect nearly the same amount for all wavelengths. Most likely this is due to the denim fabric being dyed white while the nylon samples are all undyed and actually milky colored strands naturally. As more of the strands are brought together, the increased surface area reflects enough light to make the fabric appear white.

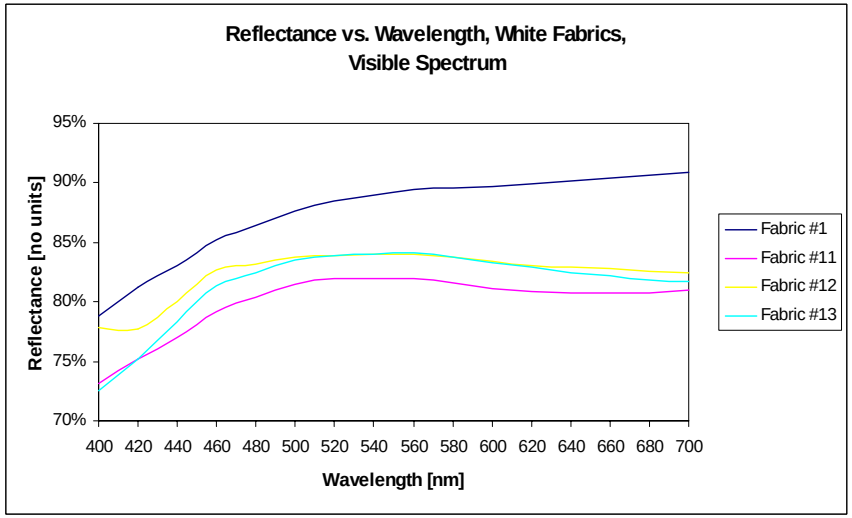

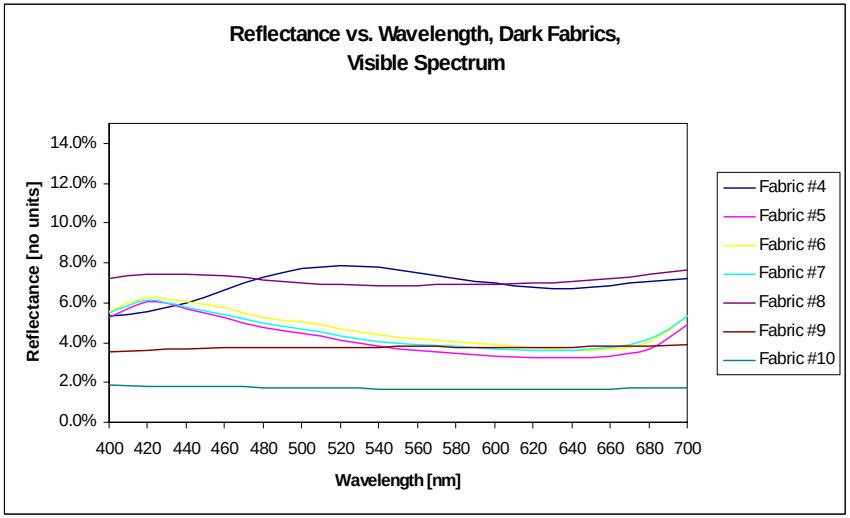

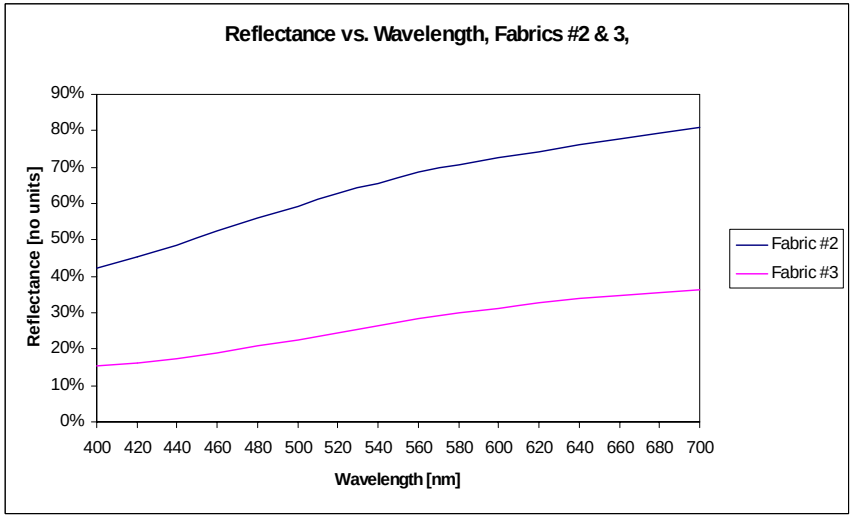

Figure 2-15 Color Comparison For Fabrics #1-13, Visible Spectrum, 400-700nm, Grouped By Color

The second graph in Figure 2-15 shows the percent reflectances for the darker fabrics, #4 – 10. Careful examination shows that the colors of the fabrics are indicated by relative maxima of their respective curve. For example, fabrics #5, 6, and 7 are blue samples, and they clearly show a peak in the 420nm range, where the accepted range for blue-violet is 390nm to 492nm. Also, fabric #4, a green fabric, has a maxima at 520nm of 7.89%. The accepted range for green is 492nm to 577nm. The three remaining samples, #8 (gray warp, white weft), #9 (black, white), and #10 (black, black) do not have an easily determined maxima, but do follow a distinct trend that with each darker color, the percentage of reflected light at all wavelengths is much less.

The remaining graph in Figure 2-15 is the final two fabrics in the sample set. Fabric #2 (tan, tan) and fabric #3 (beige, white) both could easily be described as "brown" by human standards, which is a mix of the majority of the spectrum. Thus, both show a percent reflectance somewhere between the whiter fabrics and the darker fabrics. The main difference between the two samples, is the relative darkness of the fabrics. Fabric #2 is a lighter shade of brown, while fabric #3 is darker. Thus, fabric #2 has a higher overall percent reflectance, as expected.

2.4.3.3 Comparison Of Select Visible And NIR Reflectance Data

This graph also shows a line drawn through the reflectances for all the fabrics at 630nm, which is approximately the wavelength of most helium-neon lasers on the market. The difference in the reflectance for the fabrics is extremely large, ~90%, showing that using visible light for the detector would have too much variance due to

color for usefulness. Augmenting Table 2-3 above, we can clearly see why the NIR range of light is a better selection for the study.

Table 2-4 Difference In % Reflectance For Fabrics #1-13 At Select Wavelengths

Wavelength [nm]	Average % Reflectance	Maximum % Reflectance, Test Fabric #	Minimum % Reflectance, Test Fabric #	% Reflectance Difference
630	36.60	90.13, #1	1.65, #10	88.48
1550	58.22	66.53, #12	38.53, #10	28.00
2200	55.93	62.38, #1	47.34, #13	15.04

As noted before, the NIR wavelengths have minimum reflectances above 38%, with a difference between materials and colors only 15 and 28%. In contrast the visible wavelengths have a large difference due to the color of the material, making it a poor selection for the determination of skipped stitches over a wide range of textile materials.

Also, if we add this color comparison at 630nm to the overall comparison for the NIR wavelengths of Figure 2-11, we can clearly see, as in Figure 2-16, below, that the reflectance data for the visible spectrum covers a wide range and would be unsuitable for skipped stitch detection when NIR wavelength sources are available. As an aide to the reader, lines connecting the appropriate data sets have been placed on the figure. Of important note is the visible wavelengths data ranging from as high as ~90% to a low of less than 2%, while the 1550 and 2200nm data sets stay much closer together, showing them to more suitable to use on a wide range of textile materials.

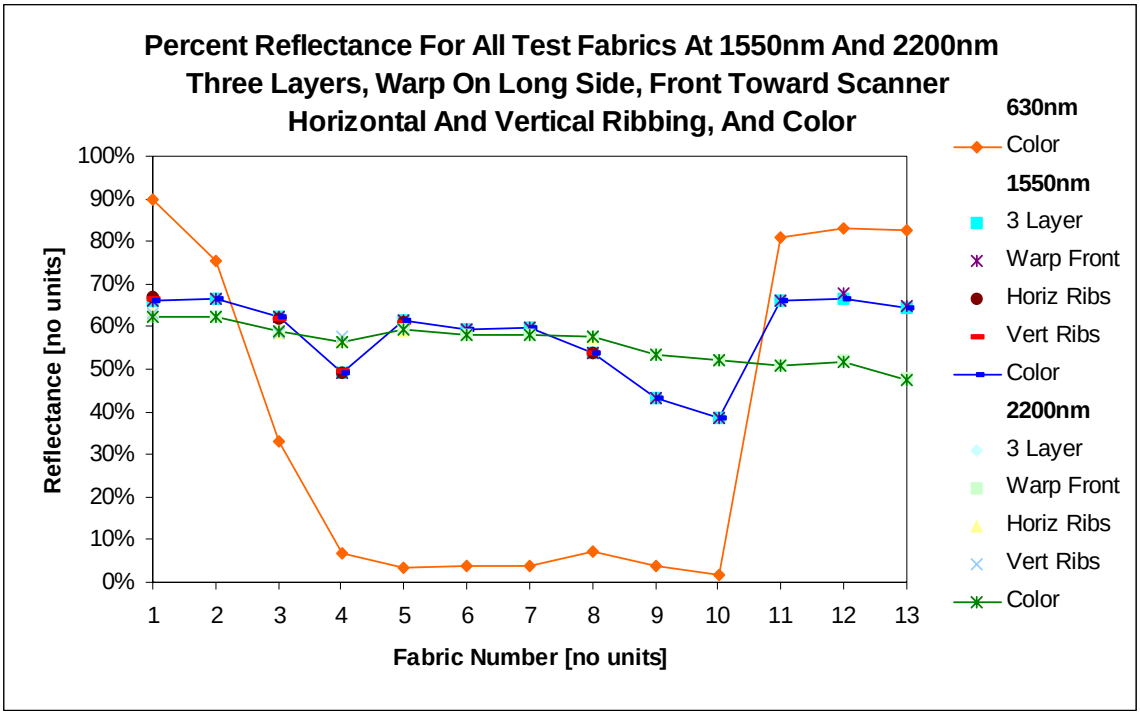

Figure 2-16 Select Wavelengths Comparison In All Categories For Fabrics #1-13, In The Visible And NIR Spectrums

2.5 Final Test Fabrics

A final set of test fabrics were chosen to aide in the repeatability of the analysis. The final six fabrics were obtained through *Test Fabrics, Inc.*, a textile industry supplier of uniform materials for use in testing. The materials *Test Fabrics* supply are made without any dyeing, treating, or special handling, unless specified by the end user. This way, anyone in the textile industry is able to obtain reliable material that eliminates variations due to manufacturing and finishing processes.

The table below outlines the material with descriptions furnished by *Test Fabrics*. There are three types of material represented, with one unifying characteristic. All of the fabrics have been bleached or left undyed to present the end user with a "pure white" material. This aides in eliminating variations due to coloring. The first material is much like Fabrics #1-10, a mercerized cotton twill, or denim. The next three are a nylon material much like Fabrics #11-13. The last two are a type of acetate material, another man-made fiber widely used in the textile industry. The main selection factor of these materials for this study are the variations in gloss or sheen of the material, as illustrated in Table 2-5.

Table 2-5 Final Test Fabric Identification Table

Fabric #	Identifying Name	Distinguishing Feature
14	White cotton twill	Lowest sheen | | | | Fabrics are ordered in increasing glossiness or sheen according to visual inspection. | | | | Highest sheen
15	Spun nylon 6.6, Dupont type 200 woven	
16	Filament nylon 6, tricot bright	
17	Filament nylon 6.6, semi-dull taffeta, scoured, heat set	
18	Acetate satin, bright filament yarn	
19	Acetate tricot, all delustered filament	

A more complete manufacturer's description can be found in the Appendix, Table A-1.

2.5.1 Common Usage Of Final Test Fabrics

The wide usage of these materials in the textile industry makes them desirable test fabrics as they span a variety of implementations. Fabrics such as #14, the denim, is mainly used in producing heavy garments meant to withstand more day to day abuse. Fabrics #15-17 are used in garment manufacturing, airbag material, and furniture coverings. Though not expected to withstand as much abuse as the denim, they are cheaper to produce, and are useful as material in rain gear and other waterproof/water resistant items. The last two fabrics, #18 and #19 are a very fine yarn material giving them a pleasing feel. They are used as support material in women's gowns (for example, crinoline slips in bridal gowns), and ribbon material for decoration and furnishings.

2.5.2 Physical Parameters Of Final Test Fabrics

The final test fabrics were further characterized by determining several physical parameters, as the first thirteen fabrics were, using several ASTM standards. The physical quantities measured were fabric weight, ASTM D3776; average yarn count, ASTM D3775; average yarn crimp ratio and average yarn take-up ratio, ASTM D3883; and the average diameter of the threads that make up the fabric, ASTM D204. The materials were also environmental conditioned for atmosphere, humidity, and temperature per ASTM D1776. The tabulated results for these measurements can be found in the Appendix, Table A-4.

2.5.3 NIR Wavelength Spectrophotometric Analysis Of Final Test Fabrics

The final test fabrics were also tested using the NIRSystems NIR Spectrophotometer to determine their percent reflectance in the NIR wavelength range. They were not tested using the Macbeth Spectralight system for the percent reflectance in the visible wavelength range as the study has already shown that using the visible spectrum becomes very complicated due to the affect of dye color in that wavelength range. The characteristic of interest here is the difference in reflectance caused by the fabrics differing levels of sheen or gloss.

Also, as was determined with the first set of test fabrics, the number of layers and ribbing orientation were not tested since the effects are minimal if detectable at all. However, these six fabrics do have a noticeable differentiation to the human eye in sheen from front to back of the samples. For completeness, three of the samples, the denim,

one nylon, and one acetate, were then tested to compare the effect of sheen contrast between front and back of a fabric on the percent reflectance in the intended wavelength range. Then a final comparison of all six fabrics was made to show their percent reflectance at the two chosen wavelengths of common availability of laser diodes.

The graphs in Figure 2-17 show the comparison of front to back of the three fabrics, #14, 16, and 18. We can see from these three graphs that there is very little difference in the front and back reflectance values. This is somewhat expected, as the long wavelengths in the NIR spectrum tend to be affected less by the natural sheen of materials than by the physical makeup of the materials themselves.

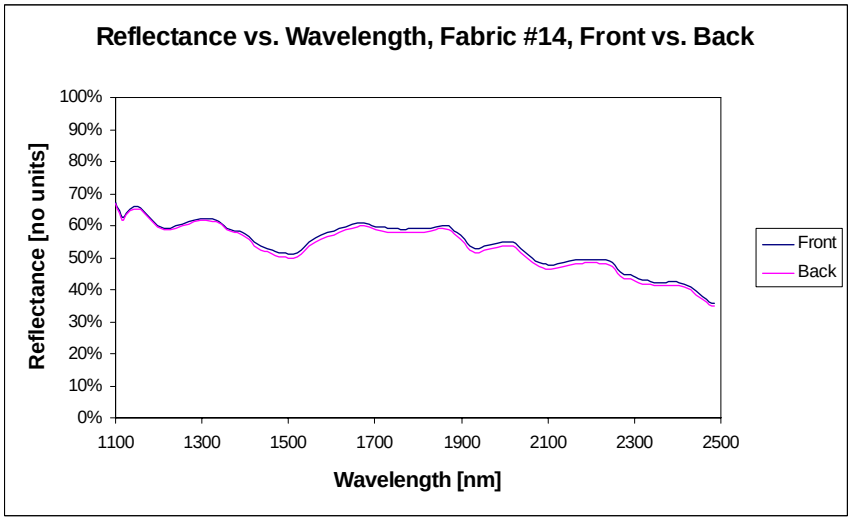

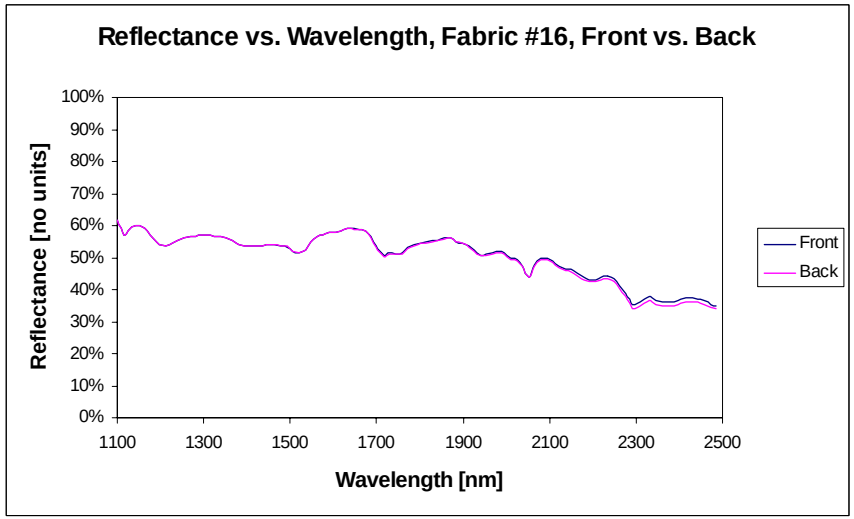

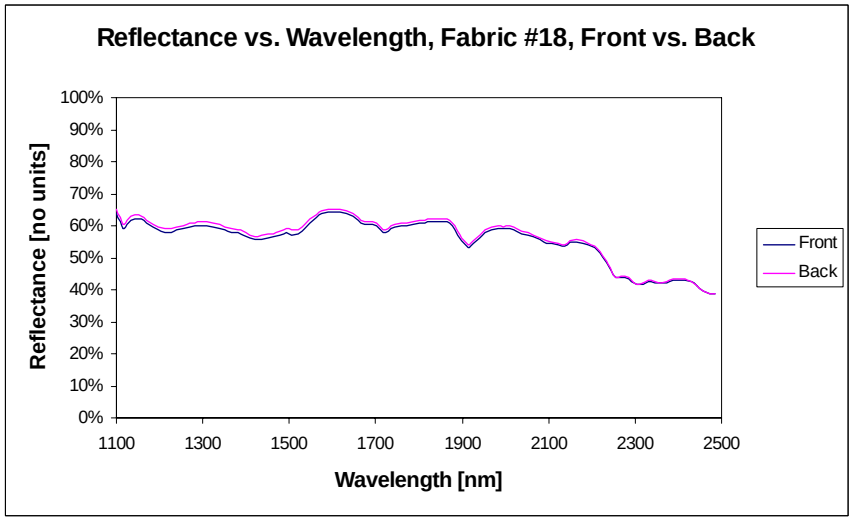

Figure 2-17 Comparison Of Front vs. Back For Fabrics #14, 16, And 18, NIR Spectrum, 1100-2500nm

The comparison of all six of the final test fabrics in Figure 2-18, below, brings no surprising results, either. This graph shows that all six of the test fabrics have similar reflectance levels at all wavelengths in the NIR spectrum. Again, this is expected as the NIR spectrum is minimally affected by the sheen of materials, and the materials all have a similar color, which was determined to be the main contributing factor to reflectance differences.

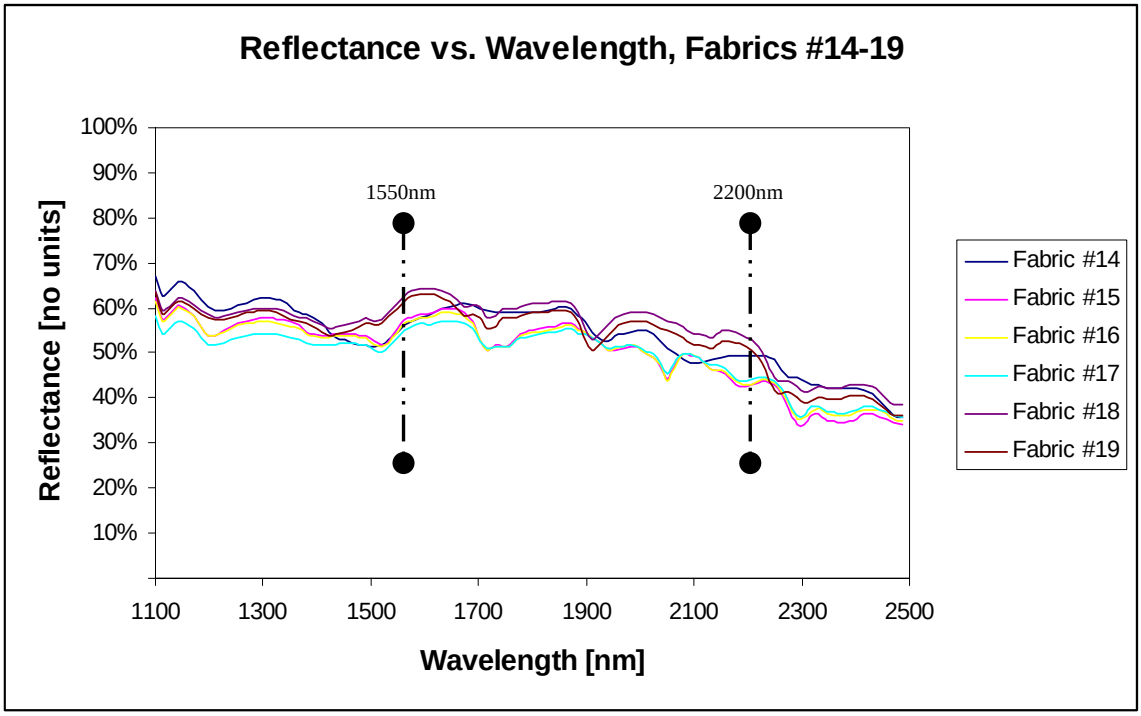

Figure 2-18 Reflectance Comparison For Fabrics #14-19,

NIR Spectrum, 1100-2500nm

Specifically for the two wavelengths selected for closer study, 1550 and 2200nm, the fabrics have a mean reflectance of 57% and 47%, respectively. Of interest also is the minimum reflectance values at the selected wavelengths. Both wavelengths show a

reflectance of greater than 40% for all fabrics, with the 1550nm wavelength having greater than 53%. This is advantageous to the study because it means that more light will be reflected off the surface of the material, carrying more information to the detector. Details of the reflectance values for these six fabrics is found in the table below.

Table 2-6 Difference In % Reflectance For Fabrics #14-19 At 1550nm And 2200nm

Wavelength [nm]	Average % Reflectance	Maximum % Reflectance, Test Fabric #	Minimum % Reflectance, Test Fabric #	% Reflectance Difference
1550	56.56	61.01, #18	53.57, #17	7.439
2200	47.35	53.50, #18	42.76, #15	10.73

Thus, the conclusion to obtain a light source in the 1550nm range of §2.3.3.5 is strengthened as it has now been shown that the reflectance off of material at that wavelength has minimal differences due to material, weave, ribbing, front or back, and now, sheen. The main variation is caused by color, but even that characteristic does not hamper the reflection of ample amounts of light to base quantitative decisions upon, such as pass/fail levels.

3. Equipment Selection And Device Arrangement

The selection of the equipment for this study required consideration of several factors. The system would need to use a light based system in the near infrared range, determined via the data collected and analyzed in Chapter 2; be powerful enough to detect over a short distance using a wavelength matched detection device, yet not dangerous to the human eye; be compact in packaging so as to be able to be added directly to a sewing machine on the factory floor, and thus less prone to contamination by dust and debris; and, be inexpensive to make it a viable option for quality control.

To this end, the following table was created to aid in the selection of the equipment. The table is arranged in order of importance to the study.

Table 3-1 Determining Factors In Equipment Selection

Factor	Qualifier
Wavelength	1550nm
Source	Laser diode
Detector	Photodiode, wavelength matched to source
Required optics	Enclosed to reduce chance of dust contamination
Required electronics	Enclosed or minimal
Packaging	As small as possible

As stated before, the NIR spectrum is very popular in the telecommunications industry because of the wavelengths high reflectivity in the optical media used there. Thus, searching the industry sources for equipment as outlined in the table above proved fruitful in short time.

3.1 Laser Diode Assembly Selection

The laser diode selected for this study was a class III InGaAsP laser, enclosed in a tube with the circuitry, apertures and lenses included. This laser diode offers a maximum output of 20mW at the peak wavelength. To control the output power, a potentiometer is set by the factory limiting it to make it safer to use around human eyes and to reduce the chance of the laser diode burning out. The laser assembly purchased for this study was set for 8.2mW at a peak wavelength of 1532nm. The aperture and lens assembly were chosen to minimize the spot size, and packaged in a small tube measuring ½" in diameter and 2" long.

3.1.1 Optics In The Laser Diode Assembly And Resulting Spot Size

To obtain the smallest possible spot size using this type of assembly, the manufacturer includes apertures and lenses to produce a "quasi-collimated" light source. The quasi-collimated lens assembly is a four element arrangement, which includes two apertures to collimate the light, and two lenses to focus the light to a known distance. The two apertures are 28° fan types turned orthogonal to one another to produce an elliptical beam. According to the specification documents for the laser diode assembly, the focal distance of the assembly is 3 inches. At this distance, the spot size was measured by the manufacturer to be 1.244mm by 0.1408mm, along the long and short axes of the ellipse, respectively.

However, initial testing of the laser diode and photodiode arrangement showed that the spot size was actually much larger. Measurements of the edges of the spot using a simple NIR photoluminescence card showed the spot size to be approximately 10mm

by 4mm, at the 3” focal length. These dimensions are actually more than the real dimensions of the spot size due to the rudimentary nature of the measurements. The photoluminescent card was moved toward each of the outside edges in turn, marked and measured. But, only when the card had received enough incident radiation did it begin to fluoresce detectably to the human eye. In reality the beam has a Gaussian shape to it, which, when measuring it in this method, makes the beam look larger than it really is due to the natural threshold of the receptive quality of the eye. A Gaussian curve is exponential as it falls off, as seen in Figure 3-1, below, while the human eye receives light intensity on a logarithmic scale. Devices used to measure the spot size more precisely calculate the size based on full width at half maximum evaluations. Measuring the spot size with the human eye, one can only mark the edges of the spot based on the intensity of light which rises above the threshold. Thus as the figure shows, the spot size according to the manual measurements made for this study are larger than the FWHM measurements made by the company.

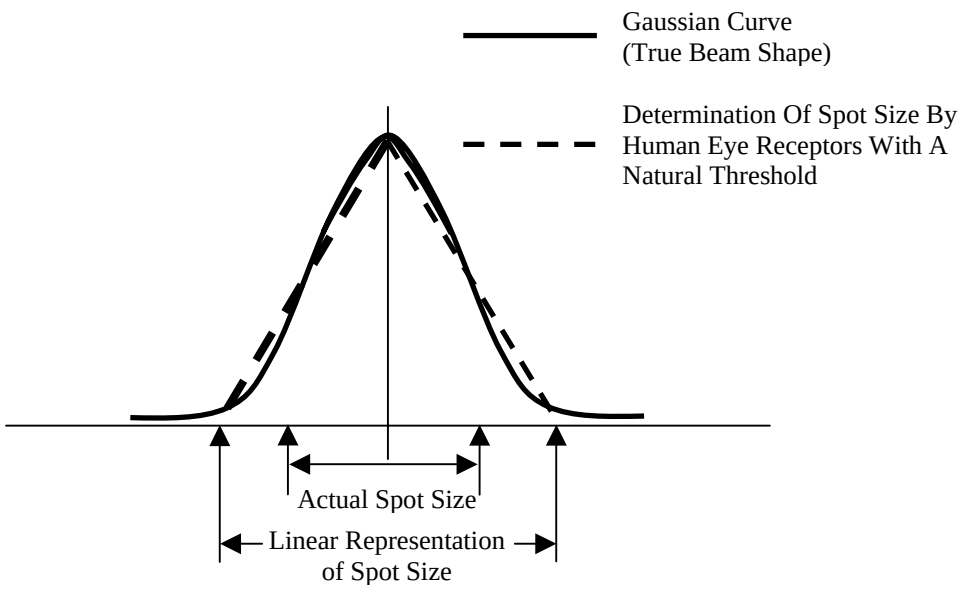

Figure 3-1 Gaussian Curve With Linear Line Overlay Showing Human Eye Interpretation Of Spot Size vs. Actual Spot Size (Not To Scale)

This determination of the actual spot size plays an important part in determining the type of stitch used in this study. Due to the size of the spot, a normal stitch was not able to be used as the stitches generally range from two to three millimeters in length. For the spot size determined for the laser diode assembly used in this study, these stitches are too small to detect separate stitches as it would cover several stitches at a time. The selection of the stitch type is discussed later in Chapter 4. For now, suffice it to say that the stitch type used for the initial testing was one known as a “basting” stitch. This type of stitch is commonly used to hold pieces together so that they may be easily handled while being sewn using a sewing machine. The basting stitch which was used for this study was a ½” basting stitch, which means that a single thread passed from front to back

of a piece of fabric through holes ½" apart. Thus, the stitch was ½" long, with ½" gaps between.

3.2 Photodiode And Filter Selection

The photodiode with the best excitation wavelength match to the laser diode's output is from the Germanium family, which are semiconductors making use of the photovoltaic effect in which a current is generated upon the application of infrared energy. They are classified as quantum, intrinsic type detectors as the detection is determined by the inherent energy gap between layers. These detectors are widely used because of their high responsivity, fast response, and room temperature (25°C) operation. Beyond material used, the sensing area is the main cost contributor to these devices. For this study, in which there was an expected scattering of light, a relatively large sensing area was chosen of a 5mm diameter circle, or a 19.6mm^2 total area. This amount of sensing area was evaluated to be large enough to collect a widely scattered signal at a close distance with sufficient levels to be able to detect changes in received light. The distance being approximately 3 inches, the same as the focal length of the laser diode assembly.

3.2.1 Interference Filter Selection

To aid in the response of the photodiode to the wavelength chosen for this study, a 1550nm interference filter was chosen to block all other wavelengths of incoming light. This allows the use of the device in a normally lit laboratory, limiting interference by light sources other than the laser diode. The Germanium photodiode has a spectral

response of 800 to 1800nm. There are many sources of light produced in this range, fluorescent lighting, sunlight through windows, etc., which would cause a great amount of noise in the signal detected by the photodiode. By choosing a filter with a bandwidth of 10.5nm full width at half maximum, it is possible to block out most light outside of a desirable 1545-1555nm range.

3.2.2 Electronics For The Photodiode Circuit

The circuitry involved with arranging the photodiode is a simple current-to-voltage converter and small gain circuit. A schematic of the circuit can be seen in Figure 3-2. The laser diode only needs a supply of +5 Volts DC, so no schematic is given. The same +5VDC supply was used to power the operational amplifier seen in the figure.

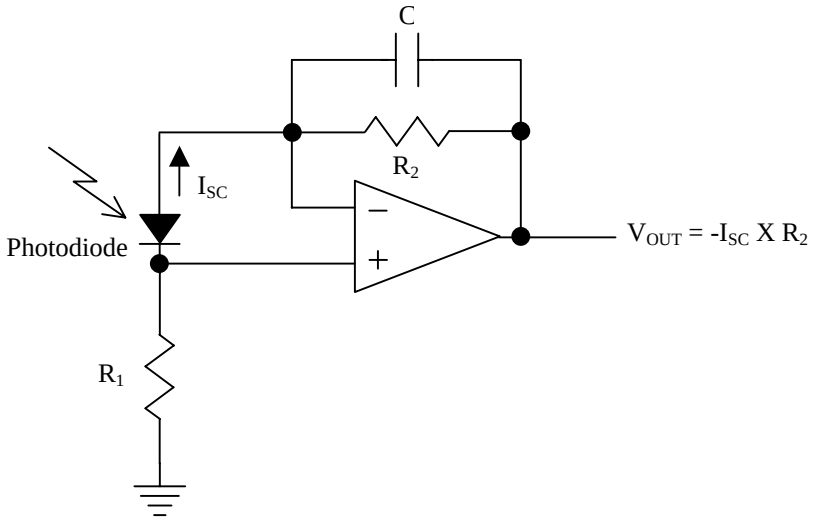

Figure 3-2 Schematic Diagram Of Photodiode Circuit

Here, the resistor R_1 acts to filter out noise from the circuit by a method known as floating the front end. Initially, the cathode of the photodiode was merely grounded, but

examination of the data revealed noise from the ground side of the circuit which comes from other circuits connected to the same ground. Adding in the resistor cuts down on this noise by giving the cathode a more defined reference to ground. The capacitor, C, and resistor, R_2, act as a low pass filter and limit the rise time of the circuit. This eliminates "ringing" in the circuit and increases the output signal from a low input signal. The voltage measured at V_{OUT} is therefore directly proportional to the intensity of light received by the photodiode and may be calculated from:

$$V_{OUT} = -I_{SC} \times R_2 \qquad \textbf{Eq. 3-1}$$

Where: V_{OUT} = Output voltage

I_{SC} = Current produced by shorting the photodiode output

3.3 Data Collection

A PC based computer was used to collect the data using a National Instruments data acquisition card through a standard analog input. The controlling software used was another National Instruments product, LabVIEW, which stands for Laboratory Virtual Instrument Electronics Workbench. The software controlled the data acquisition card and collected the data, which it wrote to a file, as well as producing a live graph on the display monitor. The data collected were in a tab delimited text format which was then examined and graphed using a spreadsheet program.

3.4 Test Apparatus Assembly

In a final application, this test system would ideally be mounted onto the sewing machine to monitor the sewing of a seam as it progresses. This would enable the system to alert the operator immediately of skipped stitches, allowing the operator to remove the material, remove the faulty stitch line, and re-sew the material with minimal loss of time and effort. However, for the test unit, it was determined that the best physical set up would be to create a table top model of the sewing process. This was done to allow control over the speed of motion, type of stitch examined, and eliminate the natural vibration of the running sewing machine. Later study can mount the device onto an actual production machine and begin to examine the effects of vibrational motion on the test device.

3.4.1 Table Top Version Assembly

The table top version of the test system, hereafter referred to as the "test system," included the optics, electronics and mounting brackets of the test system attached to a linear slide table which could be manipulated back and forth, imitating the motion of the fabric past the test systems' sensing area. Two pictures of the test system in its final configuration can be seen in Figure 3-3 and 3-4, below.

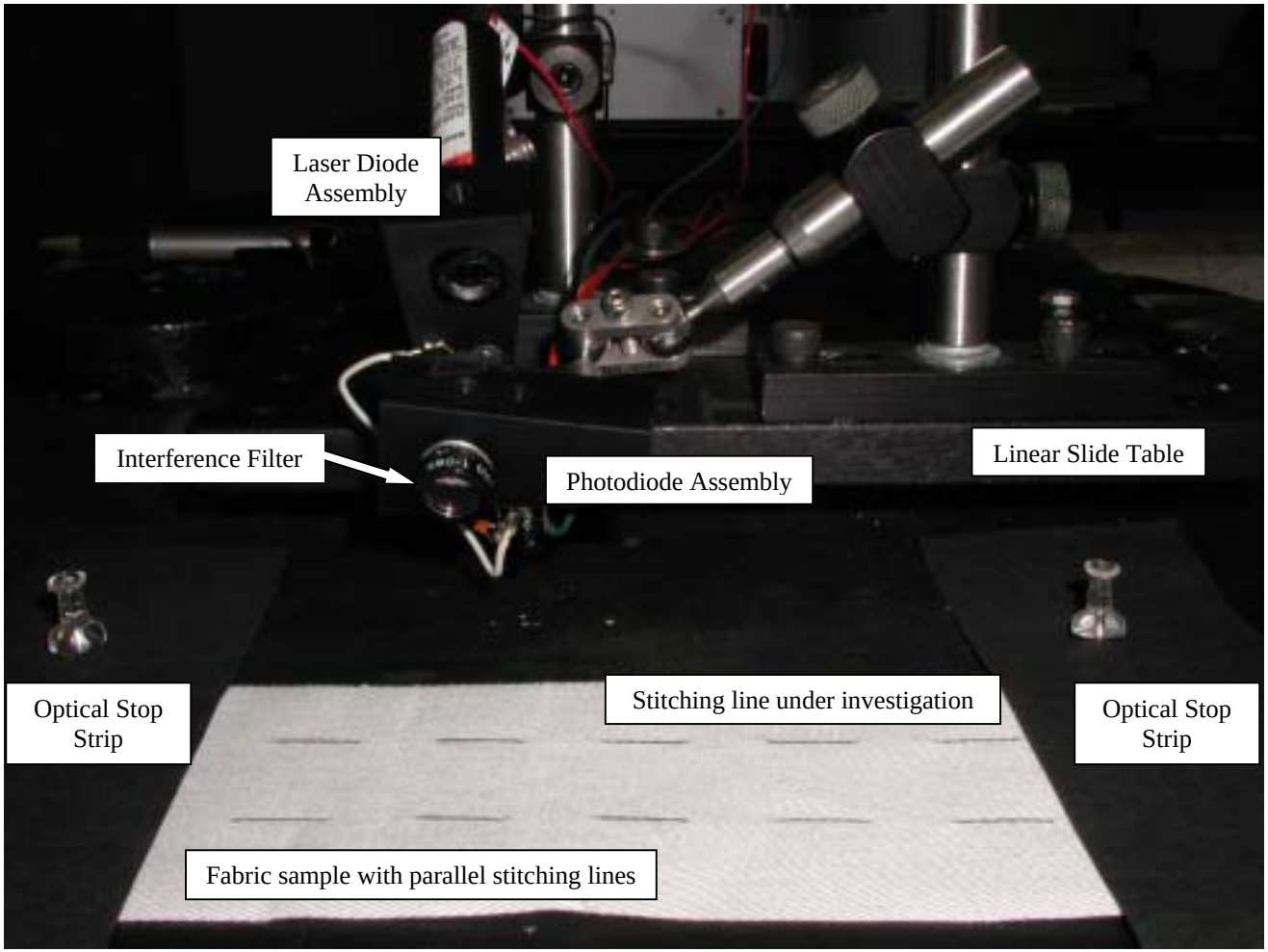

Figure 3-3 Test System Assembly, Front View

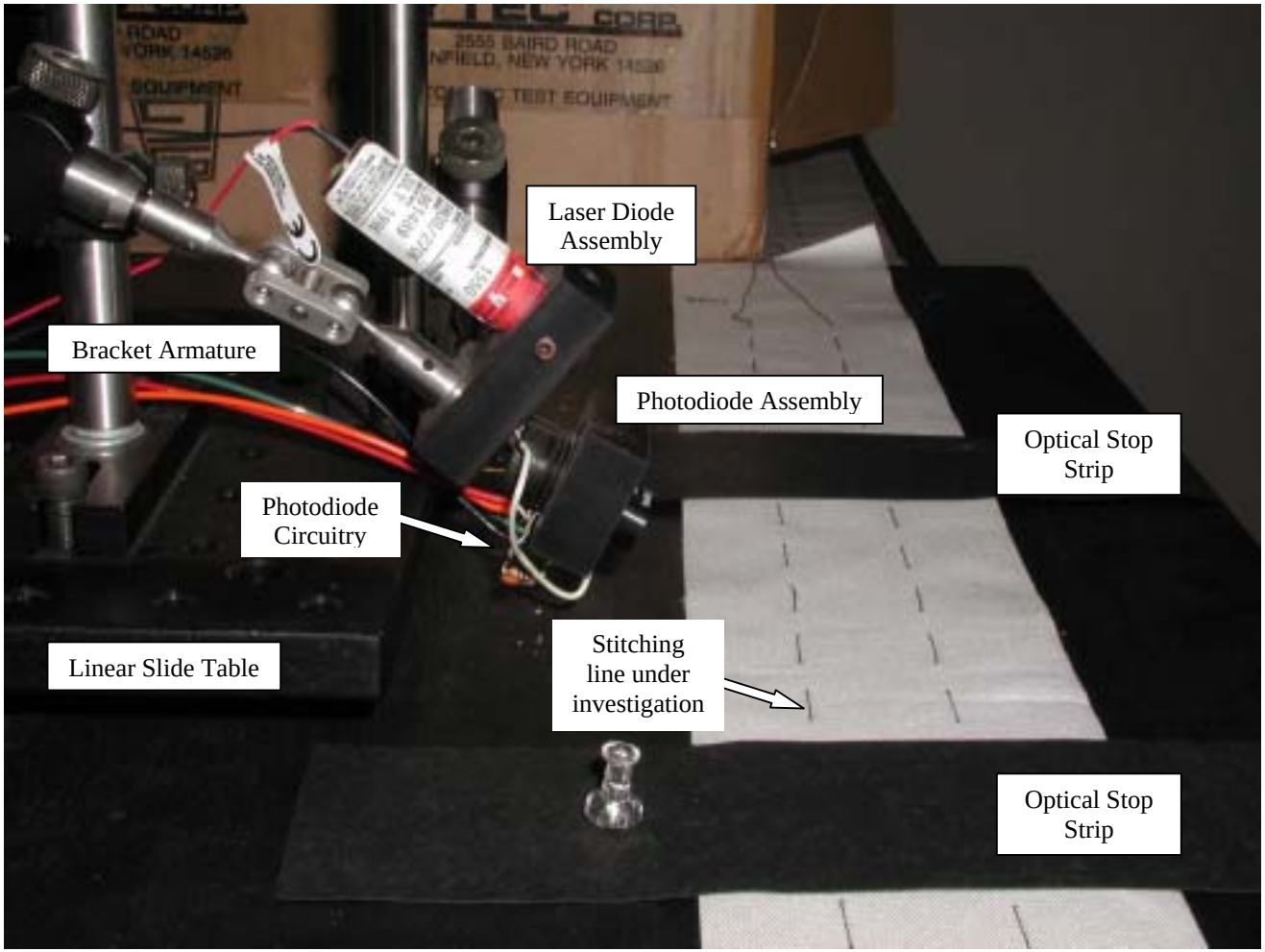

Figure 3-4 Test System Assembly, Side View

These pictures show the laser diode and photodiode as well as the mounting brackets used to orient them in relation to the measured stitch line, the closest stitch line to the assembly. The linear slide table which was used to simulate the motion of the fabric past the sensing area can be seen as the optical breadboard upon which the laser and photodiodes are mounted. The electronics for the test system are located on the back of the photodiode bracket. The +5V DC power supply for the components is out of the picture.

The fabric was placed using a removable template to ensure that the stitch line was parallel to the travel of the sensing area. The two black strips of paper pinned to the board serve as optical stops for the data collection as they make a sharp contrast in reflected intensity between the fabric surface and the paper surface. These photographs also show that five stitches were visible in the viewing area, allowing a way to clarify the data when represented graphically.

Special brackets to hold the laser diode and photodiode were machined from non-conductive Delrin material to isolate the components electronically. In the pictures, these brackets are the black blocks which the mounting posts use to hold the laser diode assembly and photodiode in place. Drawings for the brackets can be found in the Appendix, Figures A-19 and A-20.

3.4.2 Determining The Orientation Of The Components

In these photographs it is pertinent to note the orientation of the laser diode and photodiode in relation to the stitch line. The orientation of the laser diode was decided upon using geometric optics arguments with the information provided in Chapter 2. The

orientation of the photodiode was determined through extensive testing of various angles of the photodiode to determine the positions which yielded the greatest difference in light intensities between times when the laser diode was focused on a stitch and when it was focused on a space between stitches. Testing was done by setting the laser diode at an approximate 45° angle to the table surface at a distance of 3 inches from the stitch line and then moving the photodiode through a rough quarter sphere around the laser diode assembly. Limitations of the mounting assembly and an assumption of symmetry allowed the mapping to only one side of the laser diode assembly.

3.4.2.1 Orientation Of The Laser Diode Assembly

As noted in Chapter 2, the surface of the fabric and the threads cause a specular, or diffuse, reflection of the light impinging upon them. This conclusion leads to a geometric or ray optics analysis of the placement of the laser diode such as to optimize the amount of light hitting the stitch and collected by the photodiode. To begin the considerations for the arrangement, a few basic placement definitions had to be established. The two most easily recognized points to base positions from were the fabric surface, a flat plane from which "vertical" can be established as the normal to the surface, and the stitch line, which "horizontal" can be established as normal to this line in the plane of the fabric surface. Using these lines as bases for arrangement the laser diode face was then pictorially positioned such that it would be 3 inches, it's focal length, from a spot on the stitch line and moved through positions at three angles off the vertical and horizontal lines. These drawings can be seen in Figure 3-5 a through f, below. It should be noted that these drawings are not to scale, and drawn as an exercise for the argument.

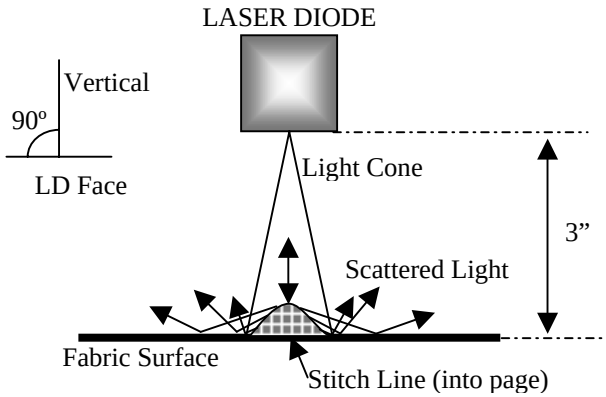

Figure 3-5a

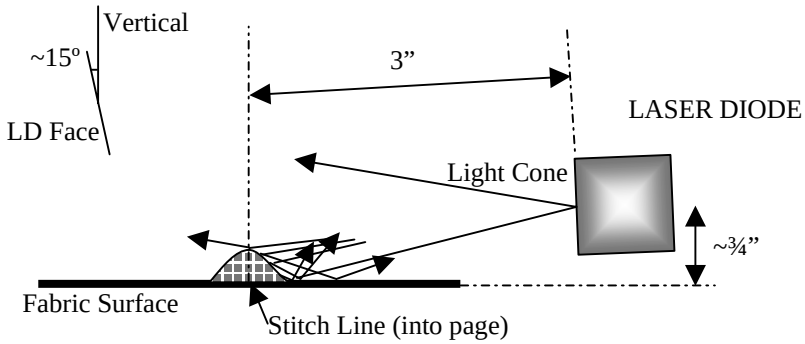

Figure 3-5b

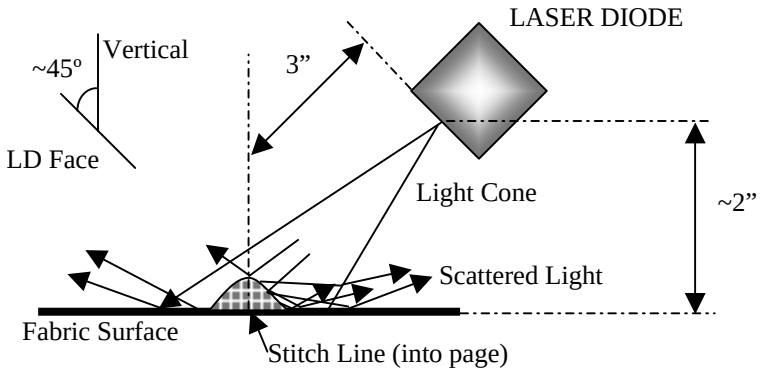

Figure 3-5c

Figure 3-5a-c Vertical Arrangement Of Laser Diode Using Geometric Optics

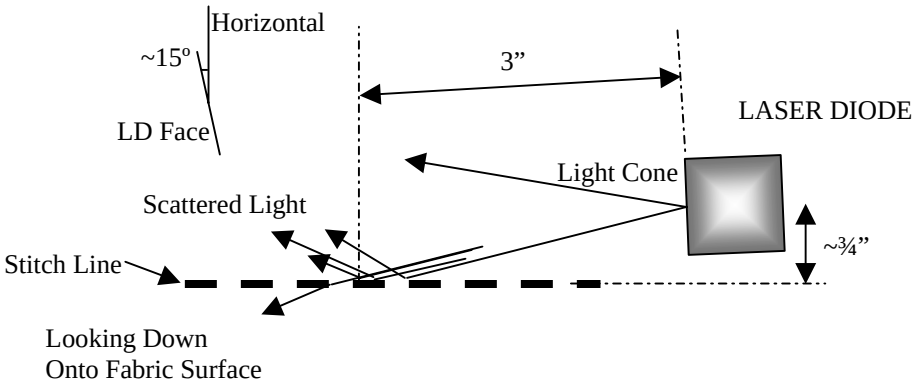

Figure 3-5d

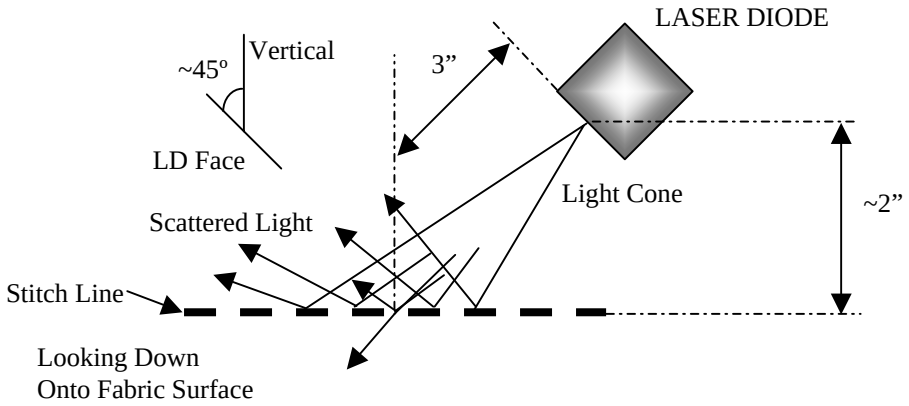

Figure 3-5e

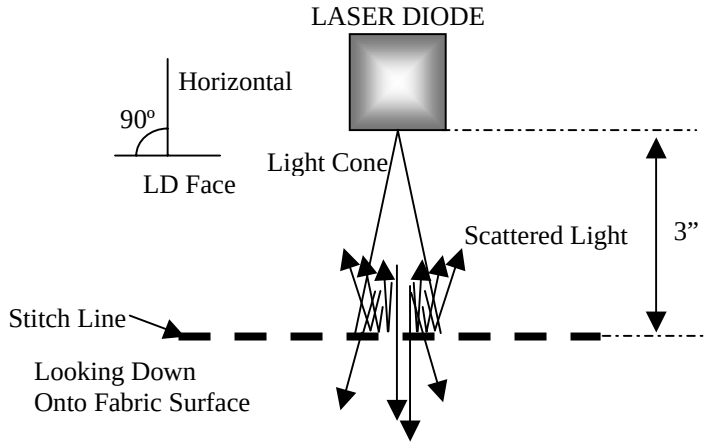

Figure 3-5f

Figure 3-5d-f Horizontal Arrangement Of Laser Diode Using Geometric Optics

These drawings show possible orientations of the face of the laser diode around the stitch line. The first three drawings show the laser diode face oriented around the vertical line defined as the normal to the surface of the fabric. Here, the fabric surface is a perpendicular plane to the page, and the stitch line is into the page. The first drawing shows the laser diode face turned at 90º to the vertical. The laser diode face is directly over the stitch line and fabric surface. The arrowhead lines show the paths of rays of light impinging on the surface and diffusely reflecting off the surfaces. As can be seen in this drawing, the wide dispersal of the rays does not point to a particularly beneficial placement of the laser diode and photodiode assemblies such as to maximize the signal received at the photodiode.

The second drawing, Figure 3-5b shows the laser diode face oriented at approximately 15º off the vertical. Recall from §3.4.1 that the laser diode and photodiode assemblies are held by machined brackets made to position the centers of their faces in the middle of the 1" wide block. This block keeps the laser diode assembly from being any closer to the surface of the fabric than ¾ of an inch. Recalling the trigonometric formula for the sine of an angle:

$$\sin\theta = \frac{opposite}{hypotenuse} \qquad \textbf{Eq. 3-2}$$

Where: *opposite* = ¾"

hypotenuse = 3"

Taking the inverse sine of the fraction yields an angle of ~15º. This drawing shows that the majority of the light cone would go over the top of the stitch and either miss the fabric entirely or strike behind the stitch and be reflected off into the distance. Only the small angle of light that hits in front of the stitch and directly onto the stitch would be reflected

in such a way as to get any information from it. Thus, this angle for the laser diode would not be ideal.

The third drawing in the series splits the difference of the first two and places the laser diode face at a 45º angle off the vertical. As can be seen here, with the center of the laser diode face pointed at the center and bottom of the stitch line, the majority of the light cone hits the stitch or the fabric surface directly in front of it to then be reflected off of the stitch itself. The portion of the cone that hits the top of the stitch or the fabric behind the stitch would be reflected off into the distance. The portion that is reflected back would be mainly concentrated into an area below the laser diode assembly. This gives an area that the photodiode assembly could easily be placed in and has the added benefit of using the laser diode assembly body to block some of the stray NIR light.

The second set of figures, Figures 3-5d through f, show a similar arrangement of the laser diode assembly for the horizontal, or normal to the stitch line, consideration. Here, the stitch line is seen as the dashed line and the fabric surface is a plane parallel to the paper. Also, the light dashed line represents the horizontal line the angle estimates were made from, as the normal to the stitch line at the center of the spot formed by the light cone. From the previous considerations, the laser diode assembly is assumed to be at approximately 45º off of the vertical. Also, as before the laser diode face is presumed to be held at the 3” focal length from the stitch line.

First, Figure 3-5d shows the laser diode face at an approximate angle of 15º again. Here, the rays are hitting the stitch line and diffusely reflecting off to the left or going between the stitches and hitting the fabric on the far side and reflecting off into the distance. This arrangement leads to no beneficial orientation of the laser diode and

photodiode assemblies such as to maximize the signal, as stated before for this angle off the vertical. Similarly, Figure 3-5e shows no easily determined benefit of orienting the laser diode face at 45º off of the horizontal. The majority of the light would be diffusely reflected off to the left and not concentrated at any point.

The final drawing, Figure 3-5f, however, shows the laser diode face oriented 90º off of horizontal, or, parallel to the stitch line. This orientation shows the majority of the rays would be reflect back towards the laser diode assembly. Combining this with the decision to place the laser diode at 45º off of vertical gives the position of the laser diode such that the photodiode assembly could be placed under the laser diode assembly, possibly shadowing it from windows or overhead lights emitting NIR light. Thus, the laser diode assembly was placed at a 45º angle off the vertical and 90º off the horizontal to the stitch line. This orientation, again using the trigonometric equations for sine and cosine in a triangle, puts the laser diode assembly at approximately 2.12" both back from the stitch line and off of the surface of the fabric, turned such that the face is at a 45º angle off of vertical, parallel to the stitch line, and at the 3" focal length of the laser diode module. This orientation of the laser diode assembly can be seen in the two digital images of the test system, in Figures 3-3 and 3-4.

3.4.2.2 Orientation Of The Photodiode Assembly

To map out the positions the photodiode would be placed in, the stitch line under investigation was used as the horizontal line off of which to base angular measurements. The incident spot, or, where the laser hit the fabric on the stitch line, was used as the point to make all measurements from the stitch line. At distances of 0.5 inches to 2.0

inches, in 0.5 inch increments, and at angles of +90, 60, 45, 30, and 0 degrees off the stitch line in both the X-Y and X-Z planes, measurements were made with the photodiodes' face perpendicular to the fabric surface, or 0° off of vertical. The bracket holding the photodiode kept the photodiode from being completely at the fabric level, maintaining a minimum distance of ½" from the surface to the center of the photodiode face. To change the angle of the face of the photodiode off of vertical, the photodiode was moved such that its' face was turned while keeping it at the distances stated above from the laser spot, as seen in Figure 3-6.

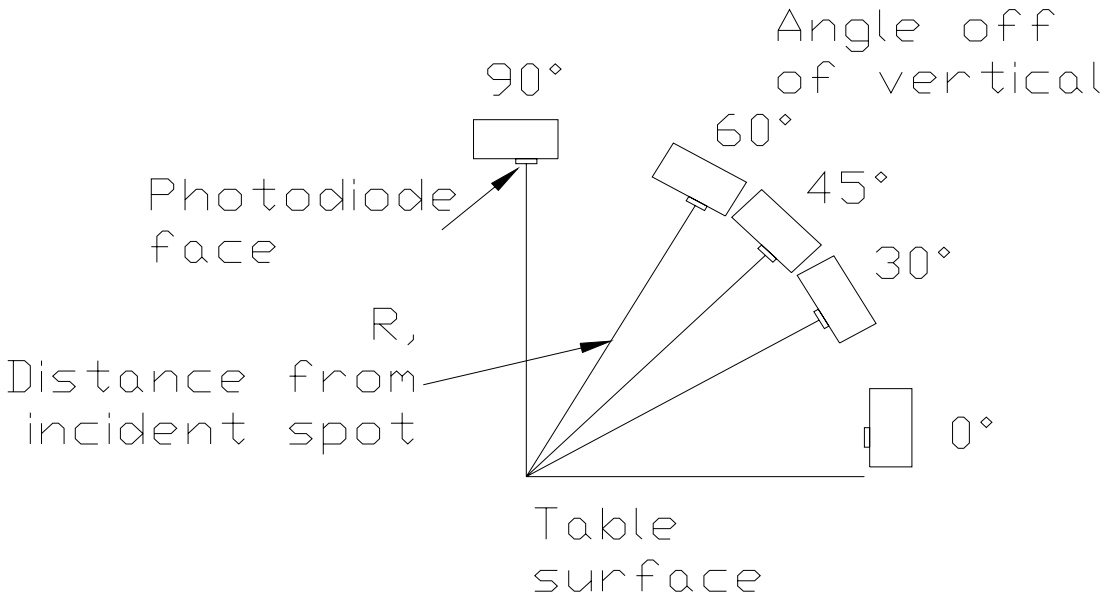

Figure 3-6 Orientation Of Photodiode For Position Determination

To establish the reflected intensity of the laser diode incident upon the photodiode, the two were aligned in a straight on arrangement. This produced a saturation voltage of 9.997 volts. This voltage limit turned out to rather be an input limit of the data acquisition board, ±10V. Measurement with a voltmeter with a much higher

input limit showed the maximum voltage created by the saturation limit of the photodiode to be 17.46 volts. Considerations were made to create a voltage divider which would bring this saturation voltage to within the limitations of the DAQ card, but it was determined from further measurements that any change in the voltage at this level would make variations expected to be seen as skipped stitches indistinguishable. Addition of a gain circuit was likewise considered and rejected due to subsequent testing which showed this also enhanced the noise levels in the signal. Thus, no voltage divider or gain circuit was added to the system. The reflected intensities recorded at the numerous positions were then compared to this maximum intensity.

Nearly all of the positions in front of the stitch line, or the side away from the laser diode assembly, such that the photodiode was facing the laser diode assembly produced the saturation limit of the photodiode. Thus, measurements made in front of the stitch line were abandoned and effort was concentrated on mapping behind the stitch line, or measuring the light reflected back toward the laser diode assembly. This mapping created a wedge shape around the incident spot, behind the stitch line, as seen in Figure 3-7. The orientation of the photodiode face is easily described in spherical coordinates, R, Θ, and Φ, where:

R = the distance of the photodiode face from the incident spot;

Θ = the polar angle, or, the angle off the Z axis; and,

Φ = the azimuthal angle, about the Z axis, projected into the XY plane

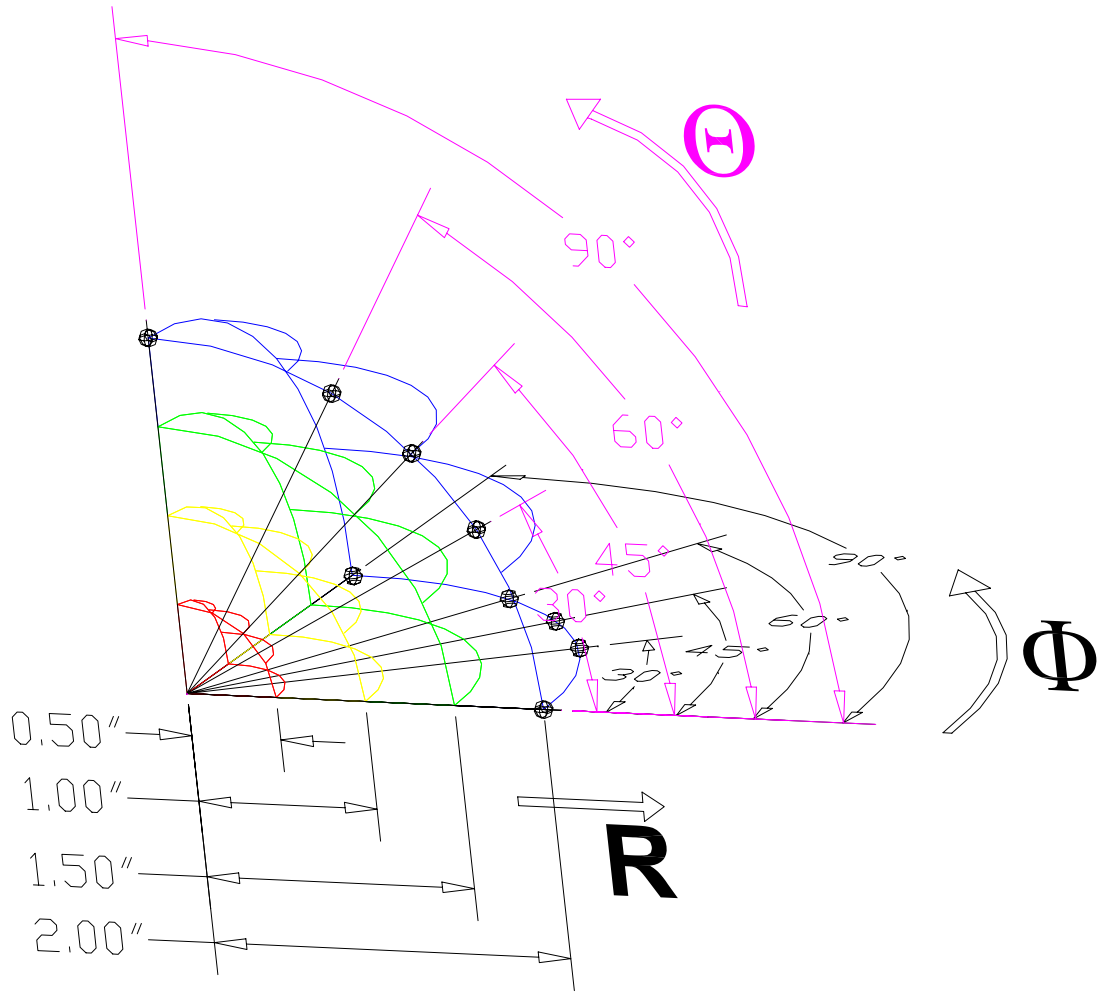

Figure 3-7 Map Of Wedge Around Laser Incident Spot For Intensity Mapping

At several of the positions behind the stitch line, the bracket holding the photodiode or the armatures attached to it blocked all or a portion of the incident beam. The arcs produced by the 0.5 and 1.0 inch distances, where not blocked by the photodiode bracket, produced the saturation voltage, eliminating them from further study. The positions that were able to produce a reading were marked and recorded using a system to show the distance from the incident spot, and the angles at which the photodiode was placed. As the photodiode was moved into position, the assembly was moved back and forth along the stitch line using the linear slide table for a total of six readings which were averaged to determine the maximum and minimum voltage levels. These levels were then used in conjunction with a qualitative discernability judgement to determine the best location for the photodiode such that the system would be able to determine the presence of skipped stitches. The results of this evaluation were tabulated and a selection can be seen in Table 3-2, or the full table can be seen in the Appendix, Table A-5.

Table 3-2 Discernability Of Voltage Variation Caused By Stitches For Photodiode Angle Tests

Position ΦR.Θ	Minimum Voltage [Volts]	Maximum Voltage [Volts]	Difference [Volts]	Discernability
11.000	maxed out			
11.030	maxed out			
11.045	maxed out			
11.060	maxed out			
11.090	maxed out			
14.000	1.50	1.00	0.50	not at all
14.030	1.50	1.00	0.50	not at all
14.090	1.75	1.50	0.25	not at all
21.000	maxed out			
21.030	maxed out			
21.045	bracket blocks			
24.000	1.75	1.00	0.75	not at all
24.030	1.75	1.00	0.75	barely
31.000	maxed out			
31.030	bracket blocks			
31.045	bracket blocks			
31.060	bracket blocks			
31.090	bracket blocks			
33.000	1.50	1.25	0.25	barely
33.030	1.75	1.50	0.25	barely
33.045	2.00	1.75	0.25	barely, worse
33.060	2.50	1.75	0.25	barely, worse
33.090	bracket blocks			
41.000	bracket blocks			
41.030	bracket blocks			
42.000	maxed out			
44.045	1.80	1.50	0.30	slightly
44.060	1.80	1.50	0.30	slightly
44.090	bracket blocks			
52.060	bracket blocks			
52.090	bracket blocks			
53.000	1.75	1.25	0.50	good
53.030	1.75	1.25	0.50	good
53.045	bracket blocks			
53.060	bracket blocks			
54.000	1.75	1.00	0.75	very good
54.030	1.75	1.00	0.75	very good
54.045	bracket blocks			

Position Legend: $\#_1\#_2.\#\#\#_\alpha$

Where:		Φ Values	R Values	Θ Values
	$\#_1$ = Φ angle			
	$\#_2$ = R position	1 = 0°	1 = 0.5 inches	000 = 0°
	$\#\#\#_\alpha$ = Θ angle	2 = 30°	2 = 1.0 inches	030 = 30°
		3 = 45°	3 = 1.5 inches	045 = 45°
		4 = 60°	4 = 2.0 inches	060 = 60°
		5 = 90°		090 = 90°

This table shows several important points of interest which bear description. First, most of the locations closest to the incident spot show that the photodiode is too close, as the photodiode receives enough reflected light to be saturated or "maxed out." Such as *11.045*, *21.030*, and *31.000*, which are all ½" from the incident spot, indicated by the "1" in the second position. Next, several other positions, such as *21.045*, *31.030*, and *52.060*, show that either the bracket holding the photodiode or the armature used for positioning block all or a portion of the laser diode beam and thus are unusable. Finally, there are several positions which received a correct level of reflected light to be able to measure the intensity without reaching the saturation limit, which can be further investigated.

Graphed data representative of the orientations which had voltage levels which could be evaluated can be seen in Figure 3-8. As stated before, the assembly was moved back and forth in front of the stitch line six times to get a good representation. For clarity, however, only one pass is shown here. Since the assembly was moved by hand, the timing of the movement was not repeated precisely, while the data collection was handled by computer and was repeated precisely. Thus, the sets show different numbers of passes for the same number of data points taken, giving variable widths to the stitch/space intervals. The discerning factor between forward and backward passes is seen as the elongated flat levels of data taken, indicating the times the assembly was positioned over the black paper strips used as optical stops. Colored lines on the graphs indicate evaluated locations of stitches and spaces. It should also be noted that as the distinction between stitches and spaces becomes more noticeable, the pattern of the variation becomes visible.

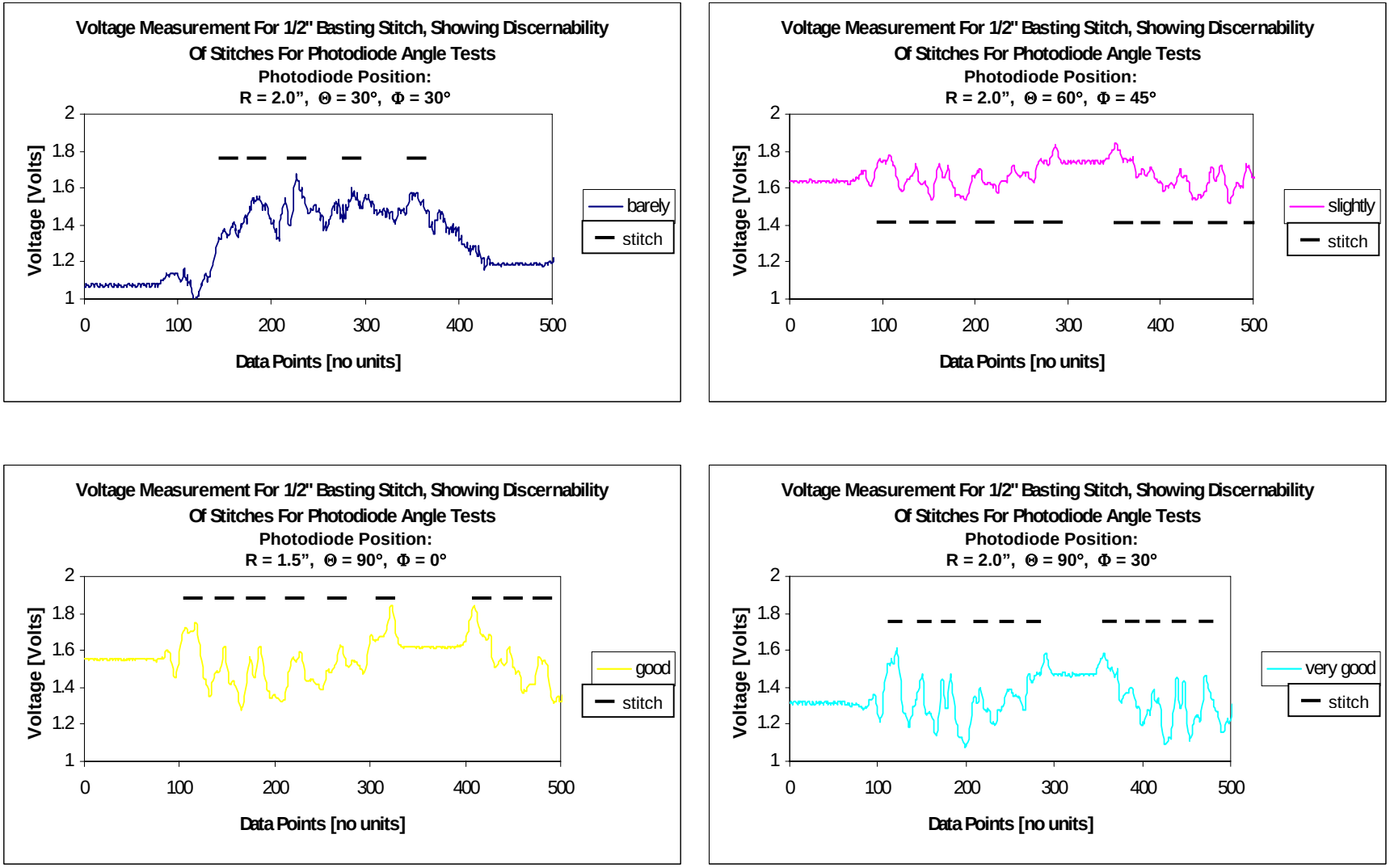

Figure 3-8 Voltage Measurement For ½" Basting Stitch, Showing Discernability Of Stitches For Photodiode Angle Tests

We see from the bottom two graphs especially that the voltage difference is not a square wave figure, as might be expected, but is a sloped decline down to a low point, and then a matching rise back up to the stitch level. In the stitch area the voltage relatively levels off for a short time then begins to drop when a space is reached, but there is not a corresponding level portion in the space region. This is due to overlapping stitch reflections caused by the large spot size of the beam. It should also be noted that at this point in the study, the interference filter had not been added and the addition of the resistor to the grounded cathode of the photodiode had not been included. Thus, the signal seen here is considerably more "noisy" than that of the final signal which are shown in later figures. Elimination of this noise is the reason these devices were later added, and aided in the selection of the devices used.

The majority of the positions, unfortunately, showed little or no discernable variation between reflected intensities for a stitch or a space. An example of this is position *24.030*, or, with the photodiode face oriented at a distance of 2.0" from the incident spot, 30° off the stitch line and 30° off of vertical. As can be seen in the top left graph of Figure 3-8, this orientation showed only a "barely" discernable variation in reflected intensity between stitches and spaces. Other positions showed what were concluded as "slightly" discernable variations, such as *44.045*, or, with the photodiode face at 2", 60° off the stitch line, and 45° off of vertical. The top right graph of Figure 3-8 shows the data collected at this position. Here we begin to clearly see a differentiation in stitch/space intervals.

Finally, only a few positions of the photodiode assembly closely located near the laser diode assembly were described as "good" to "very good" discernability. These

positions, as with the ones labeled “slightly,” clearly show a difference between the reflected intensities of a stitch and a space. Two such positions’ data, which can be seen in the bottom two graphs of Figure 3-8, were *53.000* and *54.030*, or, with the photodiode face oriented 1.5” and 2.0” from the incident spot at 90° off the stitch line and at 0° and 30°, respectively, off of vertical. These two positions showed the greatest variation in maximum and minimum voltage levels, with a high degree of variation between stitch voltage level and space voltage level.

3.4.3 Final Orientation Of The Laser Diode And Photodiode Assemblies In The Test System

In the end, the placement of the laser diode assembly, the voltage variation of the signal received by the photodiode, the discernability between stitch and space voltage levels, and ease of production and installation of a final test unit were the deciding factors in the final position of the photodiode assembly. The first factor is discussed in §3.4.2.1, and the next two of these have been discussed in the preceding paragraphs of §3.4.2.2. The final one is a matter of convenience and reliability. By placing the photodiode assembly close to the laser diode assembly, it will be easier to design and fabricate a single assembly to hold both the laser diode and the photodiode. This will also make it easier to compensate for machine vibration as the assembly will vibrate as a single unit, and easier to mount the assembly onto a production machine to detect skipped stitches in a real time situation. Thus, the position *54.030*, or with the photodiode face a distance of 2 inches from the incident spot, perpendicular to the stitch line and raised such that it was 30° off of vertical, was chosen as the final position for the photodiode assembly as it

showed the best discernable voltage difference and was closest to the laser diode assembly, without blocking the beam.

The final orientation of the laser diode and photodiode assemblies can be fully realized by looking at Figures 3-3 and 3-4, which are the digital photographs of the test system. The laser diode assembly is on the top, with the face at an angle of 45º and distance of 3” diagonally from the stitch line, or 2.12” back from the stitch line and 2.12” off of the fabric surface. The photodiode assembly is underneath the laser diode assembly and its’ face is turned at an angle of 30º off of the vertical, at a distance of 2 inches from the stitch line, or ~1.73 inches back from the stitch line and 1” off of the fabric surface.

4. Test Samples Final Preparation And Organization

Using the groundwork of information laid out in the previous chapters, the remaining organization of the final test samples was made. The type of stitch to use was outlined by the spot size of the laser diode . Classification, organization, and size of the test samples was determined through the physical testing and test system arrangement. Finally, a cross section of testing the final test samples for fabric type and stitch thread color was used to further show the systems' reliability for all fabric types and color variations.

4.1 Stitch Type

As outlined in §3.1.1, the spot size of the laser diode ended up larger than ideal, forcing a re-evaluation of the type of stitch that could be used. A stitch type was required that has a sizeable distance between stitches. One such type of stitch is the basting stitch. This stitch is a common tool in the pre-assembly of garments, especially in design of new garments, but is not meant to be used in final production. This is because the basting stitch is used to temporarily hold pieces of fabric together for final stitching by passing a single thread back and forth through the two fabrics. Other stitches require at least two threads, a "top" thread and a "bottom" thread, which are interlocked on the underside of a seam, or on the interior of the final garment, in the sewing process to form a strong, wearable garment made from separate pieces of fabric.

4.1.1 Stitch Size

The types of basting stitch vary only in size, or length, of the stitches and spaces. Again, due to the spot size of the laser diode, and also to assure a clear distinction between stitch and space reflected light levels received by the photodiode, the size of the basting stitch selected for this study was ½ inch. This indicates a ½" length stitch followed by a ½" length space, as indicated in Figure 4-1.

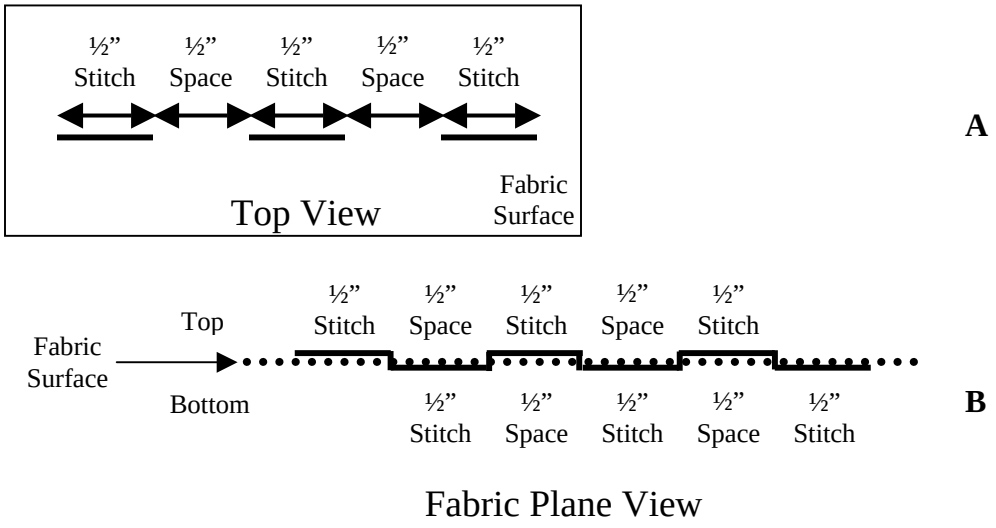

Figure 4-1 Basting Stitch, Top View (A) And Fabric Plane View (B)

This figure shows a top view of the fabric with a ½" basting stitch, as well as a view in the plane of the fabric. Figure 4-1a shows what we see when looking straight down on the fabric. The fabric plane view, Figure 4-2b, shows that the stitch is made from a single thread alternating from side to side of the fabric. This is similar to the view of the laser diode-photodiode assembly, the top side of the sample only, with stitches and spaces alternating.

4.1.2 Stitch Alignment And Uniformity

Since the basting stitch is used as a temporary tool with only one thread, it is sewn into fabric by hand. In general then, the length of the basting stitch is rough, at best. To ensure uniformity for this study, great care was taken to create two straight stitch lines per sample, with one inch between them along the length of the test sample. Size and shape of the samples is discussed in the next section. Two lines were made on each sample to allow multiple data collections per sample and for detecting any mistakes made during sewing, or obvious stitch thread abuse.

Using a straight-edged ruler with a T-head, the sample was marked every ½" along its' length. The T-head was used to create a straight line along the long side of the rectangle-shaped samples. This careful alignment and positioning of the stitches was used to create a standard pattern which would be easily discernable in the data collected as it related to the reflection levels received by the photodiode.

4.2 Final Sample Preparation

Based on the size and arrangement of the test system a final test sample size was decided to be 3" by 24" cut from the larger pieces of fabric as received from *Test Fabrics, Inc.* The 3" width was decided upon to allow two stitch lines per sample length at 1" and 2" from a long edge. A 24" length was selected based on the test systems' travel length. This allowed a single piece to be measured in the middle without concern for end effects. The basting stitch lines as described in the previous section were thus along the 1" and 2" distances from a long edge, and began and ended 4" from either end

of the test sample. The ½" stitch/space lengths thus allowed 16 stitches to be visible from the top side of the test sample.

4.2.1 Edge Fraying Resolution

One problem that was immediately noted with the original test samples, fabrics #1-13, as well as the large fabric pieces of the final test samples, fabric #14-19, was the fraying that occurred at the edges. Mainly with the nylons and acetates, but also to a degree with the cotton samples, when they were cut by hand using scissors or sharp blades and straightedge tools, and then with subsequent handling for testing, the samples became ragged along the edges to the point of not being useful for the study. This is due to the low coefficient of friction between the threads that are woven together to form the fabric. This low coefficient of friction is also what makes a fabric more pleasing to human touch.

Test Fabrics, Inc. suggests the cutting of samples for testing using a heated cutting tool to melt or burn the ends of threads together. This method of cutting has little effect on the cut sample except in close locale to the edges. Thus, to cut the samples to exact measurements and use a heated cutting tool, test samples were cut using an automated CO_2 laser cutting system. This system accepts a 2-D computer input image of sample size and shape using a CAD-based program to cut to exacting specifications. Final test samples were therefore cut as 3" by 24" pieces from the larger fabric pieces using the laser cutting system, assuring no fraying of the edges would occur.

For each of the six final test fabrics, eight test samples were cut to accommodate the eight stitch thread colors chosen. Thus, there were 48 samples cut, each then had two

stitch lines sewn into them, as described in the previous section. A final selection of which thread colors and fabrics to test the system on is described in §4.4, below.

4.2.2 Environmental Conditioning

After the fabric samples were cut, marked, and then hand sewn for use in the study, they were environmentally conditioned via ASTM D1776. The samples were conditioned as described in §2.2.1 in a controlled laboratory environment for a minimum of 24 hours prior to conduction of the tests.

4.3 Test Sample Arrangement On The Test System

To hold the test samples in place and to introduce a slight amount of tension to hold the fabric flat without pulling the stitch thread taut, the test system as described in Chapter 3 was mounted onto a board approximately 22” by 18”, and the samples were held by clamps at the ends along the long side of the board. To keep the board from bowing and to allow it to hang over the edge of a table for easy clamp placement, a 21” by 3” by ½” aluminum block was mounted on the underside of the board, directly under where the test samples would be laid. The main purpose of the aluminum block was to maintain an equal distance between the fabric surface and the laser diode/photodiode assembly by forcing the board to lie as flat as possible, minimizing any difference in received light at the photodiode caused by a difference in distance between it and the fabric surface. The fabric was then laid on top of the board and held flat by clamps at the ends as described above. This ensured that the fabric surface and the laser diode/photodiode assembly, which was mounted to a linear slide, which was, in turn,

mounted to the board, were in reasonably parallel planes as they were both connected to the board held flat by the aluminum block.

To arrange uniform placement and alignment of the test samples, a template was made to align the stitch lines parallel to the path of the laser diode spot, at the correct distance. Then, the black paper strips were used to shift the test sample into position along the travel path. Each 24" long test sample was laid on the table with approximately 1" overhanging each end of the board for clamping, then the stitch line template was pinned into place on the board. The test sample was then moved until the first stitch line, or the one closest to the test system, was aligned parallel to, and at the correct distance in the path of, the laser diode spot. Next, the optical stop strips were laid into place and pinned down, and the test sample was moved such that five complete stitches were clearly visible between the stops. This was done to aid in the comparative study for all the test samples. After positioning the test sample, the stitch line template was removed. The optical stop strips were left in place to show distinction between fabric and strip surface as viewed by light reflected back to the photodiode.

4.4 Cross Sectional Selection Of Final Test Samples For Analysis

As the preliminary NIR spectrophotometric analyses showed, there is negligible or little difference in reflectivity levels using the 1550nm wavelength light as compared for different types of fabrics, different weaves, orientation of those weaves, and color. Thus, a cross sectional representation of the final test samples was chosen for fabric type,

stitch thread color and diameter, and fabric sheen. Multiple tests were made for each group, and included changing the direction of the test system movement.

4.4.1 Stitch Thread Selection For Study

The color comparative study of the initial test samples described in §2.3.3.4 showed that the color of materials is not of intense concern. To further support this, three of the final six fabrics were chosen to evaluate with all the stitch thread colors. As a reminder, the eight stitch thread colors were black, blue, green, orange, purple, red, tan, and white. The three test samples chosen, #14, 16, and 18, were selected to represent the three types of fabric used in the final test sample group. The fabric types were cotton, nylon, and acetate.

The other three test samples had two stitch thread colors studied, specifically purple and tan. Selection of these two threads to study was done based on the measured diameter of the threads, as described in §2.2.5, rather than color. Purple represented the smallest diameter thread of the study at 0.37mm. On the opposite end, tan represented the largest diameter of the stitch threads with an average measurement of 0.46mm.

4.4.2 Sheen Of Material

As stated in §2.5, the main reason for the selection of the final six test samples was a comparison for different levels of gloss or sheen. The samples range from low sheen, as fabric #14, a cotton denim, illustrated; to medium sheen, as with fabrics #15-17, all three being nylons; and high sheen, represented by the acetates of fabrics #18 and #19. Thus, all six samples were tested for at least the minimum and maximum thread

diameters found in the purple and tan threads, as described previously. A final comparison could then be made for the effect of the sheen of a material on the reflected light intensities received at the photodiode.

4.4.3 Number Of Stitch Lines Tested

For all six final test samples, and all stitch thread color variations, both the first and second stitch lines sewn into the test samples were analyzed. After performing the test on one stitch line, the test sample was removed, turned 180º in the surface plane, and resituated according to the previous section, for analysis of the second stitch line. Here, the first/second stitch line designator is purely dependant upon which line is laid toward the test assembly first.

4.4.4 Test System Movement Direction

For all the tests done with the test system, the movement of the system was consistently done right to left, facing the test assembly, as in Figure 3-3, in Chapter 3. For balance with the final test fabrics, three of them, #14, 16, and 18 were also analyzed moving the test system from left to right, and labeled “reverse” for organization.

4.4.5 Data Organization And File Nomenclature

As with the initial test samples, a data file nomenclature was developed to help organize the data. Following the system developed in §2.3.2, the following structure was developed, as seen in Figure 4-2:

C:\Final Data\$\#_f \alpha_1 \#_1$[rev] where :

$\#_f$: test fabric number

α_1 : color of stitch thread

$\#_1$: stitch line number (1 or 2)

[rev] : denotes test system movement left to right [when applicable]

and colors of stitch threads :

BK, BL, GN, OR, PU, RD, TN, and WH

Figure 4-2 Final Data File Name Format

Thus, data files may be "14RD," indicating data for test fabric #14, red stitch thread color. Or, "16BL2REV," indicating the data for test fabric #16, blue stitch thread, stitch line 2 of 2, and the test system was moved left to right.

5. Test System Data And Analysis

As an introduction to the data form expected as collected by the test system, §3.4.2.2 shows preliminary data, in Figure 3-8, collected to aid in the orientation of the photodiode assembly. As stated there, this data is in a rough form and subsequently reformed using a set laser diode/photodiode orientation and filtering with the addition of the narrow bandwidth interference filter at 1550nm and the addition to the photodiode circuit of the resistor to ground on the cathode side of the photodiode to give the circuit a more definite reference to ground, generally referred to as floating the front end.

5.1 Final Test System Manipulation And Resulting Data Presentation

Before presenting the data, the final manipulation of the test system needs to be detailed. As noted before, the test fabric was sewn with a ½" basting stitch on a straight line formed with a ruler and straight-edge. The fabric and stitch line in question were then placed onto the test system using a measured template to ensure that the stitch line was as close to parallel to the travel path of the test system as possible.

With the stitch line in position, data collection was initiated on the computer and the table top-system was moved from one end to the other of the linear slide in an approximate one second time span. As pointed out in §4.3.2.2, the system was manually moved and therefore the data will show a difference in the time span shown in representation of the stitch and space lengths. These differences do not correlate to any

standard and thus there were no comparisons done to determine length of stitch/space to qualify a properly formed stitch.

Also, as detailed in the description of the test system in §3.4.1, two black paper strips were laid perpendicular to the path of travel to act as optical stops. The difference between reflection off of the paper surfaces and off of the fabric/stitch surfaces would act as obvious start/stop points of areas of interest in the data. With the final test assembly in place and working, the different materials did show a remarkable distinction, where the test material levels were in the 0.25 to 2.5 Volt range and the optical stops show almost no reflection to the photodiode, falling to the millivolt range near zero. For ease of reporting the data and examining details, the graphed data extends only to the point where the voltage markedly drops off indicating the test system was over the optical stops.

5.2 Placement And Organization Of The Final Test Samples

The form of the data can be surmised to follow a standard pattern due to the work in previous chapters of this study. Mainly, we expect to see a distinct difference in the levels of voltage produced by the photodiode circuit as more light is reflected back by a stitch than reflected away by a space. This is, in fact, what we do see in the data in its' final form. The data is graphed and presented in reflected voltage, where the scale spans one half of a Volt to be able to see details, to 2 ½ Volts for the largest range differences, versus a time scale, which shows the entire 6 space – 5 stitch span was passed in approximately one second.

As shown in the NIR analysis in §2.3.3, the color of the material is not a primary concern at the selected 1550nm wavelength. The main difference in collected reflectance data was instead seen to be the material used and the gloss, or sheen, of the material. One other area comes to light as a factor in the data. The diameter of the thread used in the stitch line in general should cause a variation in the amount of light reflected back as the increasing diameter forms a larger face of material open to the test assembly on the surface of the fabric. For a sketch of this, refer to Figure 3-5c. Thus, the final data presented here is categorized according to the following, Table 5-1.

Table 5-1 Final Test System Data Organization

Fabric #	Identifying Name	Distinguishing Feature	Stitch Thread Colors Tested	Comparisons Made With Final Data
14	White cotton twill	Lowest sheen | | | | | | |	All	All diameter threads for color comparisons and material comparisons
15	Spun nylon 6.6		Purple, Tan	Minimum and maximum thread diameters for stitch thread size comparisons and material comparisons; both stitch lines
16	Filament nylon 6, tricot bright		All	All diameter threads for color comparisons and material comparisons
17	Filament nylon 6.6, semi-dull taffeta	Fabrics are ordered in increasing glossiness or sheen according to visual inspection. | | | | | | Highest sheen	Purple, Tan	Minimum and maximum thread diameters for stitch thread size comparisons and material comparisons; both stitch lines
18	Acetate satin, bright filament yarn		All	All diameter threads for color comparisons and material comparisons
19	Acetate tricot, all delustered filament		Purple, Tan	Minimum and maximum thread diameters for stitch thread size comparisons and material comparisons; both stitch lines

5.3 Collected Data Graphed For Analysis

Examples of data collected and graphed as outlined above can be seen in Figures 5-1 through 5-6, which correspond to Fabrics #14 through 19, respectively. For clarity and conciseness, Figures 5-1, -3, and -5, for Fabrics #14, 16, and 18, show graphs for all 8 stitch threads, where Figures 5-2, -4, and -6, for Fabrics #15, 17, and 19, show only graphs for the minimum and maximum stitch thread diameters, purple and tan, respectively. Figures 5-2, -4, and -6 also show the first and second stitch line data for the two thread diameter extrema to show similarity for thread size and color on a particular material. To aid in differentiation of the graphs for discussion, a letter corresponding to the graphs position of the page has been placed in the upper left hand corner of each graph. Also, to aid the reader, horizontal bars are placed on each graph indicating the voltage level representative of a stitch, where discernable.

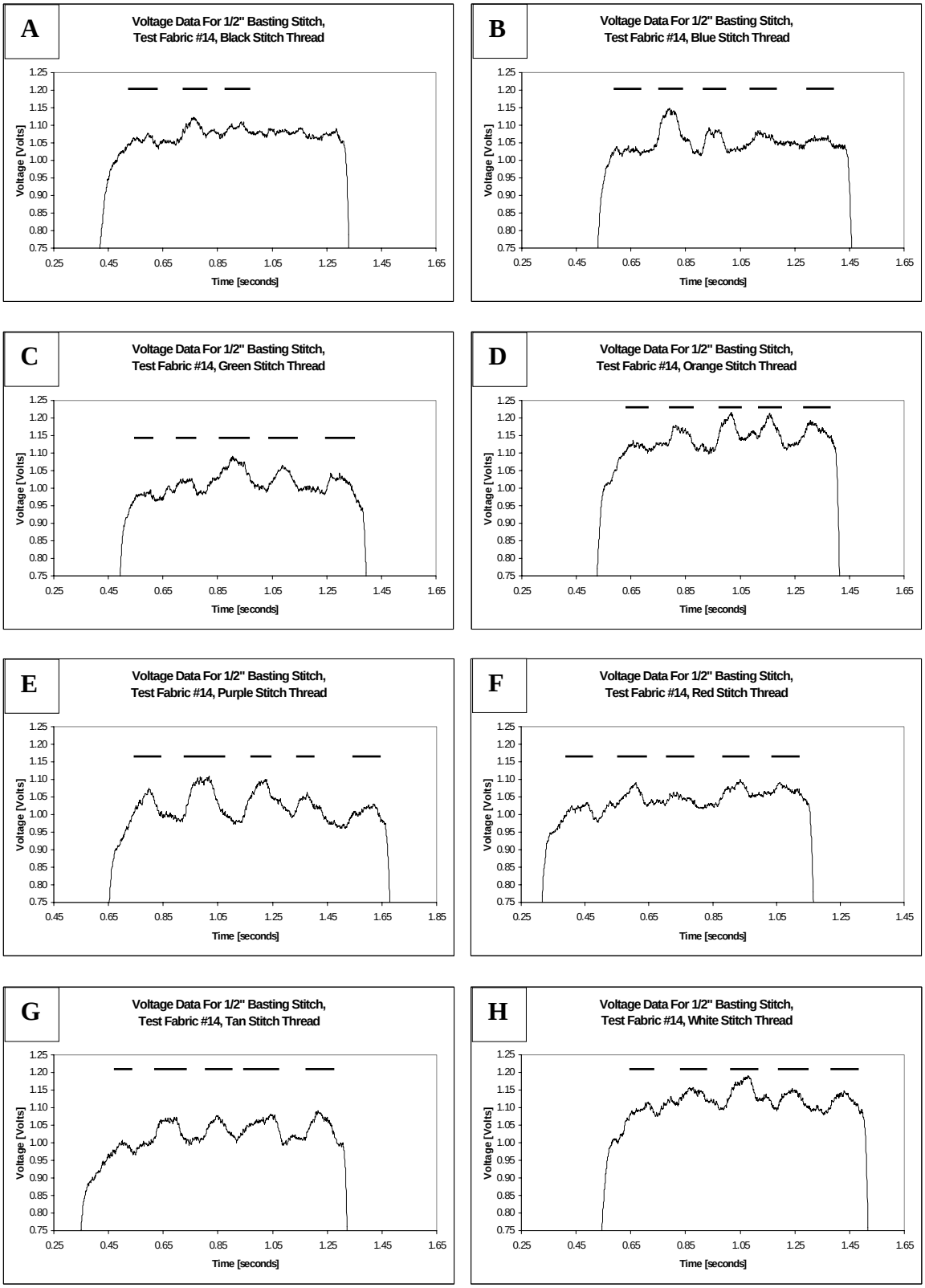

Figure 5-1 Final Collected Data For Stitch/Space Variance For Fabric #14, All Thread Colors

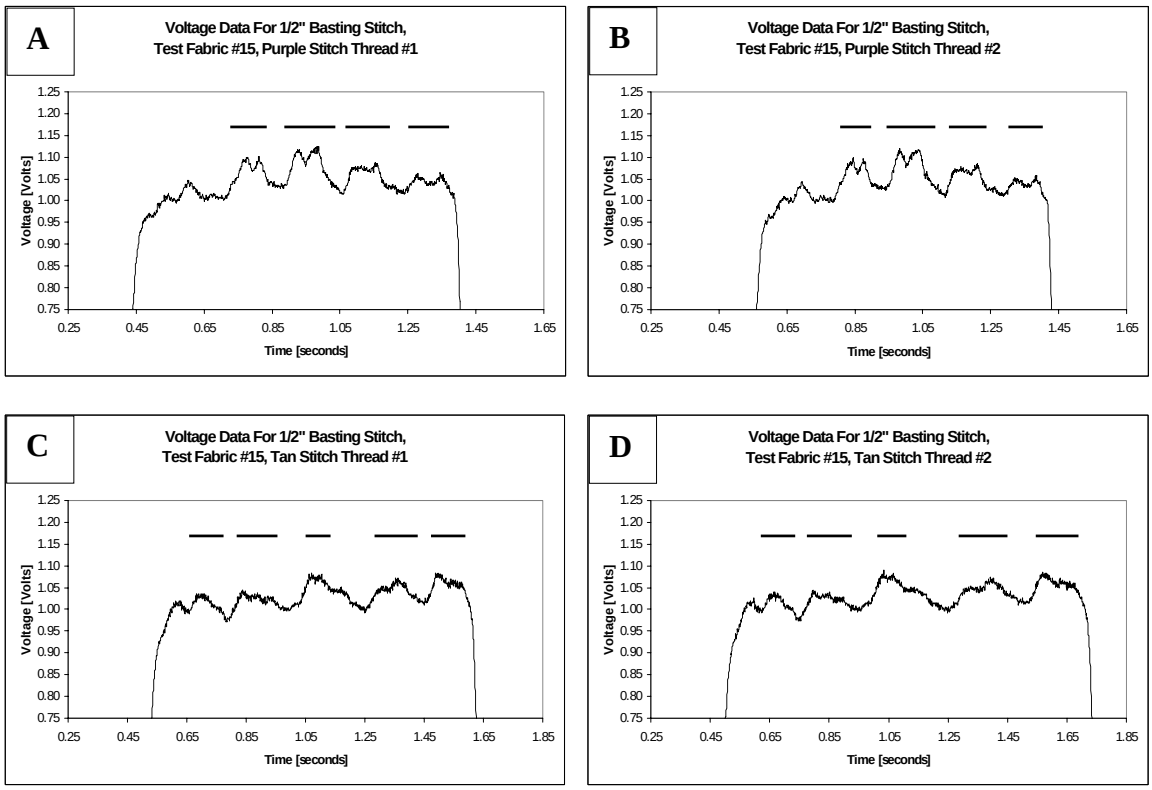

Figure 5-2 Final Collected Data For Stitch/Space Variance For Fabric #15, Minimum And Maximum Stitch Thread Diameters

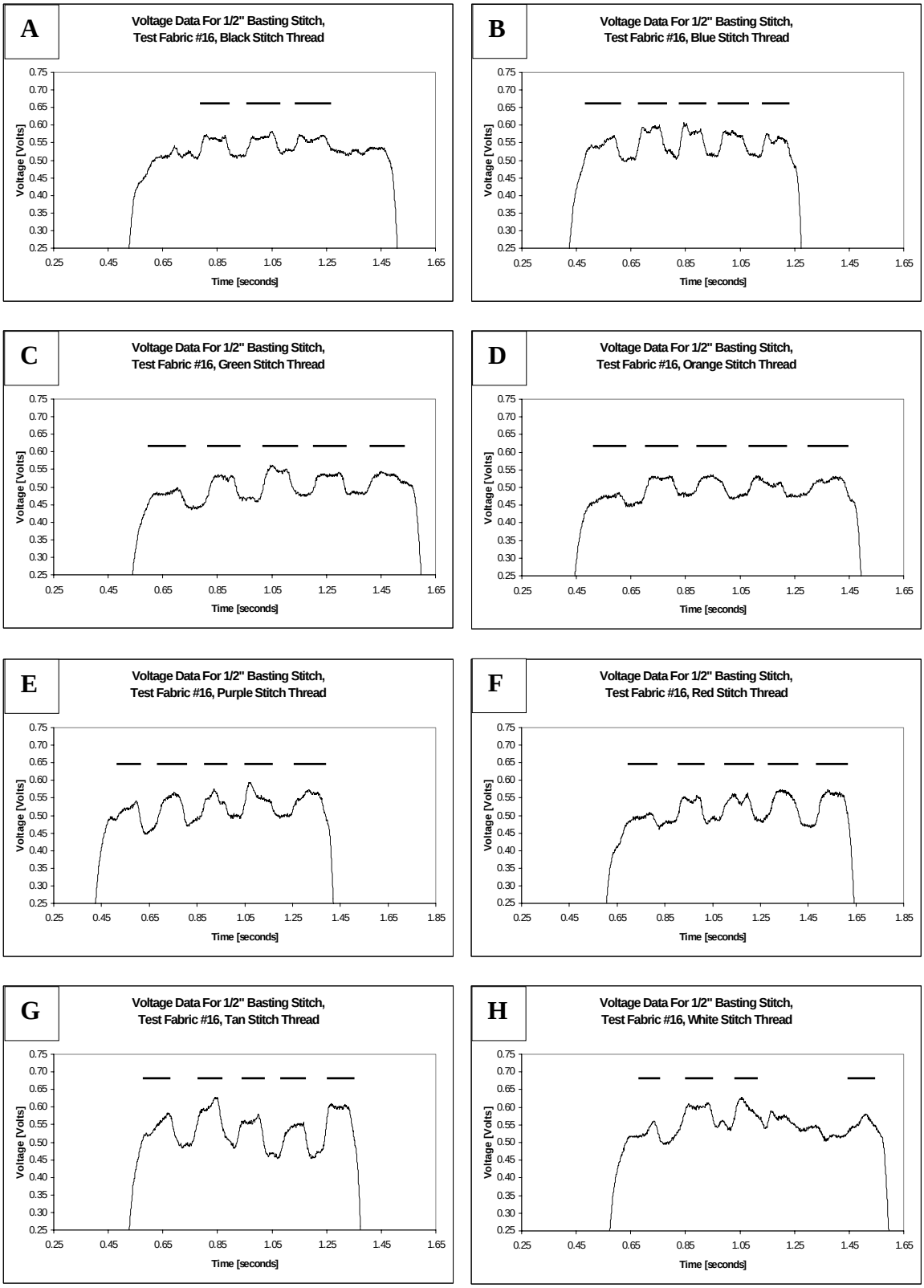

Figure 5-3 Final Collected Data For Stitch/Space Variance For Fabric #16, All Thread Colors

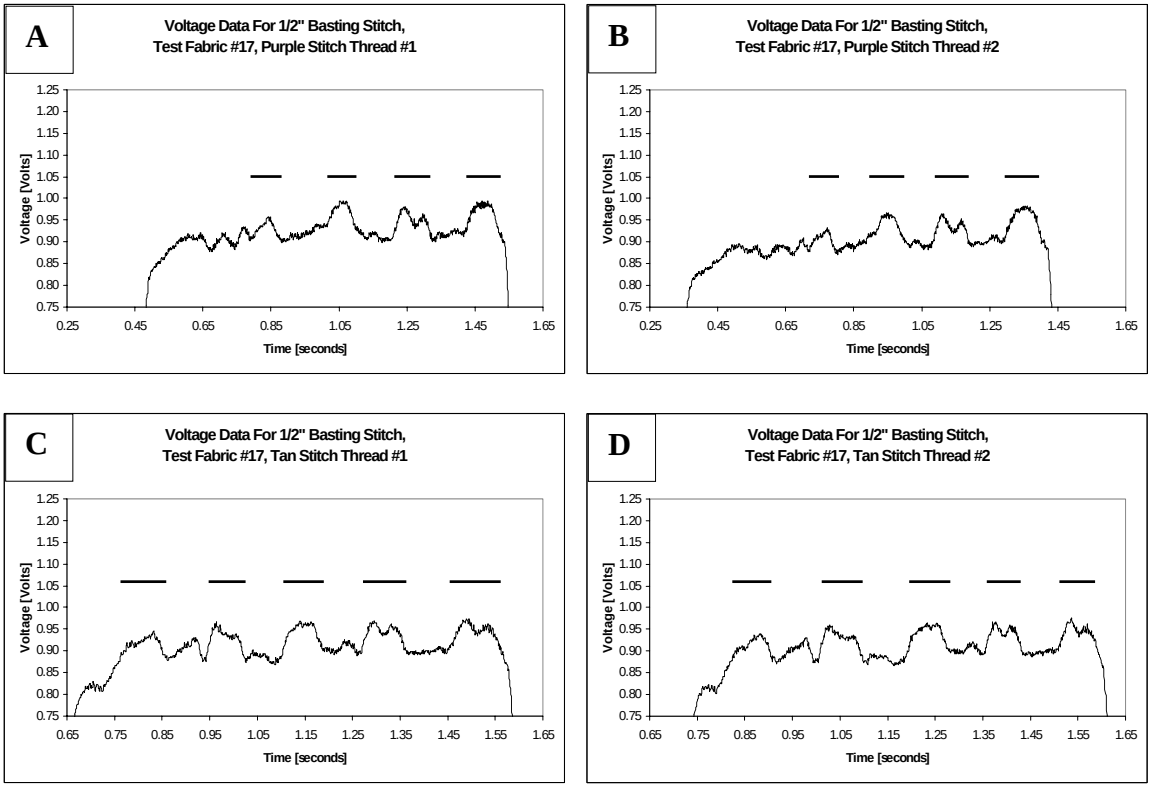

Figure 5-4 Final Collected Data For Stitch/Space Variance For Fabric #17, Minimum And Maximum Stitch Thread Diameters

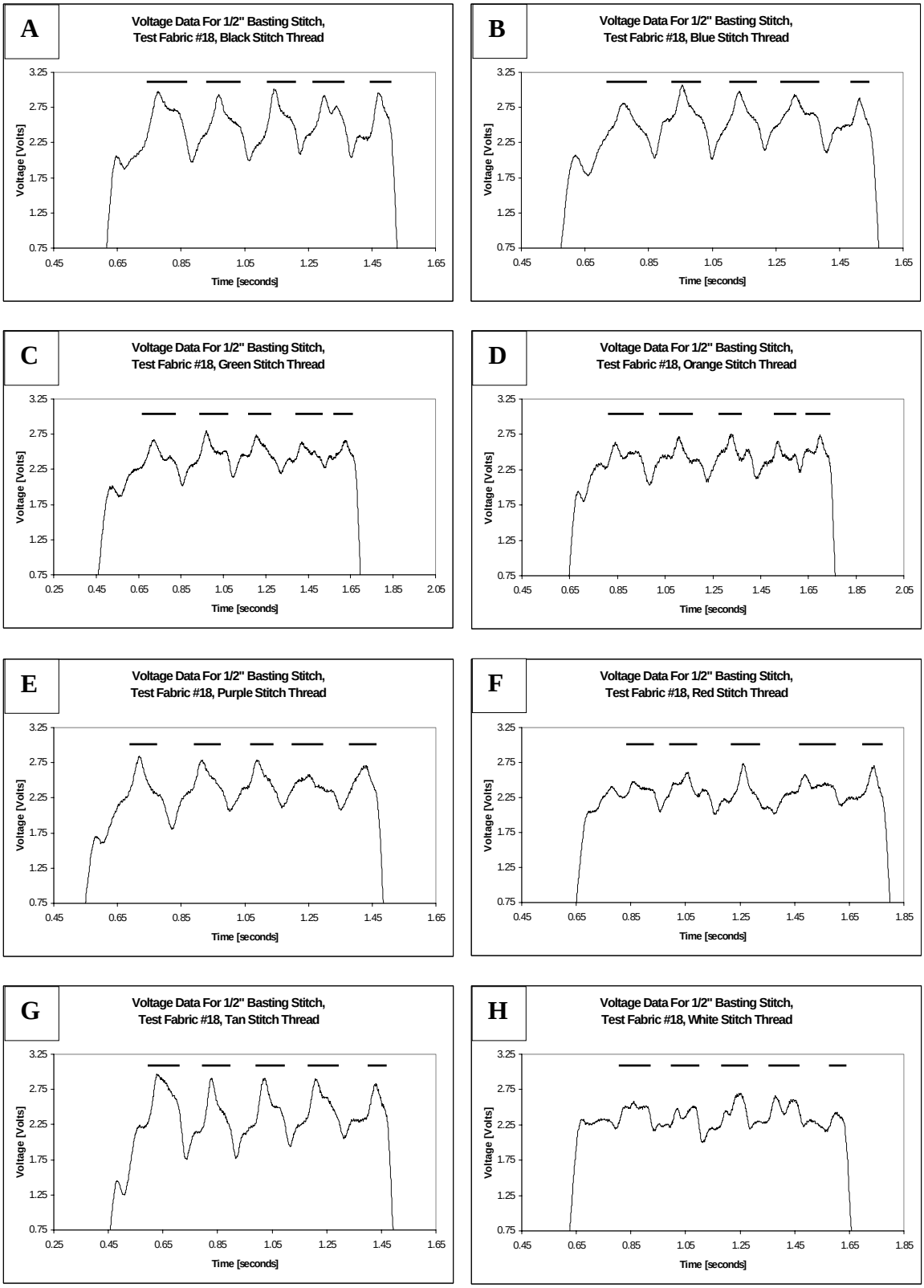

Figure 5-5 Final Collected Data For Stitch/Space Variance For Fabric #18, All Thread Colors

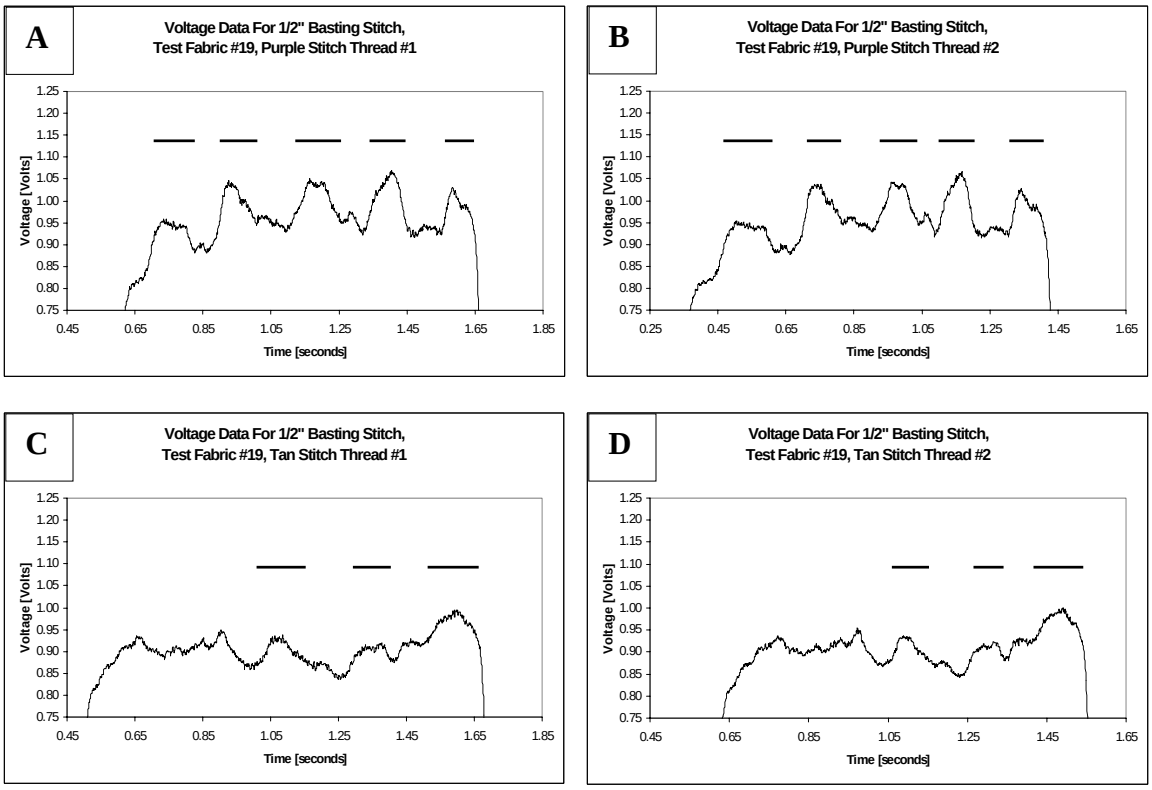

Figure 5-6 Final Collected Data For Stitch/Space Variance For Fabric #19, Minimum And Maximum Stitch Thread Diameters

These figures immediately confirm the original hypothesis that there is a distinguishable variation between reflected light levels from stitch and space intervals of the ½" basting stitch line. These variations range from approximately 10mV to nearly 200mV. Some of the variations are difficult to distinguish, such as in Figure 5-1A, where the most distinguishable portion is the drop off of the voltage to near zero due to the location of the optical stops mentioned above. These stitches however, can be discerned upon closer examination, as in Figure 5-7, below.

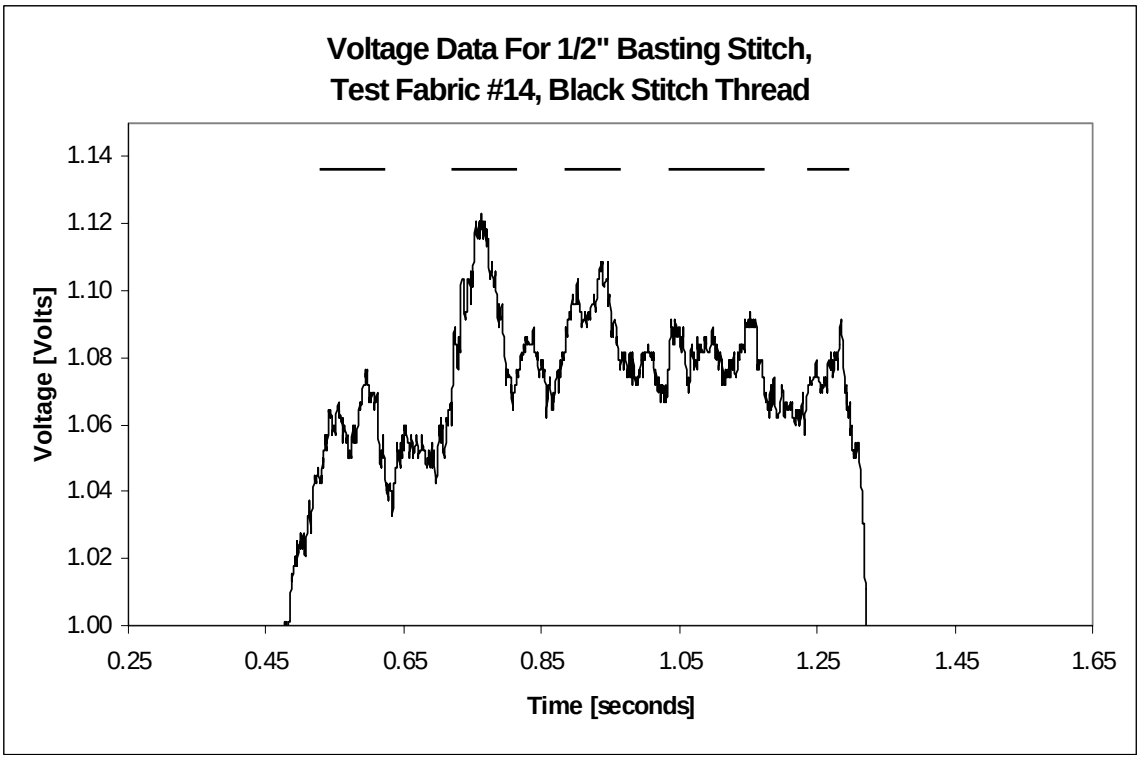

Figure 5-7 Voltage Variation Data For Stitch/Space Levels For Fabric #14, Black Stitch Thread

These graphs also show consistent forms for the data for each fabric type, but vary slightly in their overall levels when comparing one color thread to the next. This

consistency of form will aid in the final evaluation of data, but the variation of the data levels has need for explanation. As will be shown later, the data for the separate thread colors for a particular material are not actually as disparate as they look at first glance. The important point of the data levels are the differences in the bottom and top of each peak, which will be described in detail later as the contrast. This contrast value is consistent for each material, regardless of the stitch thread used. Alternate explanations for an example of the variation of Figure 5-1c, for fabric #14 with a green stitch thread and voltage levels between 0.95V and 1.10V for the bottom and tops of the peaks, and Figure 5-1d, for the same fabric, but an orange stitch thread, with voltage levels of 1.10V to 1.23V fall into three possible categories. First, due to the manual manipulation of the table top test system, extra pressure may have been inadvertently applied to the linear slide table forcing the laser diode/photodiode assembly to be closer to the surface in the orange thread case. This would cause a slightly higher voltage to be produced by the photodiode due to its' reception of more reflected light. Another possibility is the slight mis-orientation of the fabric sample and thus the stitch line closer to or further from the laser diode/photodiode assembly. Finally, the diameter of the threads may be causing a difference as seen from graph to graph for individual materials. Larger diameters would present a larger face to the laser diode/photodiode assembly thus reflecting more light back and causing a higher voltage to be produced by the photodiode. However, as the analysis of the data for contrast will show later, the variations of the voltage levels are more likely due to the first two causes than the latter one.

At this point the discernment of stitch/space voltage levels is partly quantitative and partly qualitative. Practice was the main factor in learning the methods of

determining stitch/space levels. To begin with, the data graphs which more readily show the voltage variance were used. Such as Figure 5-3c, seen in larger view in the figure below.

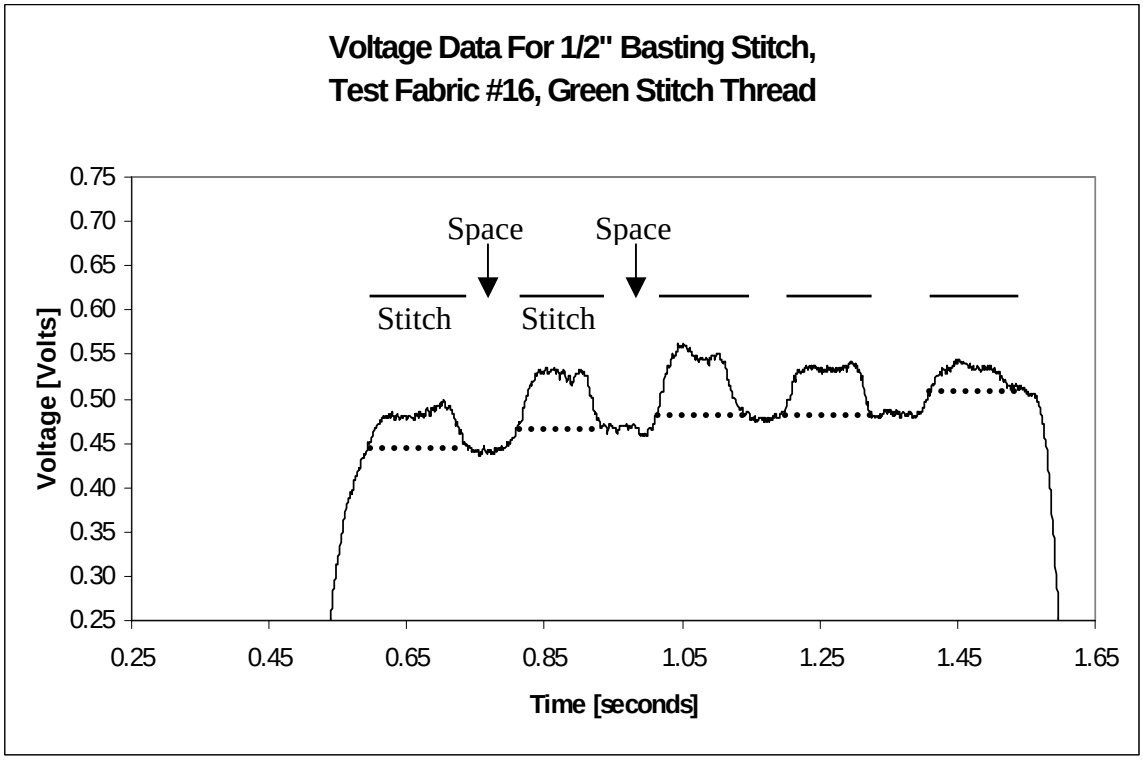

Figure 5-8 Voltage Variation Data For Stitch/Space Levels For Fabric #16, Green Stitch Thread

Here, a closer view of the data for Fabric #16 with green stitch thread shows a more clearly definable stitch/space voltage variation, seen as the quasi-square wave form where the peaks are stitch levels and the valleys are the spaces. This voltage level distinction can be deduced from the fact that more light would be reflected back from the areas where a stitch is present than from an area with a space where more light would reflect off of the surface of the fabric and be scattered into the distance. The additional

light reflected back by the stitch would be evident in the raised voltage levels produced by the photodiode circuit. This figure shows the horizontal bars representing the stitches and the spaces between them represent the spaces between the stitches. The dotted lines present at the bottom of each peak are rudimentary sketches of the levels used to differentiate the widths of the stitches. As stated before, however, the test system was moved manually, with the non-uniformity of speed of motion causing a different stitch length for nearly every stitch, thus not allowing a stitch length/peak length correlation.

These lines do begin to show the development of the method to discern the space voltage level versus the stitch voltage level. As seen in the figure the dotted lines connect what appears to be the bottom points of the peaks near the regions where the data flattens out for the space level. Searching for the beginning of this flattening of the data at the lower points is the main thrust of the qualitative method. For the most part the data was not at the same level for the spaces on each side of the stitch levels. This was due to two possible factors: the material sheen had an effect on the light level reflected back to the photodiode, and the stitch thread on the underneath side of the material caused a “bulge” in the material at the space intervals. Recall from §4.1.1 that the stitch thread passes from one side of the fabric to the other, forming the basting stitch, and that the material was laid flat on the table top surface, which would cause the material to bulge at the space intervals due to the underlying stitches. This bulging of the material in the space intervals then reflects more light back to the photodiode, increasing the voltage level. Uneven fabric placement, thread twisting and table top surface are other contributing factors to the difference in levels on a space by space basis.

However, there is still a discernable difference between the stitch and space levels seen in Figure 5-8. We may deduce from these graphs that the areas where voltage levels begin to flatten or "knee out" are the beginning of the space intervals and thus the ending of the stitch intervals. As can be seen in Figure 5-8 also, the levels of the space intervals are not the same from one to the next, and thus, the evaluation of the stitch level was generally held to begin at the higher knee out and was carried across to the opposite side of the stitch voltage peak. While not an ideal qualifying method for setting pass/fail levels for automated evaluation, for this preliminary study this subjective method is quite satisfactory.

As another example, let us more closely examine Figure 5-4c in the figure below.

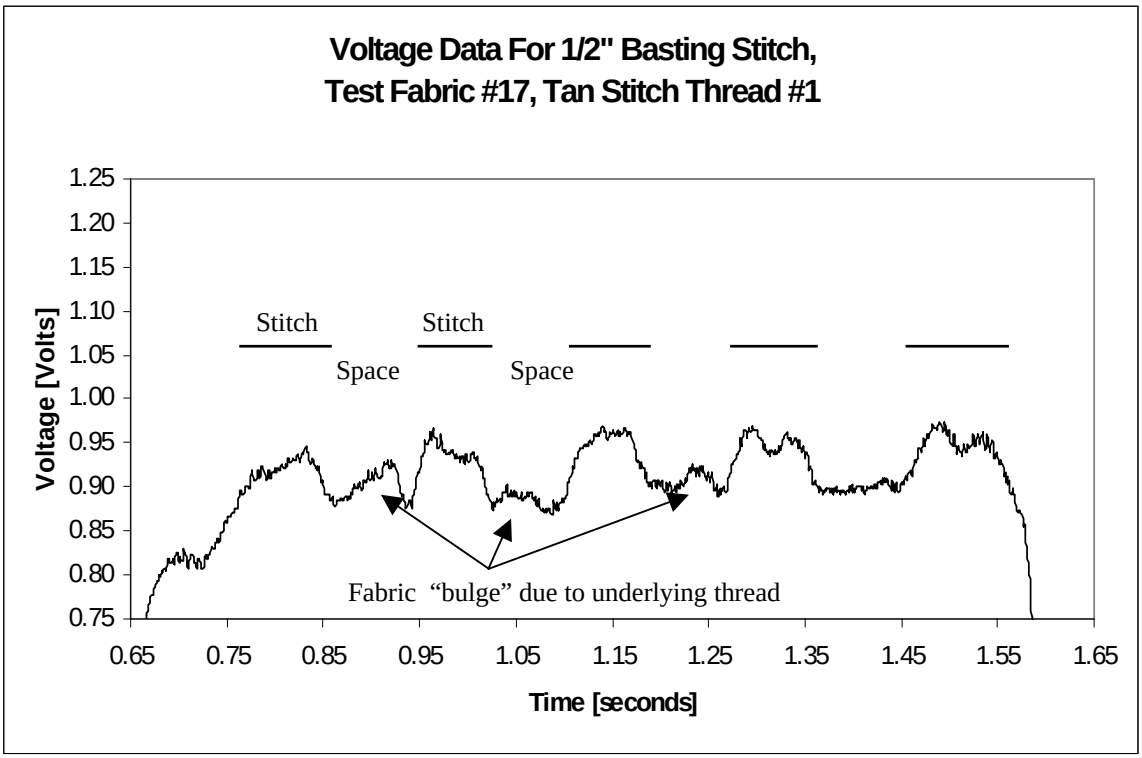

Figure 5-9 Voltage Variation Data For Stitch/Space Levels For Fabric #17, Tan Stitch Thread

In Figure 5-9, we can more closely see the effect of the bulging of the fabric material caused by the underlying stitch thread as the minor peaks which occur between the larger ones. The sizes of these minor peaks helps to eliminate them as possible stitch peaks when compared side by side as in the figure. This figure also more sharply shows the turning point for the stitch/space intervals as the voltage begins to rise again due to the underlying stitch.

An important note should be made here about the bulging of the fabric due to the underlying stitch thread. This occurrence is particular to the method of sewing involved in this study. This research focused on the stitch line as it passed through a single layer of material, which in most cases would not have sufficient stiffness to keep the bulging to a minimum. This can be seen as the progression through the data shows from a thicker material, such as fabric #14, a heavy denim, to a medium density material, such as the nylon in fabric #16, to a particularly light material such as the nylon taffeta of fabric #17. This is also clearly evident in the case of fabric #18, a light density acetate satin, as evidenced in Figure 5-10, below.

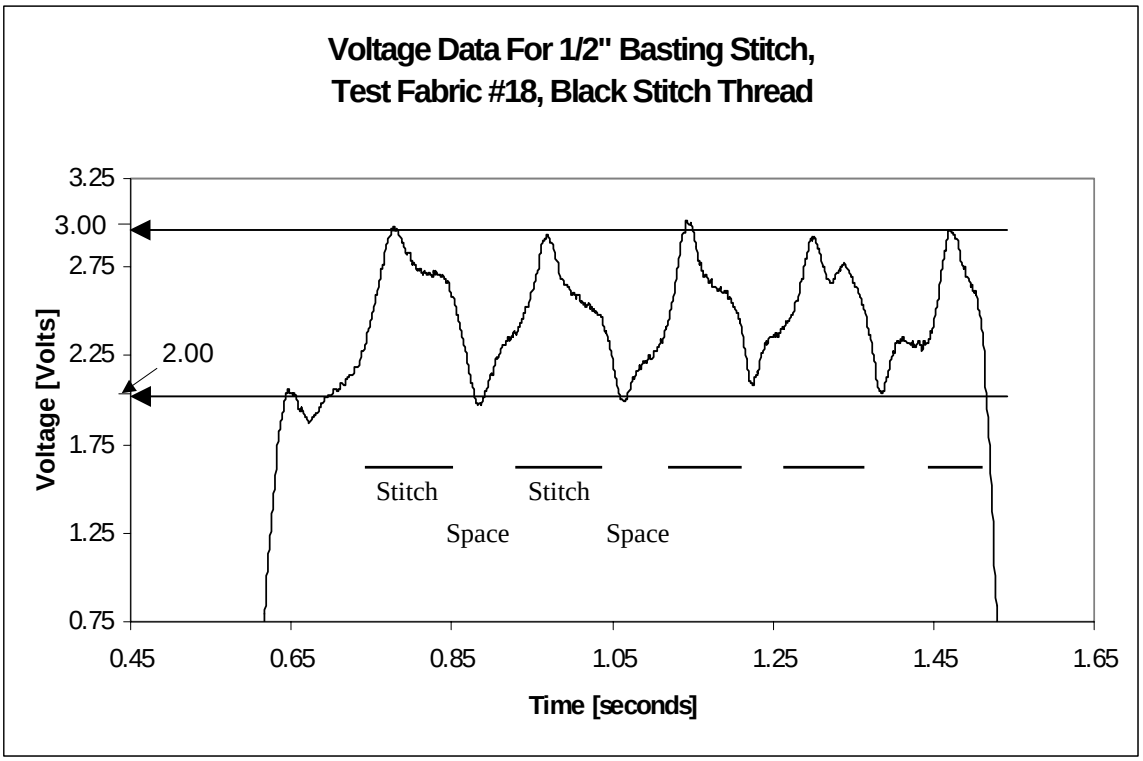

Figure 5-10 Voltage Variation Data For Stitch/Space Levels For Fabric #18, Black Stitch Thread

Here, the stitches are seen as sharper peaks rather than the squared off peaks of the other materials. This is due to the bulging caused by the underlying stitches causing more light to be reflected back to the detector in the space intervals, especially right at the stitches. For example, the first large peak on the left shows a rapid increase from the minimum voltage of ~1.75V to the maximum of ~3.0V. Then, as the system continues moving, the voltage begins to drop off, then levels off at ~2.65V. This is most likely caused by a combination the bulging of the fabric and the large spot size of the laser diode assembly, as described in §3.1.1. As the spot is moved from the stitch interval into the space interval, a portion of the beam is in both intervals which causes the voltage to level out.

As the spot continues to move into the space interval, the majority of the beam is now projected onto the bulge, which is physically lower than the stitch, and the voltage again drops off precipitously to a true low of ~2.0V. Then, continuing on, the spot moves into the stitch interval again and we see the sudden increase in the voltage due to the quick increase in reflected light from the larger stitch face being in the spots' path. This pattern continues through the five stitches, only differing in the last stitch where the pattern is reversed, but still the same principal applies. One important note for this argument is the fact that all of the major peaks have nearly the same value, ~3.0V, and all the valleys hare nearly the same value, ~2.0V.

A rough sketch of the fabric bulges is seen in Figure 5-11, below. Here, the stitch thread passes back and forth through the fabric, but the flimsiness of the material allows a bulging to occur near the stitches in the space intervals. Note that this bulging is less than the stitch height, but enough to cause a variation in the reflected light. Also, as will be shown in forthcoming analyses, the sheen of the material plays an important roll in the reflection of the light, and adds to the variation in the light levels evidenced here.

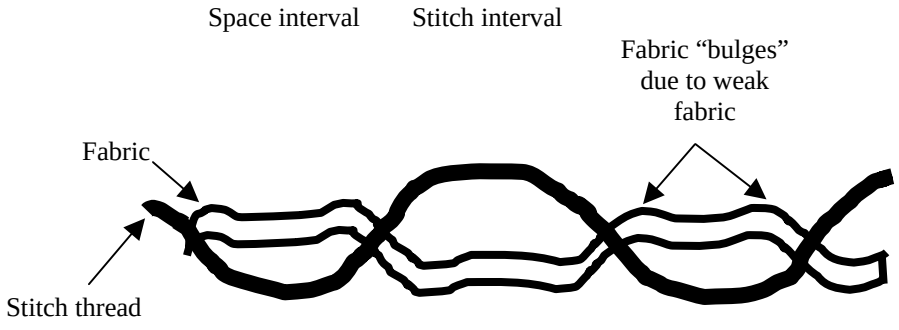

Figure 5-11 Sketch Of Fabric "Bulges" In Space Intervals Due To Thin Material

Later study for an actual application of this research would most likely reveal that this problem of fabric bulging would disappear. Mainly due to the facts that most seams in real application are a minimum of two layers of fabric thick, and the difference in the type of stitch used. The doubling of the fabric would provide enough stiffness to the seam to decrease the bulging caused by the stitch from the underside. Also, in practice, the stitches are similar to the chain stitch shown in Figure 1-2, where the stitches are not separated by a space but rather differentiated by the thread dropping down through the fabric, being caught with the looper thread on the underside, and rising again through the same hole to form the next stitch. This type of undulation is a more standard form of stitching in practical situations, but was beyond the scope of the current research.

One other important point should be made of the graphs and data of Figure 5-1 through 5-6. As stated in the test fabric/stitch line preparations sections of Chapter 4, two stitch lines were sewn on each fabric piece. Each of the stitch lines was used to make a data set for this final analysis. If became evident that as each sample was tested, the stitch lines for each sample were producing nearly identical data sets, except for variations due to sheen and fabric bulge, as outlined above. For conciseness, only six data sets are shown here for this demonstration. Figures 5-2, -4 and –6 show the data for the minimum and maximum thread diameters, purple and tan, respectively. Included along side these graphs are graphs of the data of the 2nd stitch line from the same piece of fabric. Examining, for example, 5-4a and –4b, we see that the stitch lines produce close to the same patterns for each sample, with only minor variations in the data at the beginning of the sample. This set of graphs, as well as the other five, show that for a

particular material, and particular stitch thread diameter, the data collected is consistent for those samples.

5.4 Using Voltage Contrasts To Evaluate Voltage Variations

Due to the subjective nature of the previous sections' data analysis, a more finessed method of evaluating the data for stitch/space intervals is needed to clarify the data for quantitative pass/fail levels. A commonly used method for evaluating the difference on data of the form presented here is to use contrasting between the upper and lower levels of the peaks. Contrasting is based on the following equation:

$$C = \frac{A - \overline{B}}{A + \overline{B}} \qquad \textbf{Eq. 5-1}$$

Where: C is the contrast;

A is the peak value; and,

$\overline{B}$ is the mean base value

And, $\overline{B}$ is derived from:

$$\overline{B} = \frac{B_1 + B_2}{2} \qquad \textbf{Eq. 5-2}$$

Where: B_1 and B_2 are two minimum values located to each side of the peak

With these two equations, the difference between the maximum and minimum of the peak at the center can be determined. The equation for the average B value is used to determine the center of the peak when there is not a measured average width useable for

the determination. The average base value and peak value are then used in Equation 5-1 to determine the contrast for comparison with other peaks and other data, such as that presented in this research.

Determination of the base values to use for Equation 5-2 for this study was based on the methodology of determining the stitch/space intervals outlined in the preceding section. This subjective method would be refined in a finished production unit, which will be discussed in the future recommendations of Chapter 6. As an example of this method for determining the contrast value for a particular peak, see Figure 5-12, below.

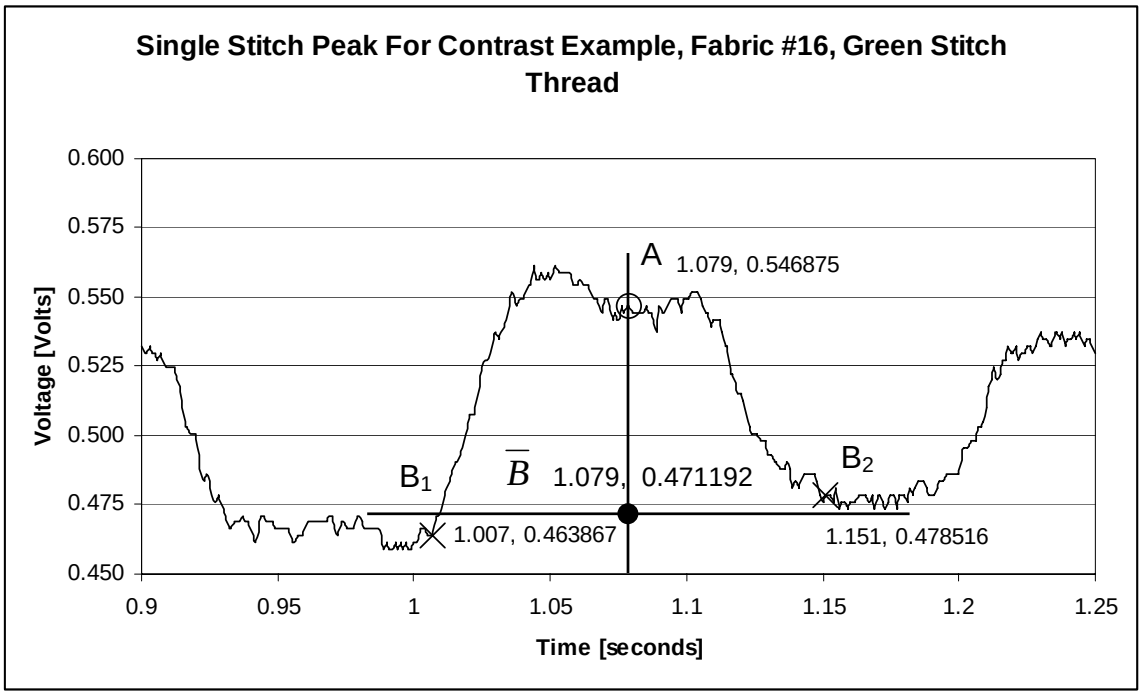

Figure 5-12 Example Graph Of Single Peak Evaluation For Contrast Measurement

This figure shows the points used to determine the values for A and $\overline{B}$. Then, using Equation 5-1, the contrast can be calculated to be 0.07434. Another way of stating

this is to say there is an approximate 74 millivolt difference between the evaluated extrema for this peak.

For this study, the determination of peaks was limited to the inner three peaks of the data taken to eliminate any errors caused in the determination of the minimum values of the outer peaks due to the rapid reduction of reflected light by the optical stops. In a few cases only two peaks were identifiable. In all cases the peaks that were evaluated presented a definable contrast which were then averaged together by fabric type and stitch thread color/diameter. The averages determined and used for comparison in this study are found in the following table, Table 5-2. A detailed table of the data collected for this contrast method can be found in the Appendix, Table A-6.

Table 5-2 Average Contrasts For Fabrics #14-19, Sorted By Thread Color

Fabric #14	Contrast		Fabric #15	Contrast
thread color	averages		thread color	averages
black	0.017934884		purple #1	0.025330725
blue	0.031600805		purple #2	0.023469617
green	0.027919912		tan #1	0.02050909
orange	0.027557339		tan #2	0.01973599
purple	0.039821046			
red	0.020285658			
tan	0.027734148			
white	0.024384065			
Fabric #16			**Fabric #17**	
black	0.039609686		purple #1	0.025395649
blue	0.059011771		purple #2	0.023770527
green	0.057256573		tan #1	0.030131177
orange	0.045728212		tan #2	0.030432135
purple	0.068233395			
red	0.05995745			
tan	0.088279939			
white	0.053418673			
Fabric #18			**Fabric #19**	
black	0.171281835		purple #1	0.047451108
blue	0.168991255		purple #2	0.048338998
green	0.088338555		tan #1	0.028011541
orange	0.110667353		tan #2	0.023369255
purple	0.1215722			
red	0.097045971			
tan	0.198555763			
white	0.065021535			

The left columns of Table 5-2 show the averages for three peaks for fabrics #14, 16, and 18 for each of the stitch thread colors used. These will be used to compare different types of materials and different thread diameters for the voltage contrast. The right columns show the averaged data for fabrics #15, 17, and 19 for the minimum and

maximum thread diameters used in this study. There are two sets for each thread diameter indicating the data was taken on two different stitch lines. This data will be used to compare min/max thread diameter differences, and to show similarity for separate stitch lines of the same color/diameter in the same material.

5.4.1 Final Data Comparisons

To begin the data comparison, the average contrasts determined from the data were compared for the three fabrics #14, 16, and 18 for all the thread types used. The thread types were organized alphabetically, as in Table 5-2, such that thread #1 was black, #2 was blue, and so forth. Figure 5-13 shows the graphed data for these three fabrics and eight stitch threads. This figure begins to show that the difference of contrasts is not dependant upon thread color, rather that is a difference based on the sheen of the material, as expected.

Note that, according to Table 5-1 and Figure 5-13, as the sheen of the material increases, the contrast data for the fabrics increase as well. Yet, for the fabrics individually, the contrast levels stay fairly similar. This is to be expected, for if we return to Chapter 2, Figure 2-16, we see that the NIR reflectance levels for fabrics #14-19 increase slightly for each materials progressive sheen evaluation. For error calculations for the data, the separate series fall within one standard deviation according to the formula:

$$\text{Standard deviation} = \left(\frac{\sum_{i=1}^{n} (X_i - \overline{X})^2}{n-1} \right)^{1/2} \qquad \textbf{Eq. 5-3}$$

Where: X_i = individual data points;

$\overline{X}$ = average of the data; and,

n = total number of data points

According to statistical models, 68% of the data is expected to fall within one standard deviation. As the graph shows, the data for fabric #14 and 16 have 7 out of 8 points, or 88% of the data within one deviation, and fabric #16's data has 5 points, or 63% within one deviation. The larger error bars for fabric #18 are due to the wider spread of the contrasts for that series of data. This larger variation in contrast can be attributed to the subjective method of determining the base points for the peaks in the stitch/space voltage level data, and the bulging variations caused by the lower density fabric that is used in fabric #18.

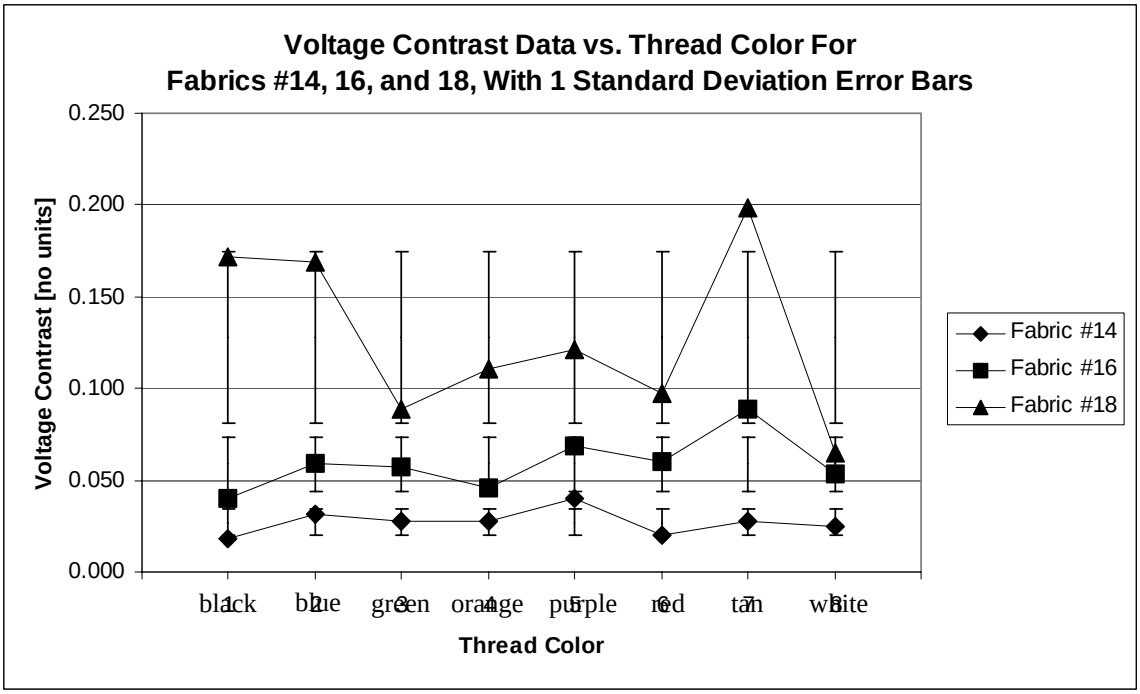

Figure 5-13 Voltage Contrast Data For Fabrics #14, 16 And 18

Another comparison made from the data organized in Table 5-2 is the voltage contrast for each of the material against the smallest and largest diameter stitch threads used, purple, 0.37mm, and tan, 0.46mm, respectively. The graph for this data can be seen below in Figure 5-14. Here, we see that the diameter of the thread only has a limited amount of effect on the reflected light and subsequent voltage contrast. This is somewhat expected as the difference in the thread diameters is a mere nine hundredths of a millimeter.

Recall from Chapter 2, where the study details the selection of materials used for this research, that these threads were specifically chosen for their general representation of threads used in the textile industry. Thus, the slight variation of diameters is common among all thread types used for forming seams: large enough to provide adequate

strength, yet small enough to not cause unwarranted damage to the fabric as the threads pass through to form a stitch.

Indeed, the contrasts for the two diameters stay relatively near to one another for each of the fabrics with only two exceptions. The two flimsiest pieces of fabric, #16 and 18, show that the contrast for the larger diameter stitch thread is higher than that of the smaller diameter. This could be caused by the difference in diameters of the threads on the surface of the fabrics, but, again, is more likely due to the thinness of the material allowing the stitch thread to force the material to bulge at the space intervals.

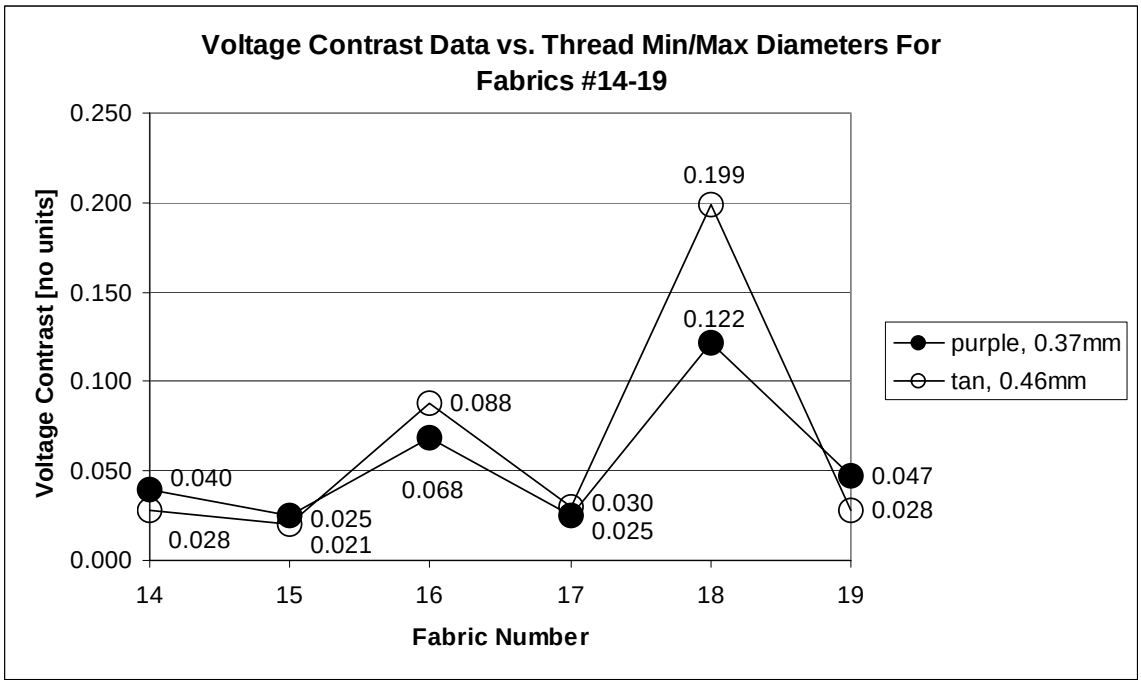

Figure 5-14 Voltage Contrast Comparison For All Fabrics vs. Min/Max Thread Diameters

Further, upon examining the data for all six fabrics for increasing thread diameter, there is no discernable increase in the contrasts, as seen in Figure 5-15, below. This graph is somewhat confusing for the fact that both the black and red threads have the same diameter. However, ignoring that and keeping in mind that the diameter increases from left to right on the graph, there is not a discernable increase for the data. This is not unexpected, as the thread diameters only range 0.09mm from smallest to largest. Only the increase at the end of the data series for fabrics #16 and 18 show the contrast rising with increase in diameter. However, given the other data series values, this is not an appreciable trend, and is more likely attributable to the thinness of the material and subsequent bulging between the stitches.

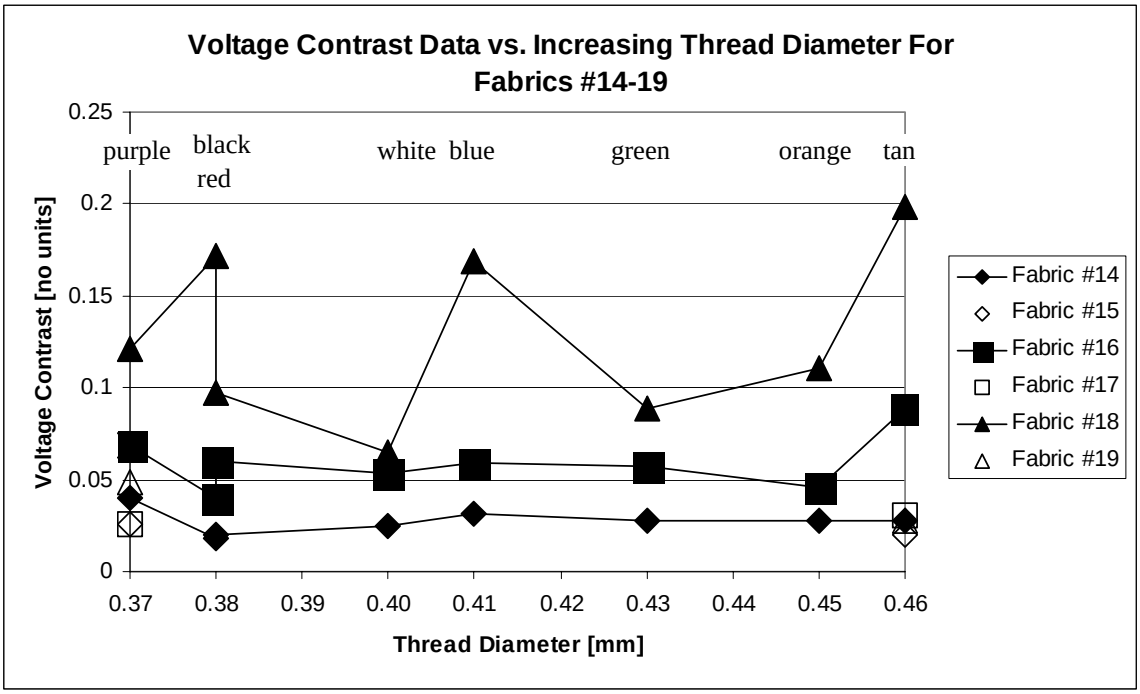

Figure 5-15 Voltage Contrast Data vs. Increasing Stitch Thread Diameter

One final comparison can be made with the data presented here to confirm once again that the color of the thread does not have an appreciable effect on the reflected light, and thus the contrast of the voltage variations between stitch and space intervals. Figure 5-16, below, shows the accepted wavelengths for five of the colors used. The other three colors, black, white, and tan, are considered an absence of color or a mixture of all or some of the colors of the visible light spectrum, respectively, and thus have no accepted average wavelength. As this data shows there is only a slightly decreasing trend in the data as the wavelength increases for the three fabrics tested, #14, 16, and 18. Consider the data presented in Chapter 2, Figure 2-10, a graph of reflectance versus NIR wavelengths for the initial set of test fabrics which show, for increasing fabric color wavelength, the amount of reflected light at the 1550nm selection decreases. This is also evident in the graph of Figure 5-16, below.

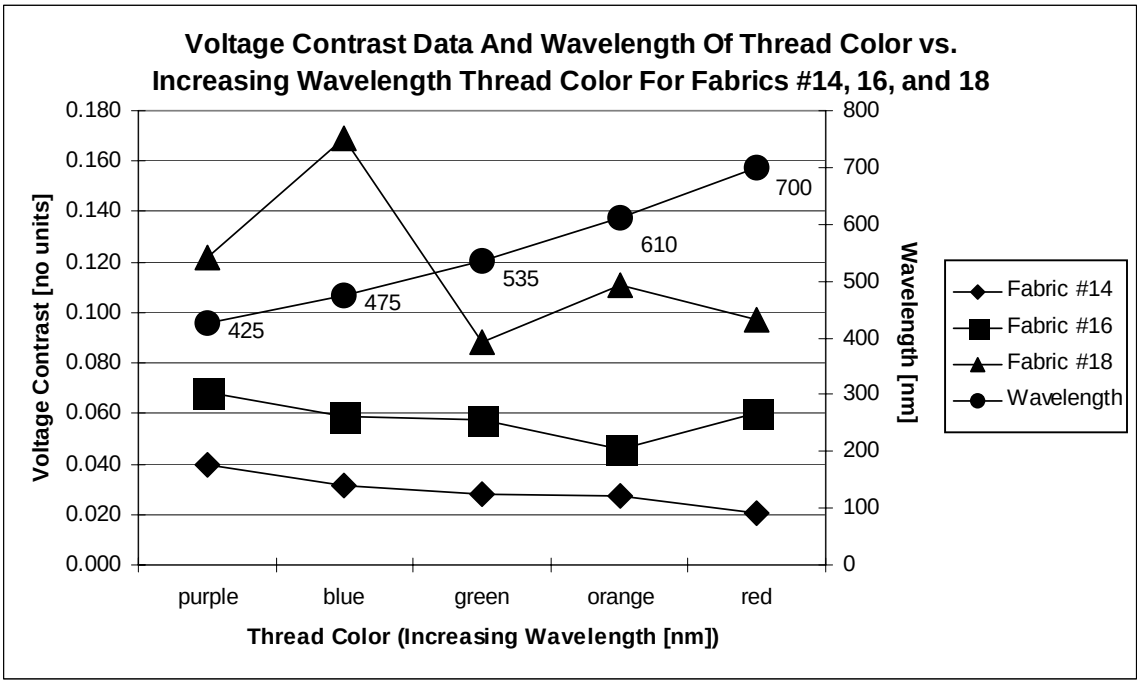

Figure 5-16 Voltage Contrast Data vs. Thread Color In Increasing Wavelength

5.5 Evaluation Of Contrast For Quality Control Pass/Fail Levels

A final analysis of the data can be made to evaluate its' use for quality control testing of properly formed stitches in a sewing application, which is the main point of this research. For this method, the contrast levels of the stitch/space intervals can be used to determine a pass/fail level. With the data collected for this study, we can begin to develop a mathematical method of determining a pass/fail qualifying level by weighting the values for the upper and lower bounds of the peaks. For a weighted mean for analysis of the levels, we start with the equation:

$$\bar{x} = \frac{\sum_{i=1}^{n} w_i x_i}{\sum_{i=1}^{n} w_i} \qquad \textbf{Eq. 5-4}$$

Where: x_i = individual data point

w_i = a weighting factor, such that:

$$\text{total weight} = \sum_{i=1}^{n} w_i \qquad \textbf{Eq. 5-5}$$

Here, the weighting factor w_i, could be a complex calculation based on voltage levels, stitch density and other factors beyond the scope of the current research.

This weighting of the data could then be used to give and upper and lower boundary for the stitch/space voltage levels which could then be used to create an "accepted" contrast level against which each individual peak could be evaluated. The

contrast levels of each peak could be qualified as pass or fail based on their contrast being within a certain percentage of this accepted contrast level.

As an example let us examine the graph of Figure 5-4c in closer detail here in Figure 5-17:

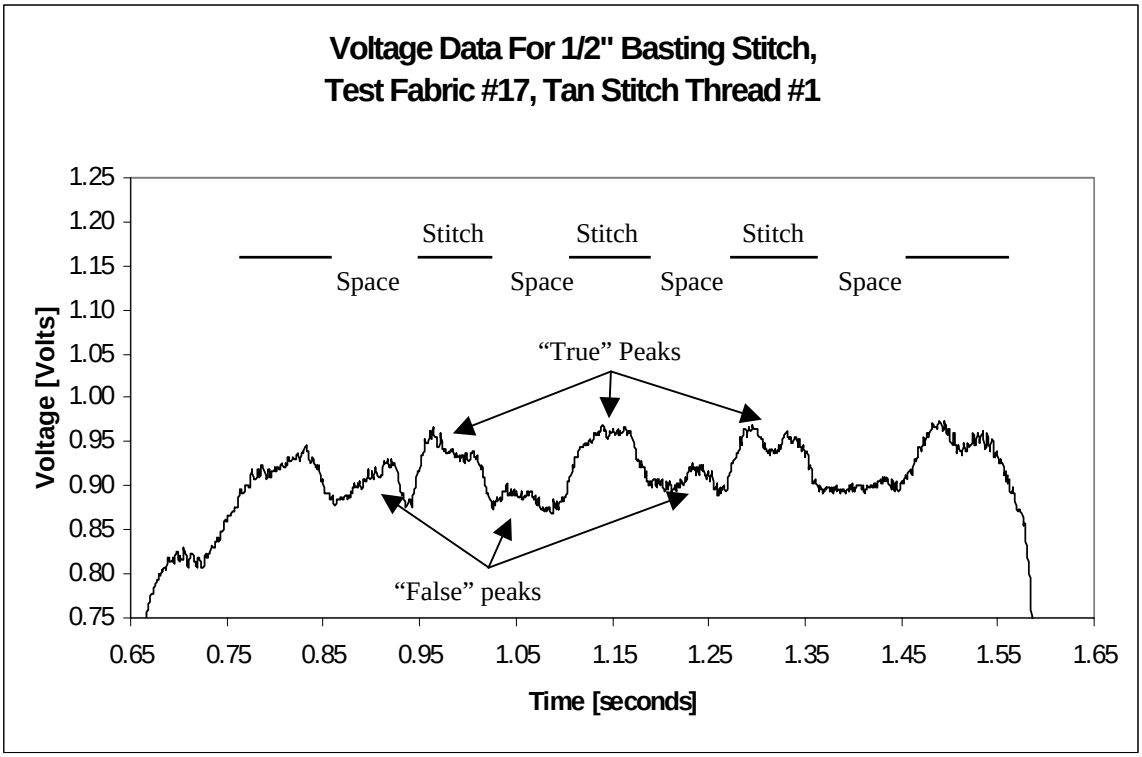

Figure 5-17 Voltage Variation Data For Stitch/Space Levels For Fabric #17, Tan Stitch Thread

This graph was chosen due to the presence of "false" peaks, namely the bulges caused by the underlying stitch thread as described in the previous section. Following the method outlined above to determine the contrast for the three inner peaks representing

stitches, the smaller, false peaks were evaluated for their contrast levels and the following table sums up their results.

Table 5-3 Contrast Data For True/False Peaks For Fabric #17, Tan Stitch Thread

	Peak #	Contrast
"True" Peaks	1	0.034251
	2	0.029547
	3	0.026596
"False" Peaks		
	1	0.016349
	2	0.006935
	3	0.012795

This table shows the evaluation of the peaks leads to different contrasts for the "true" and "false" peaks, as designated in Figure 5-17. The true peaks contrast values show the heights of the peaks to be between 25 and 35mV, while the false peaks only range between 6 and 16mV.

With the limited number of data points we have here, Equation 5-5 becomes simplified as w_i =1, and the sum of w over n points is therefore n. Thus, Equation 5-4 simplifies to a simple average:

$$\frac{1}{n}\sum_{i=1}^{n} x_i \qquad \textbf{Eq. 5-6}$$

Where: n = total number of points; and,

x_i = individual data point

Thus, for the true peaks of Figure 5-17, the average is 0.0301313, or an average separation of base and peaks of nearly 30mV. Given that a standard deviation has 68%

of all the data fall within the maximum, a level of 20mV could be set as the acceptable pass/fail level and the three false peaks would be excluded as they are below this threshold.

In real practice, this method of determining the contrast levels for pass/fail qualifications would be slightly inverted. Instead of determining the location of false peaks, the system would need to determine false valleys. From Chapter 1, consider Figure 1-2, which shows the top view of a properly and improperly formed stitch line. The optical system developed for this research would need to look for the absence of breaks between the peaks rather than at the levels of the peaks themselves. For this research, however, the quantifying of the contrast for stitch/space intervals shows that the optical system could be used to differentiate such intervals.

Similar analysis could be done using a computer system on a real world applied assembly in a textile plant environment. Beyond the scope of this study, the analysis could be set to initiate according to a signal received by a timer/encoder attached to the sewing machines' motor. When the signal is given, the computer begins the analysis and formulates an initial pass/fail level which later peaks could be evaluated against. We've seen in the data presented here that the voltage may vary due to fluctuations in the material, or in a real world application, the vibration of the sewing machine. With the advanced speed of computers available today, the process of formulating a pass/fail level could be an ongoing process which evaluates some number of stitches at a time and then reformulates the qualifying levels as the seam production progresses.

6. Conclusion

This research has shown that the application of an optical skipped stitch detection system is a viable option to the slower, more costly efforts used currently. Through the use of spectrophotometric analysis in the near infrared and visible wavelength ranges of light, the suitable wavelength to cover a wide range of materials, weaves, and properties has been seen to lie in the NIR range. This range is less susceptible to variations caused by material, weave and color. By selecting an affordable laser diode and matching photodiode in the 1550nm wavelength, the research has shown that the levels of light reflected back from the surface of a seam can be used to determine a pass/fail level for the identification of skipped stitches.

6.1 Future Recommendations

Further research on this subject would effectively cover three areas for improvement and implementation of the system. First, selection of an optics arrangement that produced a smaller spot would aid in carrying the system over from inspecting a hand made stitch to the inspection of a machine produced stitch. As the true application stitches are actually end to end in formation, rather than separated by a space as the stitch type used in this study, a smaller spot size is needed to allow the system to focus on the seam in a stitch by stitch analysis. Then, as the spot moves over the area where the thread drops below the surface of the fabric, the difference in reflected light would be noted and categorized as a properly formed stitch, or if the thread does not form properly, the change in reflected light would not be detected and an operator could be informed of a faulty stitch.

A second area that further research may cover is the application of the device onto a sewing machine. The design and manufacture of the system would need to include allowances for vibration of the system, minimized package size to keep the device out of the operators way, and simple attachment measures for attaching the device to different types of seaming machines. In the research done by Cox [4], the application of a piezo-electric tensiometer to the top threads in a seam sewing application is tied in via an encoder system to time the motion of the thread across the sensor with the downward motion of the needle. In his research, the timing and voltage produced by the tensiometer were crucial variables in the determination of a properly formed stitch. A similar application could be tied in with the research presented here with few modifications. Knowing the stitch density, or stitches/inch, ranging from 8 to 12 generally, and a precise location of the laser spot on the sewn seam, a computer system could uses the encoder information to evaluate where a stitch/space interval should occur and further qualify a properly formed stitch line for an entire seam length.

Finally the system would need the methodology of determining stitch pass/failure levels refined. With further data collection in a real world application, a better understanding of the form of the data received may show a truer way of determining a pass/fail level that could be applied for all materials, all seam types and all stitch types. With the advancement in the computer industry, a rapid “learning” system could be used to collect a library of standard levels and values that might be used across the entire textile industry. Alternately, with the tie in of a computer/encoder system, a method could be developed for a time-based investigation for skipped stitches. Combining a better understanding of the form of the data collected, and a time-based mapping for the

form, the optical skipped stitch detection system could be applied in a textile factory setting for reliable quality control.

Literature Citations

1. Bahners, Thomas, E Schollmeyer, M Magel, H Fuchs, R Seifert, P Raue and P Offermann "Surface Characterization of Textile Fabrics Part 2 : Modern Mathematical Profile Evaluation Process" *Melliand Textilberichte* pp. 181-3 (pp. E46-47), March 1994.

2. Bellio, Stephen L "Method and Apparatus for Detecting Skipped Stitches for a Chain Stitch Sewing Machine" US Patent #5233936 Issued August 10, 1993.

3. Brydon, Alan "The Laser Card Web Monitor" *Textile Technology International* pp. 238-40, 1991.

4. Cox, Robert Norman "Analysis of Sewing Dynamics to Recognize and Model Stitch Formation Defects in the 401 Chainstitch" *Masters Thesis, North Carolina State University*, 1997.

5. Dobrjanskyj, Leo "Skipped Stitch Detection System" US Patent #4170951 Issued October 16, 1979.

6. Fieguth, Paul W and DH Staelin "High-Accuracy Profiler That Uses Depth From Focus" *Applied Optics* pp. 686-9, Vol. 33, No. 4, 1 February 1994.

7. Fuchs, Hilmar, M Magel, P Offermann, P Raue, E Schollmeyer and T Bahners "Surface Characterization of Textile Fabrics Part 1 : Surface Characterization Parameters" *Melliand Textilberichte* pp. 30-3 (pp. E13-15), January 1993.

8. Kuznair, Michael "A Break In The Action" *The Needle's Eye* pp. 28-31 December 1988 - January 1989.

9. Liu, Wei, Y Tan, and X Wang "Electronic Speckle Pattern Interferometry Using Mulitmode Fiber Optic Bundles for Sensing Measurement" *SPIE Optical Sensors* pp. 112-8, Vol. 1814, 1992.

10. Mizunuma, M, S Ogawa, C Nishimura, and H Kuwano "A Displacement Measurement Method by Laser-Beam Scanning for Mapping the Interior Geometry of Pipes" *Transactions of the ASME* pp. 188-92, Vol. 116, May 1994.

11. Nickolay, Bertram "Automatic Fabric Inspection - Utopia or Reality?" *Melliand Textilberichte* pp. 70-6 (pp. E33-7), January 1993.

12. Obry, Norbert "Successful Innovation in Industrial Sewing" *JSN International* pp. 28-32, September 1991.

13. Porat, I and MJ Alagha "An Optical Technique to Detect Miss Stitch in Real Time" *International Journal of Clothing Science and Technolog*y pp. 23-27, Vol. 4, No. 4, 1992.

14. Ramgulam, RB, J Amirbayat and I Porat "Measurement of Fabric Roughness by a Non-contact Method" *Journal of the Textile Institute* pp. 99-106, Vol. 84, No. 1, 1993.

15. Ribolzi, S, J Merckle, J Gresser and PE Exbrayat “Real-Time Fault Detection On Textiles Using Opto-electronic Processing” *Textile Research Journal* 63(2) pp. 61-71, February 1993.

16. Rockerath, John L and JH Blum “Skipped Stitch Detector for Chain Stitch Sewing Machines” US Patent #4102283 Issued July 25, 1978.

17. Sick, Erwin “Detection Apparatus for Finding Holes in Webs” US Patent #4302105 Issued November 24, 1981.

18. Sodomka, Lubomir and Jiri Komrska “Laser Diffraction Measurements of the Parameters of Fine-Mesh Woven Textiles” *Textile Research Journal* pp. 232-6, April 1991.

19. Stenemur, Bertil “Method and Device For Monitoring Fiber Orientation Distribution and Web Uniformity On Running Webs of Paper and Nonwovens Based on Light Diffraction Phenomenon” *INDA Journal* pp. 42-5, Vol. 4, No. 2, Spring 1992.

20. Toba, E and M Sawaji “The Detection of Defects in Woven Fabrics by Means of Laser Light” *Journal of the Textile Institute* pp. 42-54, Vol. 73, No. 2, March/April 1982.

21. Tsai, I-Shou, C-H Lin, and J-J Lin “Applying an Artificial Neural Network to Pattern Recognition in Fabric Defects” *Textile Research Journal* pp. 123-31, Vol. 65, No. 3, 1995.

22. Tsai, I-Shou, K Shentu, C-H Lin and C-K Lu “Pattern Recognition of Fabric Representation Structure By Image Processing” *Melliand Textilberichte* pp. 77-80 (pp. E37-38), January 1993.

23. Viertel, Ellen “Structure Sensor For Measuring Thread and Stitch Counts” *Melliand Textilberichte* pp. 536-7 (pp. E222-3), July 1991.

24. Von Stein, Walter “Running Several Tufting Machines With One Operative” *Textile Praxis International* pp. 714-6 (pp. VI-VII), Vol. 43, No. 7, July 1988.

25. Wiese, David R “Automating the Inspection of Carpets -- With Lasers” *American Textile Institute* pp. 82-5 March 1988.

26. Zheng, K and DJ Whitehouse “The application of the Wigner distribution function to machine tool monitoring” *Proceedings of the Institute of Mechanical Engineers Part C Journal of Mechanical Engineering Science* pp. 249-64, Vol. 206, 1992.

27. “Automatic Laser-Scan Fabric Inspection” (Trade journal article, no author listed) *International Textile Bulletin Weaving* p. 214, 1982.

28. “Detection of Yarn Breakages” (Trade journal article, no author listed) *Knitting International* p. 72, July 1983.

29. “Dual Sensor Simplifies Thickness Measurements” (Trade journal article, no author listed) *Machine Design* p. 32, 7 February 1994.

30. “Getting The Breaks In Yarn Detection” (Trade journal article, no author listed) *Textile Month* pp. 32,35, May 1992.

31. “Inspection System For Piecegoods” (Trade journal article, no author listed) *ITS/ITI Documentation* pp. 77-8 1993.

32. “Measuring System For Textile Goods” (Trade journal article, no author listed) *Chemiefasern/Textilendustrie* p. 406 (p. E61), Vol. 43/95, May 1993.

33. “Non-contact, Opto-electronic Measurements In The Production Process of Running Nonwoven and Textile Rolls” (Trade journal article, no author listed) *Melliand Textilberichte* pp. 712-4 (pp. E334-5), September 1990.

34. “Optical Crimp Control in Synthetic Staple Fiber Production” (Trade journal article, no author listed) *Chemiefasern/Textilendustrie* p. 399 (p. E43), Vol. 44/96, June 1994.

35. “Practice for Conditioning Textiles for Testing”, *American Society for Testing and Measurement (ASTM)*, Standard D 1776, 1990.

36. “Sewing Solutions” (Trade journal article, no author listed) *Apparel International* pp. 8,11, May 1994.

37. “Standard Test Method for Fabric Count of Woven Fabric”, *American Society for Testing and Measurement (ASTM)*, Standard D 3775, 1990.

38. “Standard Test Methods for Mass Per Unit Area (Weight) of Woven Fabric”, *American Society for Testing and Measurement (ASTM)*, Standard D 3776, 1990.

39. “Standard Test Method for Yarn Crimp or Yarn Take-up in Woven Fabric”, *American Society for Testing and Measurement (ASTM)*, Standard D 3883, 1990.

40. “Standard Methods for Testing Sewing Threads”, *American Society for Testing and Measurement (ASTM)*, Standard D 204, 1986.

41. “Thread Pitch Measurement” (Trade journal article, no author listed) *Wool Record* p. 17, January 1994.

Appendix

Appendix List Of Tables

Table A-1 Test Fabrics' Manufacturers' Description Table

Fabric #	Description	Source	Source ID #'s
1*	white cotton twill	Testfabrics, Inc.	423
2*	tan cotton twill	Levi Mfg., Inc.	3908
3*	beige cotton twill	Levi Mfg., Inc.	2480
4*	dark green cotton twill	Levi Mfg., Inc.	7225
5*	blue #1 cotton twill (brightest blue)	Levi Mfg., Inc.	20270
6*	blue #2 cotton twill (2nd brightest blue)	Levi Mfg., Inc.	3826
7*	blue #3 cotton twill (3rd brightest blue)	Levi Mfg., Inc.	1662
8*	black #1 cotton twill (gray warp, white weft)	Levi Mfg., Inc.	37615
9*	black #2 cotton twill (black warp, white weft)	Levi Mfg., Inc.	(no number)
10*	black #3 cotton twill (black warp, black weft)	Levi Mfg., Inc.	27690
11**	airbag #1 (nylon, loosest weave)	Reeve's Automotive Airbag	Loom #45; Style 000827-2000
12**	airbag #2 (nylon, middle weave)	Reeve's Automotive Airbag	Loom #37; Style 00050-2000
13**	airbag #3 (nylon, tightest weave)	Reeve's Automotive Airbag	Loom #18; Style 00032-2000
14+	White, bleached mercerized cotton twill	Testfabrics, Inc.	423
15+	White, spun nylon 6.6, Dupont type 200 woven fabric	Testfabrics, Inc.	361
16+	White, filament nylon 6, tricot-bright	Testfabrics, Inc.	322
17+	White, filament nylon 6.6, semi-dull taffeta, scoured, heat set	Testfabrics, Inc.	306A
18+	White, acetate satin, bright filament yarn	Testfabrics, Inc.	100
19+	White, acetate tricot, all delustered filament	Testfabrics, Inc.	122

* Ordered for darker color

** Ordered in increasing tightness of weave, finish on the samples looks/feels the same, ID #'s were written on fabric with magic marker by loom operators

\+ Fabrics are all white to remove variability of dye, ordered in increasing glossiness or sheen according to visual inspection

Table A-2 Physical Parameters For Fabrics #1-13 And Eight Stitch Threads

Fabric #	Weight [oz/yd^2]	Weight [g/m^2]	Avg. Yarn Count [per inch]	Avg. Yarn Crimp Ratio [unitless]		Avg. Yarn Take-up Ratio [unitless]		Avg. Diameter [mm]	
			warp x weft	warp	weft	warp	weft	warp	weft
1	7.74	263	116 x 51	3.53	9.27	3.41	8.49	0.23	0.27
2	14.8	503	57 x 46	17.4	7.29	14.8	6.79	0.38	0.49
3	14.4	488	60 x 46	14.6	7.412	12.8	6.91	0.41	0.46
4	14.3	485	54 x 48	16.3	6.62	14.0	6.21	0.43	0.48
5	14.7	500	46 x 45	18.5	6.29	15.6	5.92	0.42	0.47
6	15.5	527	59 x 46	14.1	7.42	12.4	6.91	0.46	0.43
7	14.2	482	45 x 46	15.1	6.11	13.1	5.76	0.43	0.48
8	14.3	484	51 x 47	20.8	5.89	17.2	5.57	0.44	0.47
9	14.8	504	48 x 44	12.6	6.53	11.2	6.13	0.41	0.48
10	14.0	474	44 x 45	16.5	6.80	14.1	6.37	0.46	0.52
11	4.33	147	19 x 21	1.53	1.07	1.51	1.06	0.92	0.74
12	5.71	194	25 x 26	0.93	2.67	0.93	2.60	1.03	0.97
13	5.47	185	49 x 50	2.65	2.58	2.58	2.52	0.58	0.60
Stitch Threads									
Black									0.38
Blue									0.41
Green									0.43
Orange									0.45
Purple									0.37
Red									0.38
Tan									0.46
White									0.40

Table A-3a Visible Spectrophotometric Data For Fabrics #1-4

Fabric #, Warp color, Weft color	Light Type*	Luminosity L*	Red/Green Content a*	Yellow/Blue Content b*
	Scale:	Dark → bright (0 → 100)	Red → Green (-20 → +20)	Yellow → Blue (-20 → +20)
1 white, white	D	95.51	-0.55	3.40
	F	95.63	-0.41	3.86
	C	95.50	-0.64	3.41
2 tan, tan	D	85.19	1.96	14.55
	F	85.94	1.29	16.51
	C	85.20	1.50	14.65
3 beige, white	D	59.12	3.64	15.52
	F	59.97	2.49	17.63
	C	59.14	3.10	15.65
4 green, white	D	32.73	-4.18	3.96
	F	32.62	-3.04	4.23
	C	32.70	-4.19	3.97

* D = Northern Daylight (blue sky); F = Fluorescent (experimental lab); C = Full Sunlight

Table A-3b Visible Spectrophotometric Data For Fabrics #5-10

Fabric #, Warp color, Weft color	Light Type*	Luminosity L*	Red/Green Content a*	Yellow/Blue Content b*
	Scale:	Dark → bright (0 → 100)	Red → Green (-20 → +20)	Yellow → Blue (-20 → +20)
5 blue, white (brightest)	D	23.17	0.20	-8.15
	F	22.69	0.19	-9.35
	C	23.17	0.41	-8.21
6 blue, white (medium)	D	24.95	-0.70	-6.86
	F	24.51	-0.40	-7.95
	C	24.95	-0.39	-6.93
7 blue, white (dull)	D	24.06	0.09	-7.08
	F	23.64	0.09	-8.18
	C	24.06	0.49	-7.15
8 gray, white	D	31.69	0.71	-1.49
	F	31.62	0.46	1.67
	C	31.69	0. 76	-1.51
9 black, white	D	22.90	-0.33	0.47
	F	22.90	-0.12	0.56
	C	22.90	-0.22	0.49
10 black, black	D	13.71	0.11	-1.04
	F	13.65	0.02	1.24
	C	13.71	0.07	-1.07

* D = Northern Daylight (blue sky); F = Fluorescent (experimental lab); C = Full Sunlight

Table A-3c Visible Spectrophotometric Data For Fabrics #11-13

Fabric #, Warp color, Weft color	Light Type*	Luminosity L*	Red/Green Content a*	Yellow/Blue Content b*
	Scale:	Dark → bright (0 → 100)	Red → Green (-20 → +20)	Yellow → Blue (-20 → +20)
11 white, white (loose weave)	D	92.33	-1.47	2.55
	F	92.36	-1.08	2.87
	C	92.32	-1.58	2.56
12 white, white (medium weave)	D	93.29	-1.21	1.85
	F	93.31	0.88	2.18
	C	93.29	-1.26	1.88
13 white, white (tight weave)	D	93.23	-1.66	2.92
	F	93.28	-1.19	3.34
	C	93.22	-1.74	2.94

* D = Northern Daylight (blue sky); F = Fluorescent (experimental lab); C = Full Sunlight

Table A-4 Physical Parameters For Fabrics #14-19, Final Test Fabrics

Fabric #	Weight [oz/yd^2]	Weight [g/m^2]	Avg. Yarn Count [per inch]	Avg. Yarn Crimp Ratio [unitless]		Avg. Yarn Take-up Ratio [unitless]		Avg. Diameter [mm]	
			warp x weft	warp	weft	warp	weft	warp	weft
14	7.60	258	112 x 52	2.99	9.46	2.90	8.64	0.31	0.35
15	3.65	124	52 x 44	2.88	13.6	2.80	12.0	0.20	0.21
16	2.15	73	40 x 23	4.50	6.25	4.31	5.88	0.31	0.33
17	1.74	59	104 x 85	2.70	4.32	2.63	4.15	0.22	0.23
18	2.71	92	65 x 92	1.09	1.82	1.08	1.79	0.23	0.23
19	2.30	78	50 x 92	0.90	5.32	0.89	5.05	0.30	0.33

Table A-5 Photodiode Angle Testing Data Table

Position ΘR.Φ	Minimum Voltage [Volts]	Maximum Voltage [Volts]	Difference [Volts]	Discernability
11.000	maxed out			
11.030	maxed out			
11.045	maxed out			
11.060	maxed out			
11.090	maxed out			
12.000	maxed out			
12.030	maxed out			
12.045	bracket blocks			
12.060	bracket blocks			
12.090	bracket blocks			
13.000	1.50	1.25	0.25	barely
13.030	1.25	1.00	0.25	barely
13.045	1.50	1.25	0.25	barely, worse
13.060	1.75	1.50	0.25	barely, worse
13.090	2.00	1.50	0.50	not at all
14.000	1.50	1.00	0.50	not at all
14.030	1.50	1.00	0.50	not at all
14.045	1.50	1.00	0.50	not at all
14.060	1.50	1.00	0.50	not at all
14.090	1.75	1.50	0.25	not at all
21.000	maxed out			
21.030	maxed out			
21.045	bracket blocks			
21.060	bracket blocks			
21.090	bracket blocks			
22.000	bracket blocks			
22.030	bracket blocks			
22.045	maxed out			
22.060	maxed out			
22.090	bracket blocks			
23.000	1.25	1.00	0.25	barely
23.030	1.50	1.25	0.25	barely
23.045	1.75	1.50	0.25	barely, worse
23.060	2.00	1.75	0.25	not at all
23.090	2.00	1.50	0.50	not at all
24.000	1.75	1.00	0.75	not at all
24.030	1.75	1.00	0.75	barely
24.045	1.50	1.25	0.25	barely
24.060	1.50	1.25	0.25	barely
24.090	1.75	1.50	0.25	barely

Table A-5 (Continued)

Position ΘR.Φ	Minimum Voltage [Volts]	Maximum Voltage [Volts]	Difference [Volts]	Discernability
31.000	maxed out			
31.030	bracket blocks			
31.045	bracket blocks			
31.060	bracket blocks			
31.090	bracket blocks			
32.000	1.75	1.50	0.25	barely
32.030	2.00	1.75	0.25	barely
32.045	2.00	1.75	0.25	barely
32.060	bracket blocks			
32.090	maxed out			
33.000	1.50	1.25	0.25	barely
33.030	1.75	1.50	0.25	barely
33.045	2.00	1.75	0.25	barely, worse
33.060	2.50	1.75	0.25	barely, worse
33.090	bracket blocks			
34.000	1.25	1.00	0.25	barely
34.030	1.50	1.25	0.25	barely
34.045	1.75	1.50	0.25	barely, worse
34.060	1.75	1.50	0.25	not at all
34.090	bracket blocks			
41.000	bracket blocks			
41.030	bracket blocks			
41.045	bracket blocks			
41.060	bracket blocks			
41.090	bracket blocks			
42.000	maxed out			
42.030	maxed out			
42.045	maxed out			
42.060	bracket blocks			
42.090	bracket blocks			
43.000	1.25	1.00	0.25	barely
43.030	1.50	1.25	0.25	barely
43.045	1.50	1.25	0.25	slightly
43.060	1.50	1.25	0.25	slightly
43.090	bracket blocks			
44.000	1.25	1.00	0.25	slightly
44.030	1.25	1.00	0.25	barely
44.045	1.80	1.50	0.30	slightly
44.060	1.80	1.50	0.30	slightly
44.090	bracket blocks			

Table A-5 (Continued)

Position ΘR.Φ	Minimum Voltage [Volts]	Maximum Voltage [Volts]	Difference [Volts]	Discernability
51.000	bracket blocks			
51.030	bracket blocks			
51.045	bracket blocks			
51.060	bracket blocks			
51.090	bracket blocks			
52.000	bracket blocks			
52.030	bracket blocks			
52.045	bracket blocks			
52.060	bracket blocks			
52.090	bracket blocks			
53.000	1.75	1.25	0.50	good
53.030	1.75	1.25	0.50	good
53.045	bracket blocks			
53.060	bracket blocks			
53.090	bracket blocks			
54.000	1.75	1.00	0.75	very good
54.030	1.75	1.00	0.75	very good
54.045	bracket blocks			
54.060	1.50	1.50	0.00	not at all
54.090	bracket blocks			

Table A-6 Contrast Data Evaluated From Fabrics #14-19 For Final Data Analysis

Fabric #14		Time [sec]	Voltage [Volts]	Time [sec]	Voltage [Volts]	Time [sec]	Voltage [Volts]	Time [sec]	Voltage [Volts]	Contrast	Contrast Averages
thread color	stitch #	B1		B2		B(avg.)		A			
black	1	0.716	1.064453	0.808	1.064453	0.762	1.064453	0.762	1.118164	0.024608532	
	2	0.87	1.071777	0.982	1.071777	0.926	1.071777	0.926	1.096191	0.011261236	0.017935
blue	1	0.727	1.027832	0.876	1.025391	0.802	1.0266115	0.802	1.137695	0.051325217	
	2	0.911	1.018066	1.005	1.020508	0.958	1.019287	0.958	1.083984	0.030760183	
	3	1.082	1.04248	1.204	1.04248	1.143	1.04248	1.143	1.069336	0.012717017	0.031601
green	1	0.655	0.979004	0.777	0.979004	0.716	0.979004	0.716	1.020508	0.020757065	
	2	0.827	1.020508	0.972	1.018066	0.900	1.019287	0.9	1.07666	0.027373307	
	3	1.033	0.991211	1.147	0.991211	1.090	0.991211	1.09	1.064453	0.035629364	0.02792
orange	1	0.786	1.120605	0.884	1.120605	0.835	1.120605	0.835	1.164551	0.019231072	
	2	0.968	1.135254	1.054	1.135254	1.011	1.135254	1.011	1.208496	0.03124992	
	3	1.115	1.140137	1.201	1.135254	1.158	1.1376955	1.158	1.213379	0.032191026	0.027557
purple	1	0.92	0.981445	1.102	0.981445	1.011	0.981445	1.011	1.103516	0.058548337	
	2	1.151	1.015625	1.289	1.018066	1.220	1.0168455	1.22	1.09375	0.036437347	
	3	1.329	0.996094	1.436	0.998535	1.383	0.9973145	1.383	1.047363	0.024477454	0.039821
red	1	0.547	1.020508	0.645	1.022949	0.596	1.0217285	0.596	1.079102	0.027309914	
	2	0.702	1.025391	0.797	1.025391	0.750	1.025391	0.75	1.057129	0.01524019	
	3	0.88	1.047363	0.969	1.047363	0.925	1.047363	0.925	1.086426	0.018306871	0.020286
tan	1	0.613	1.000977	0.735	0.998535	0.674	0.999756	0.674	1.057129	0.027893149	
	2	0.797	1.008301	0.916	1.008301	0.857	1.008301	0.857	1.071777	0.030516163	
	3	0.922	1.008301	1.082	1.008301	1.002	1.008301	1.002	1.05957	0.024793133	0.027734
white	1	0.823	1.103516	0.936	1.113281	0.880	1.1083985	0.88	1.152344	0.019438525	
	2	1.004	1.118164	1.163	1.118164	1.084	1.118164	1.084	1.184082	0.02863204	
	3	1.184	1.091309	1.31	1.091309	1.247	1.091309	1.247	1.147461	0.02508163	0.024384

Table A-6 (Continued)

Fabric #15		Time [sec]	Voltage [Volts]	Time [sec]	Voltage [Volts]	Time [sec]	Voltage [Volts]	Time [sec]	Voltage [Volts]	Contrast	Contrast Averages
thread color	stitch #	B1		B2		B(avg.)		A			
purple #1	1	0.732	1.037598	0.839	1.035156	0.786	1.036377	0.786	1.086426	0.023576846	
	2	0.893	1.035156	1.023	1.037598	0.958	1.036377	0.958	1.098633	0.029159582	
	3	1.064	1.025391	1.192	1.025391	1.128	1.025391	1.128	1.074219	0.023255747	0.025331
purple #2	1	0.804	1.035156	0.901	1.035156	0.853	1.035156	0.853	1.071777	0.017381189	
	2	0.949	1.035156	1.076	1.035156	1.013	1.035156	1.013	1.101074	0.030857164	
	3	1.121	1.022949	1.238	1.022949	1.180	1.022949	1.18	1.069336	0.022170498	0.02347
tan #1	1	0.81	0.998535	0.98	0.998535	0.895	0.998535	0.895	1.032715	0.016827077	
	2	1.033	1.013184	1.201	1.013184	1.117	1.013184	1.117	1.064453	0.024676592	
	3	1.272	1.015625	1.432	1.015625	1.352	1.015625	1.352	1.057129	0.020023601	0.020509
tan #2	1	0.769	0.998535	0.925	0.998535	0.847	0.998535	0.847	1.027832	0.014457894	
	2	0.991	1.015625	1.192	1.015625	1.092	1.015625	1.092	1.054687	0.018867688	
	3	1.282	1.010742	1.487	1.010742	1.385	1.010742	1.385	1.064453	0.025882387	0.019736

Table A-6 (Continued)

Fabric #16		Time [sec]	Voltage [Volts]	Time [sec]	Voltage [Volts]	Time [sec]	Voltage [Volts]	Time [sec]	Voltage [Volts]	Contrast	Contrast Averages
thread color	stitch #	B1		B2		B(avg.)		A		Contrast	
black	1	0.779	0.510254	0.908	0.510254	0.844	0.510254	0.844	0.561523	0.047835511	
	2	0.955	0.515137	1.089	0.517578	1.022	0.5163575	1.022	0.568848	0.04836918	
	3	1.131	0.527344	1.266	0.527344	1.199	0.527344	1.199	0.551758	0.022624367	0.03961
blue	1	0.675	0.527344	0.78	0.527344	0.728	0.527344	0.728	0.59082	0.056768059	
	2	0.825	0.515137	0.929	0.515137	0.877	0.515137	0.877	0.581055	0.060133626	
	3	0.969	0.515137	1.086	0.515137	1.028	0.515137	1.028	0.581055	0.060133626	0.059012
green	1	0.811	0.466309	0.932	0.466309	0.872	0.466309	0.872	0.522461	0.056789749	
	2	1.012	0.480957	1.139	0.480957	1.076	0.480957	1.076	0.546875	0.064133049	
	3	1.191	0.478516	1.326	0.478516	1.259	0.478516	1.259	0.529785	0.05084692	0.057257
orange	1	0.699	0.476074	0.824	0.478516	0.762	0.477295	0.762	0.527344	0.049817895	
	2	0.878	0.480957	1.004	0.480957	0.941	0.480957	0.941	0.534668	0.052884677	
	3	1.077	0.478516	1.22	0.478516	1.149	0.478516	1.149	0.512695	0.034482063	0.045728
purple	1	0.676	0.46875	0.81	0.46875	0.743	0.46875	0.743	0.556641	0.08571462	
	2	0.862	0.495605	0.993	0.493164	0.928	0.4943845	0.928	0.568848	0.070035011	
	3	1.034	0.498047	1.186	0.498047	1.110	0.498047	1.11	0.549316	0.048950555	0.068233
red	1	0.894	0.483398	1.021	0.480957	0.958	0.4821775	0.958	0.539551	0.056153371	
	2	1.085	0.490723	1.229	0.490723	1.157	0.490723	1.157	0.541992	0.049644868	
	3	1.271	0.488281	1.417	0.488281	1.344	0.488281	1.344	0.566406	0.074074109	0.059957
tan	1	0.755	0.490723	0.905	0.490723	0.830	0.490723	0.83	0.612793	0.110619148	
	2	0.917	0.488281	1.022	0.490723	0.970	0.489502	0.97	0.554199	0.06198806	
	3	1.076	0.456543	1.195	0.456543	1.136	0.456543	1.136	0.549316	0.092232609	0.08828
white	1	0.832	0.541992	0.968	0.541992	0.900	0.541992	0.9	0.600586	0.051282276	
	2	1.018	0.539551	1.14	0.539551	1.079	0.539551	1.079	0.603027	0.055555069	0.053419

Table A-6 (Continued)

Fabric #17		Time [sec]	Voltage [Volts]	Time [sec]	Voltage [Volts]	Time [sec]	Voltage [Volts]	Time [sec]	Voltage [Volts]	Contrast	Contrast Averages
thread color	stitch #	B1		B2		B(avg.)		A		Contrast	
purple #1	1	0.752	0.898437	0.883	0.898437	0.818	0.898437	0.818	0.9375	0.021276874	
	2	1.016	0.935059	1.098	0.935059	1.057	0.935059	1.057	0.98877	0.027918802	
	3	1.203	0.90332	1.324	0.900879	1.264	0.9020995	1.264	0.952148	0.026991273	0.025396
purple #2	1	0.674	0.874023	0.799	0.876465	0.737	0.875244	0.737	0.908203	0.018480504	
	2	0.887	0.895996	1.011	0.895996	0.949	0.895996	0.949	0.964355	0.036745216	
	3	1.083	0.895996	1.188	0.895996	1.136	0.895996	1.136	0.925293	0.01608586	0.023771
tan #1	1	0.942	0.876465	1.025	0.878906	0.984	0.8776855	0.984	0.939941	0.034250986	
	2	1.104	0.90332	1.189	0.900879	1.147	0.9020995	1.147	0.957031	0.029546877	
	3	1.268	0.893555	1.364	0.893555	1.316	0.893555	1.316	0.942383	0.026595669	0.030131
tan #2	1	1.005	0.874023	1.099	0.874023	1.052	0.874023	1.052	0.9375	0.035040681	
	2	1.191	0.895996	1.283	0.895996	1.237	0.895996	1.237	0.957031	0.032937998	
	3	1.352	0.893555	1.434	0.895996	1.393	0.8947755	1.393	0.9375	0.023317727	0.030432

Table A-6 (Continued)

Fabric #18		Time [sec]	Voltage [Volts]	Time [sec]	Voltage [Volts]	Time [sec]	Voltage [Volts]	Time [sec]	Voltage [Volts]	Contrast	Contrast Averages
thread color	stitch #	B1		B2		B(avg.)		A		Contrast	
black	1	0.89	2.011719	1.062	2.006836	0.976	2.0092775	0.976	2.871094	0.176588299	
	2	1.074	2.08252	1.223	2.092285	1.149	2.0874025	1.149	2.978516	0.175903639	
	3	1.226	2.089844	1.381	2.084961	1.304	2.0874025	1.304	2.890625	0.161353568	0.171282
blue	1	0.871	2.041016	1.046	2.036133	0.959	2.0385745	0.959	3.034668	0.196342576	
	2	1.058	2.143555	1.214	2.145996	1.136	2.1447755	1.136	2.961426	0.159933074	
	3	1.217	2.15332	1.403	2.15332	1.310	2.15332	1.31	2.91748	0.150698115	0.168991
green	1	0.872	2.148437	1.094	2.143555	0.983	2.145996	0.983	2.687988	0.112121182	
	2	1.108	2.214355	1.32	2.207031	1.214	2.210693	1.214	2.69043	0.097883077	
	3	1.338	2.302246	1.526	2.290039	1.432	2.2961425	1.432	2.563477	0.055011406	0.088339
orange	1	0.994	2.089844	1.225	2.084961	1.110	2.0874025	1.11	2.712402	0.130213533	
	2	1.234	2.126465	1.432	2.124023	1.333	2.125244	1.333	2.741699	0.126661644	
	3	1.449	2.229004	1.611	2.219238	1.530	2.224121	1.53	2.585449	0.075126882	0.110667
purple	1	0.84	2.060547	1.004	2.058105	0.922	2.059326	0.922	2.744141	0.142566817	
	2	1.011	2.102051	1.167	2.109375	1.089	2.105713	1.089	2.768555	0.135988009	
	3	1.173	2.133789	1.344	2.138672	1.259	2.1362305	1.259	2.539062	0.086161775	0.121572
red	1	0.959	2.050781	1.152	2.04834	1.056	2.0495605	1.056	2.597656	0.117940599	
	2	1.172	2.097168	1.333	2.087402	1.253	2.092285	1.253	2.587891	0.105894736	
	3	1.394	2.150879	1.615	2.145996	1.505	2.1484375	1.505	2.458496	0.067302578	0.097046
tan	1	0.739	1.77002	0.918	1.777344	0.829	1.773682	0.829	2.910156	0.242637341	
	2	0.932	1.965332	1.113	1.960449	1.023	1.9628905	1.023	2.905273	0.1935807	
	3	1.126	2.045898	1.312	2.053223	1.219	2.0495605	1.219	2.827148	0.159449247	0.198556
white	1	0.799	2.199707	0.93	2.199707	0.865	2.199707	0.865	2.541504	0.072090654	
	2	0.995	2.216797	1.102	2.177734	1.049	2.1972655	1.049	2.358398	0.035369711	
	3	1.176	2.216797	1.285	2.194824	1.231	2.2058105	1.231	2.629395	0.087604239	0.065022

Table A-6 (Continued)

Fabric #19		Time [sec]	Voltage [Volts]	Time [sec]	Voltage [Volts]	Time [sec]	Voltage [Volts]	Time [sec]	Voltage [Volts]	Contrast	Contrast Averages
thread color	stitch #	B1		B2		B(avg.)		A		Contrast	
purple #1	1	0.897	0.944824	1.009	0.944824	0.953	0.944824	0.953	1.022949	0.039702242	
	2	1.113	0.95459	1.254	0.952148	1.184	0.953369	1.184	1.030273	0.038769092	
	3	1.327	0.930176	1.453	0.930176	1.390	0.930176	1.39	1.057129	0.063881991	0.047451
purple #2	1	0.703	0.949707	0.813	0.947266	0.758	0.9484865	0.758	1.018066	0.035381461	
	2	0.916	0.944824	1.041	0.944824	0.979	0.944824	0.979	1.032715	0.044444635	
	3	1.097	0.927734	1.207	0.927734	1.152	0.927734	1.152	1.057129	0.065190897	0.048339
tan #1	1	1.001	0.859375	1.175	0.861816	1.088	0.8605955	1.088	0.927734	0.037542578	
	2	1.294	0.874023	1.405	0.876465	1.350	0.875244	1.35	0.908203	0.018480504	0.028012
tan #2	1	1.054	0.876465	1.161	0.876465	1.108	0.876465	1.108	0.932617	0.031038947	
	2	1.259	0.878906	1.343	0.881348	1.301	0.880127	1.301	0.908203	0.015699563	0.023369

Appendix List Of Figures

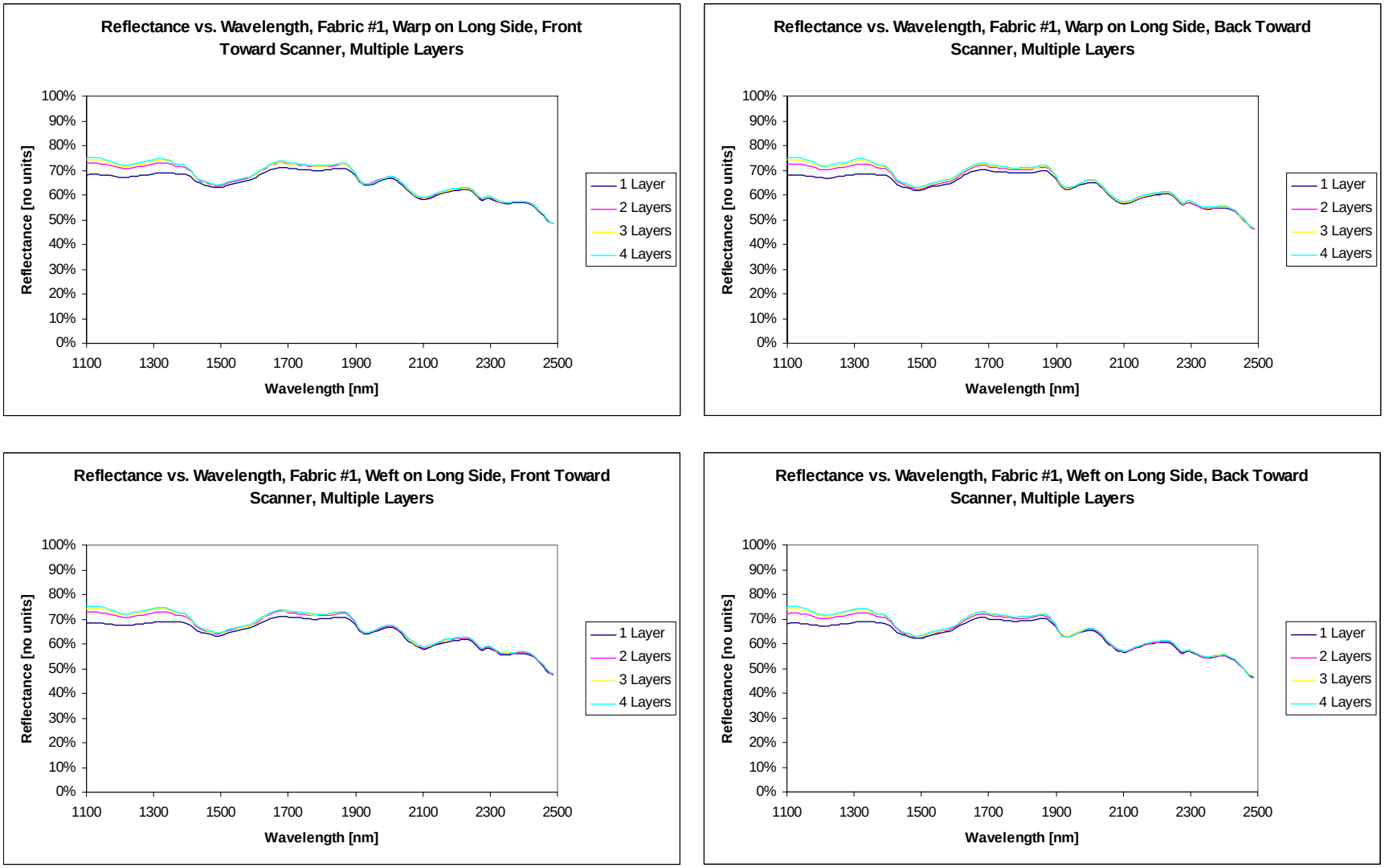

Figure A-1 Multiple Layer And Front vs. Back Comparisons For Fabric #1

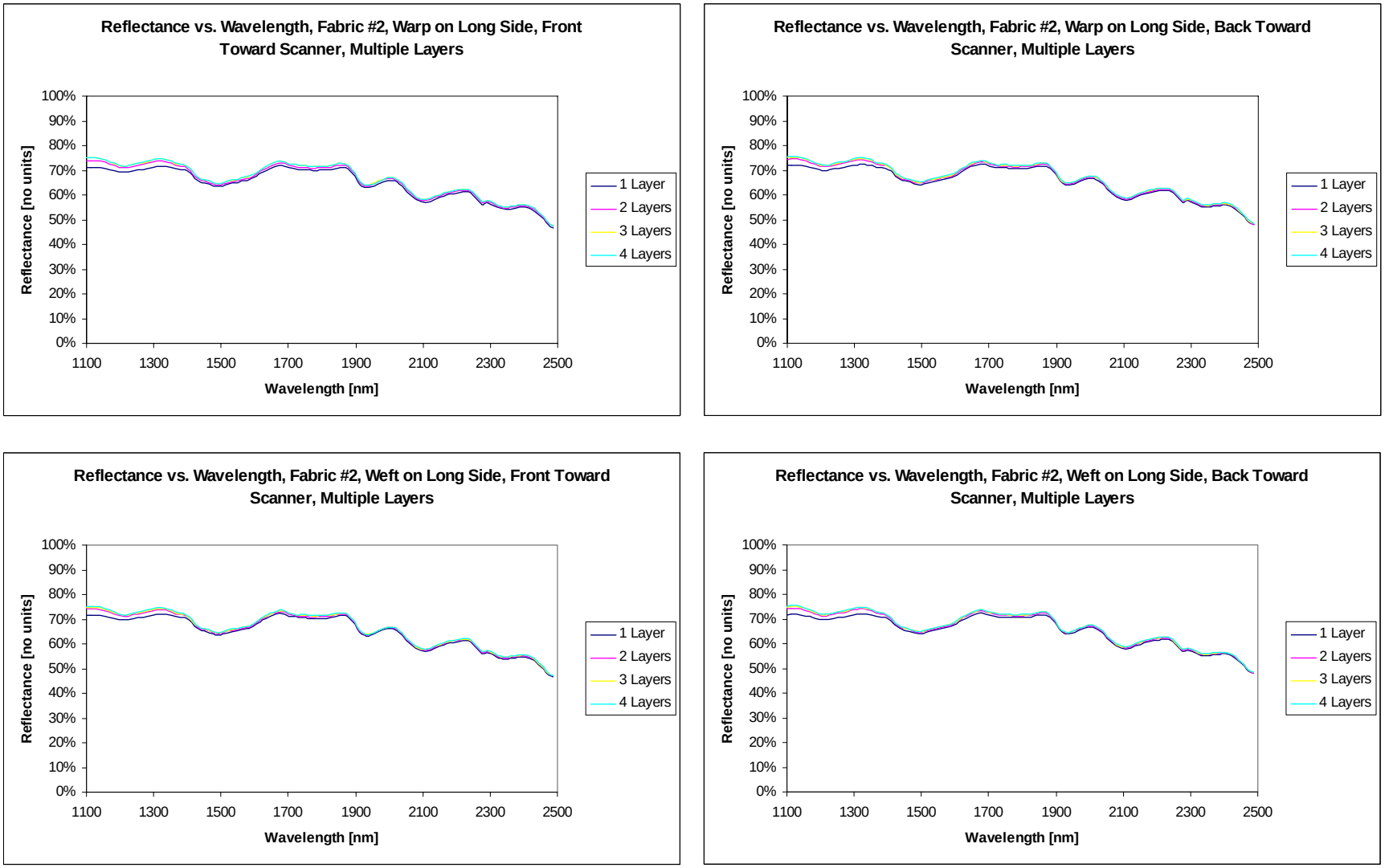

Figure A-2 Multiple Layer And Front vs. Back Comparisons For Fabric #2

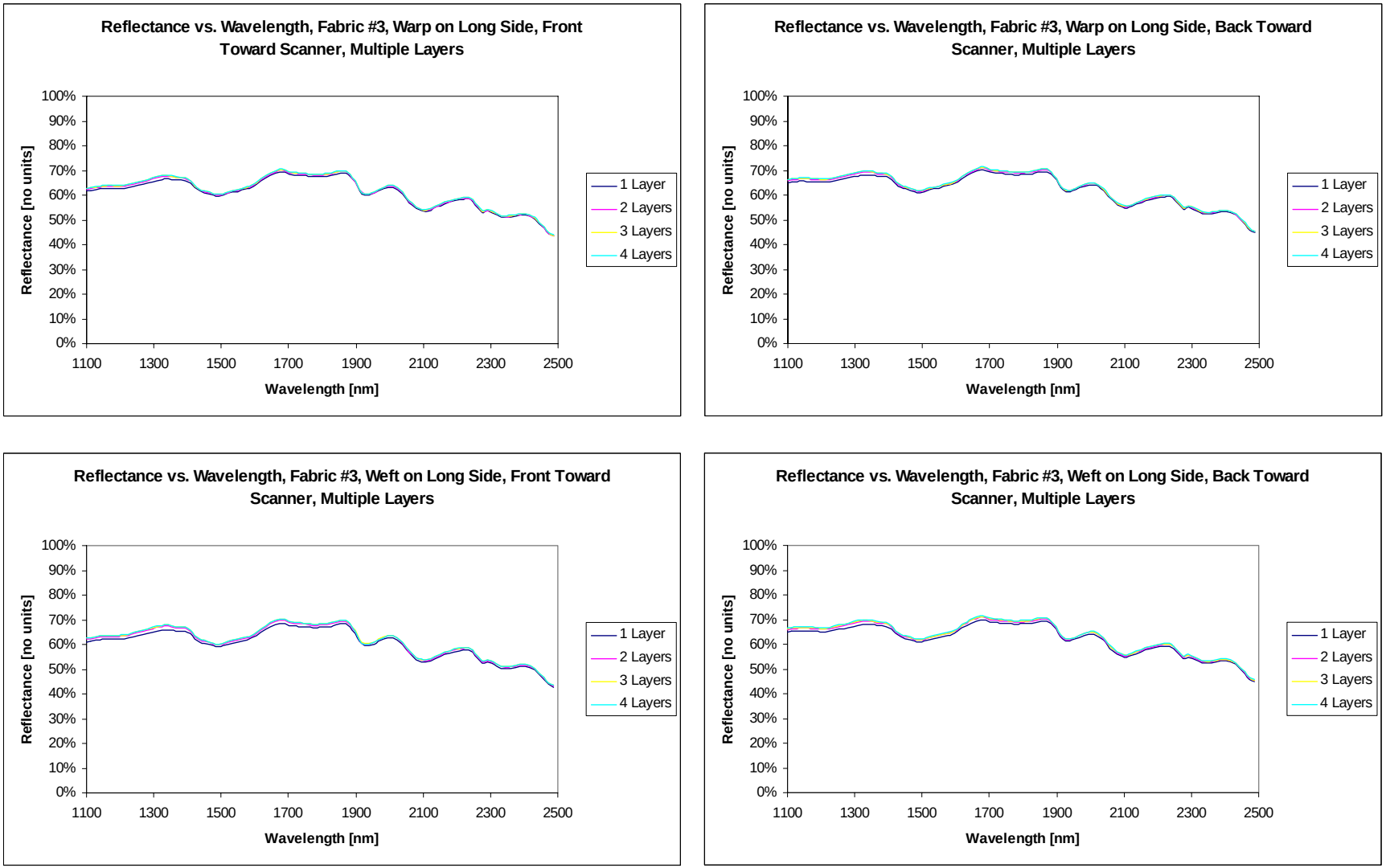

Figure A-3 Multiple Layer And Front vs. Back Comparisons For Fabric #3

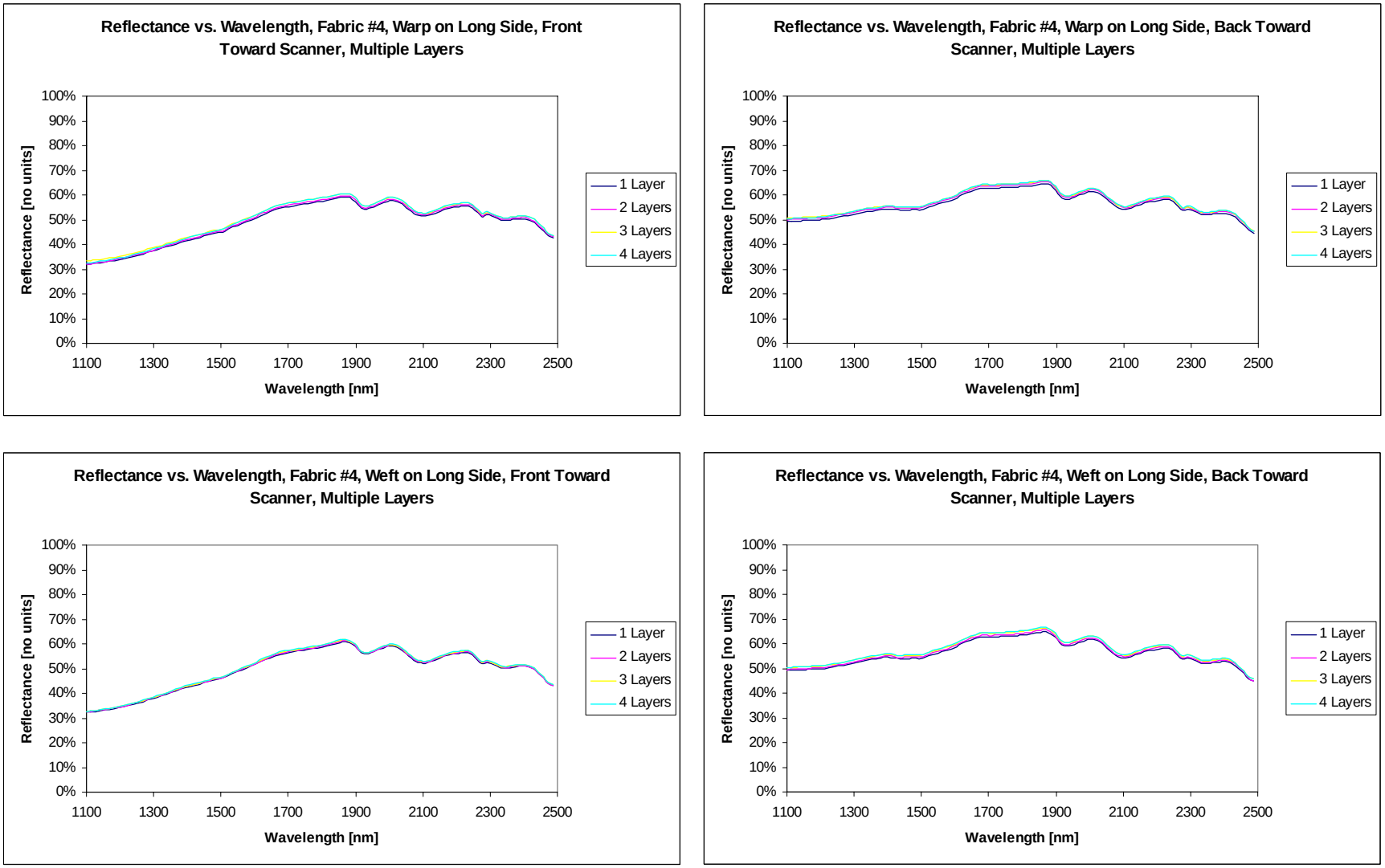

Figure A-4 Multiple Layer And Front vs. Back Comparisons For Fabric #4

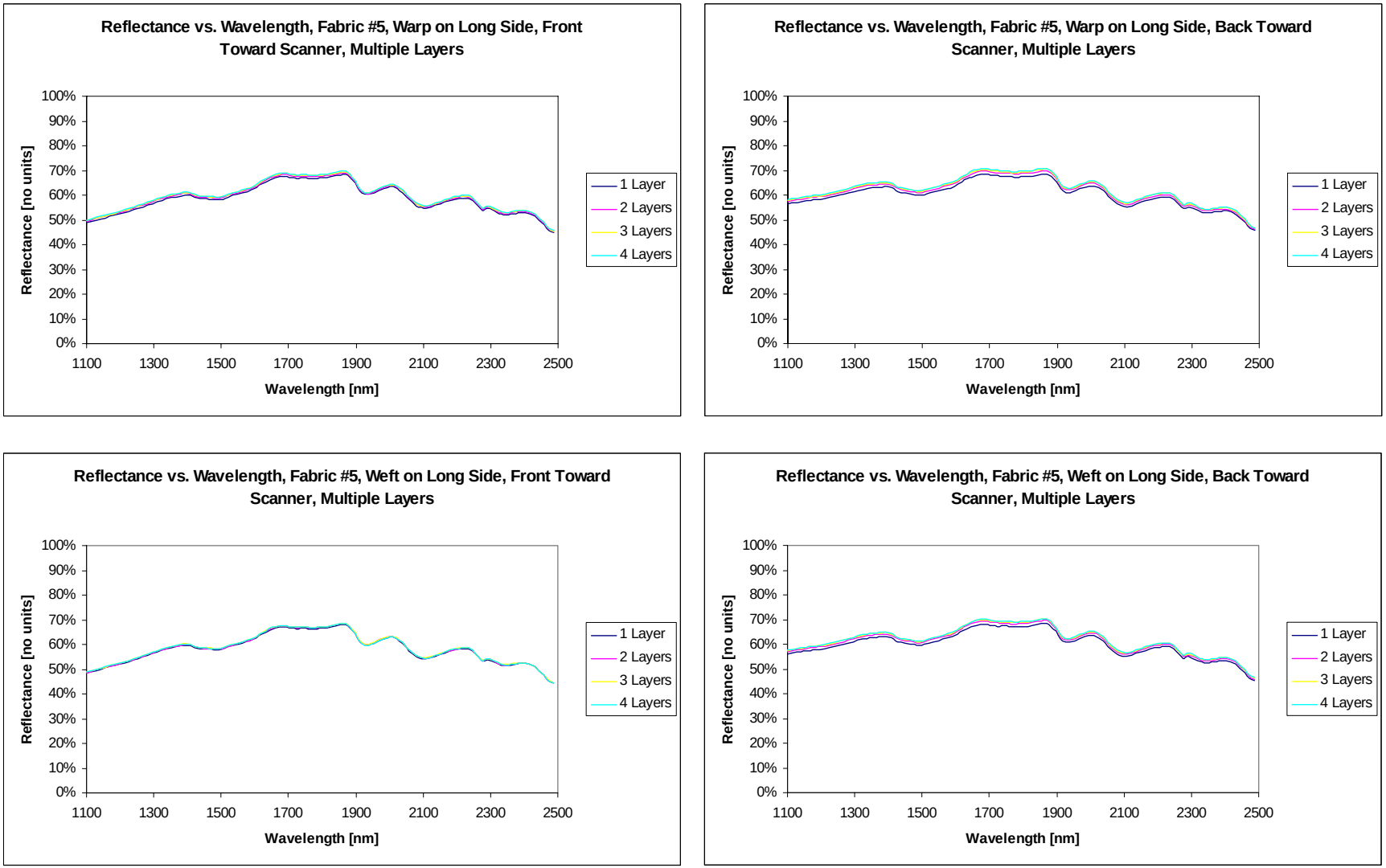

Figure A-5 Multiple Layer And Front vs. Back Comparisons For Fabric #5

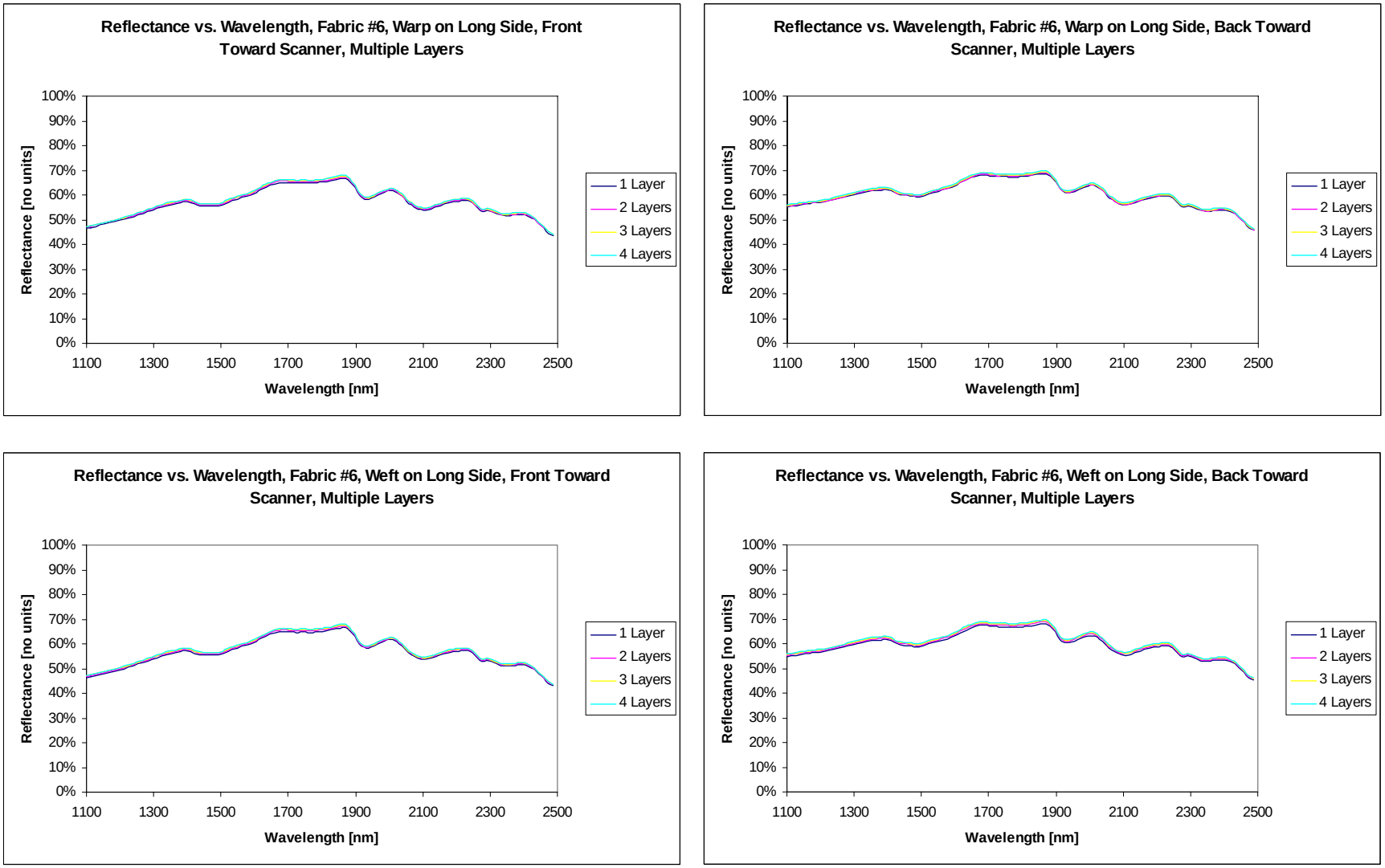

Figure A-6 Multiple Layer And Front vs. Back Comparisons For Fabric #6

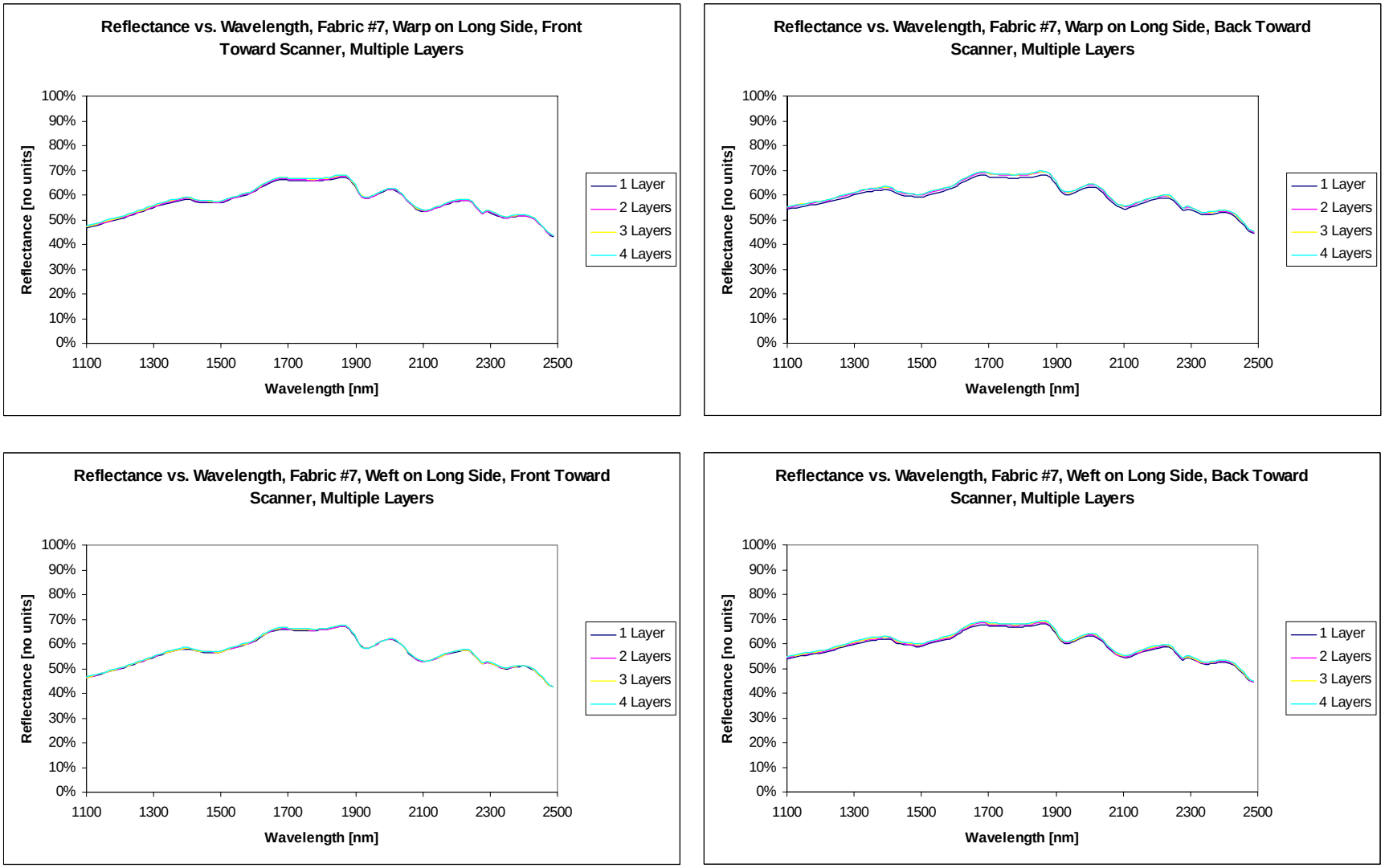

Figure A-7 Multiple Layer And Front vs. Back Comparisons For Fabric #7

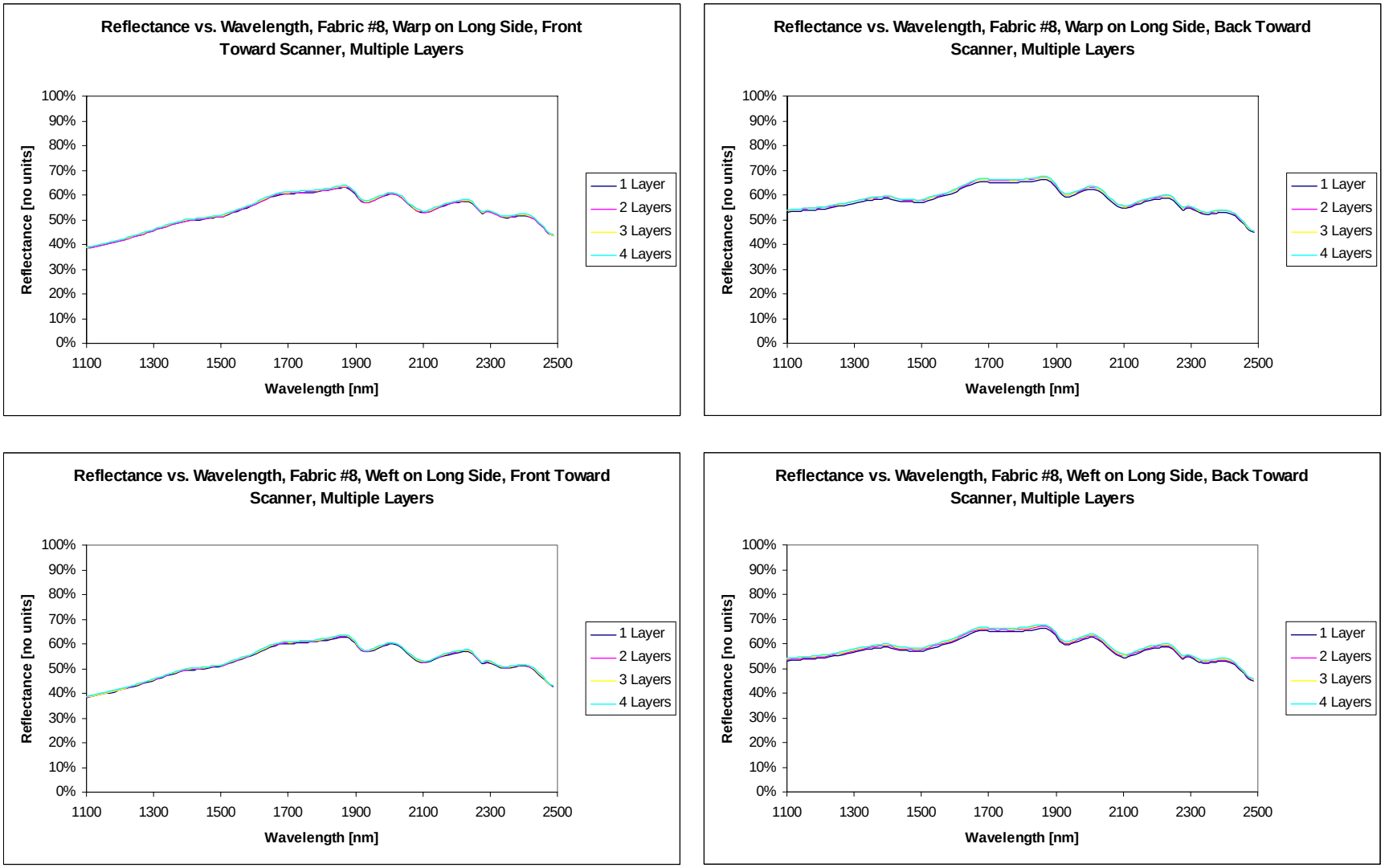

Figure A-8 Multiple Layer And Front vs. Back Comparisons For Fabric #8

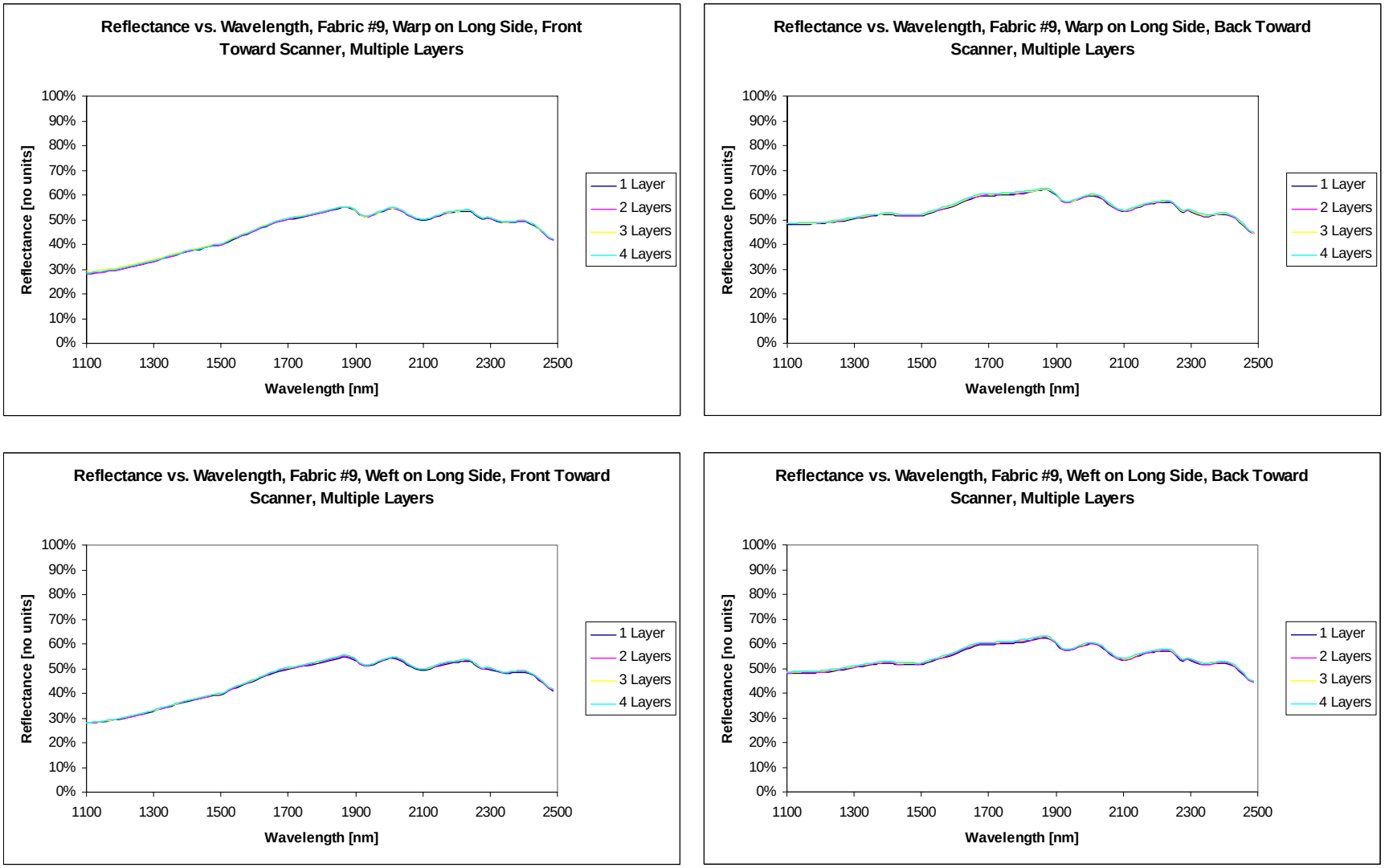

Figure A-9 Multiple Layer And Front vs. Back Comparisons For Fabric #9

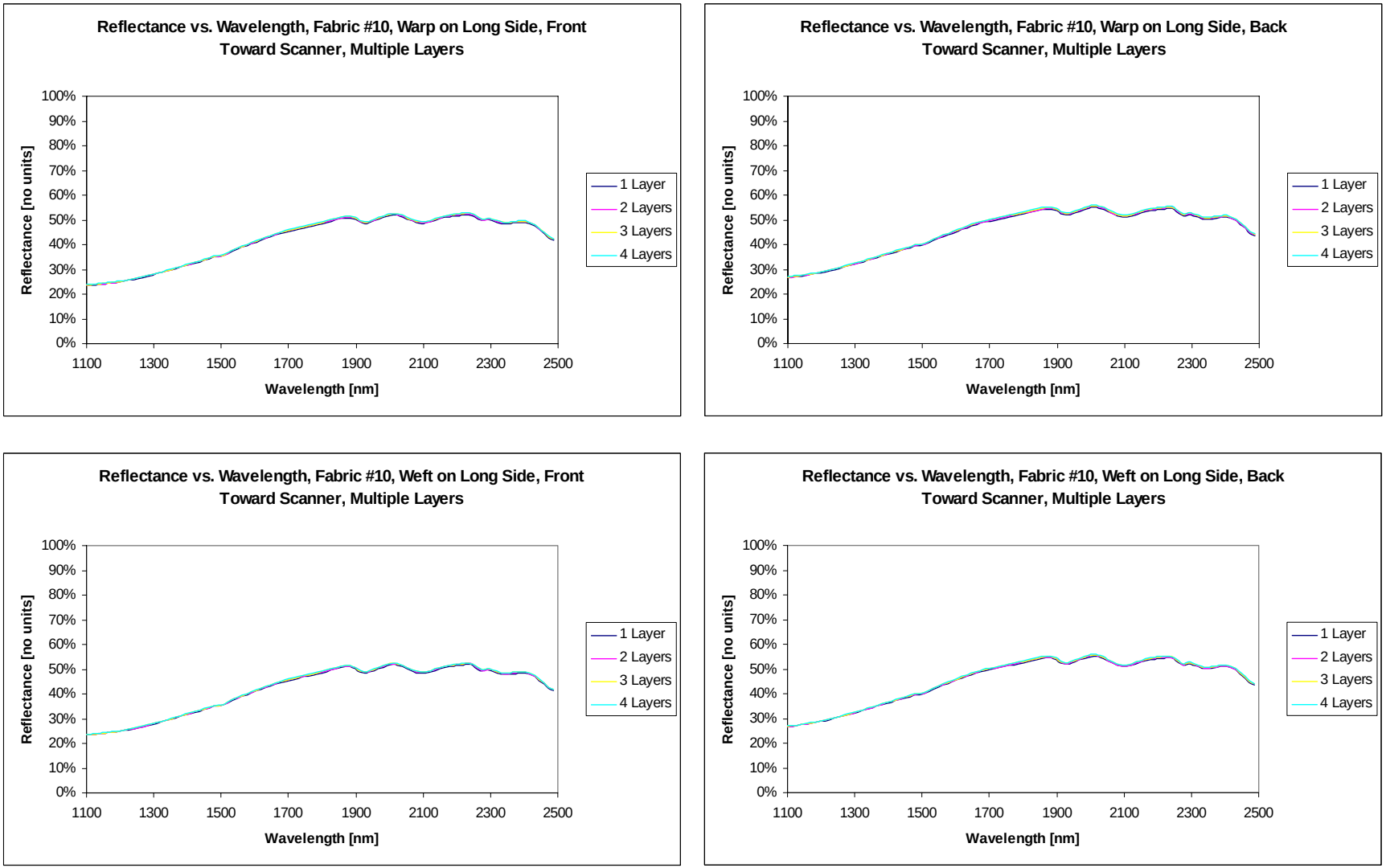

Figure A-10 Multiple Layer And Front vs. Back Comparisons For Fabric #10

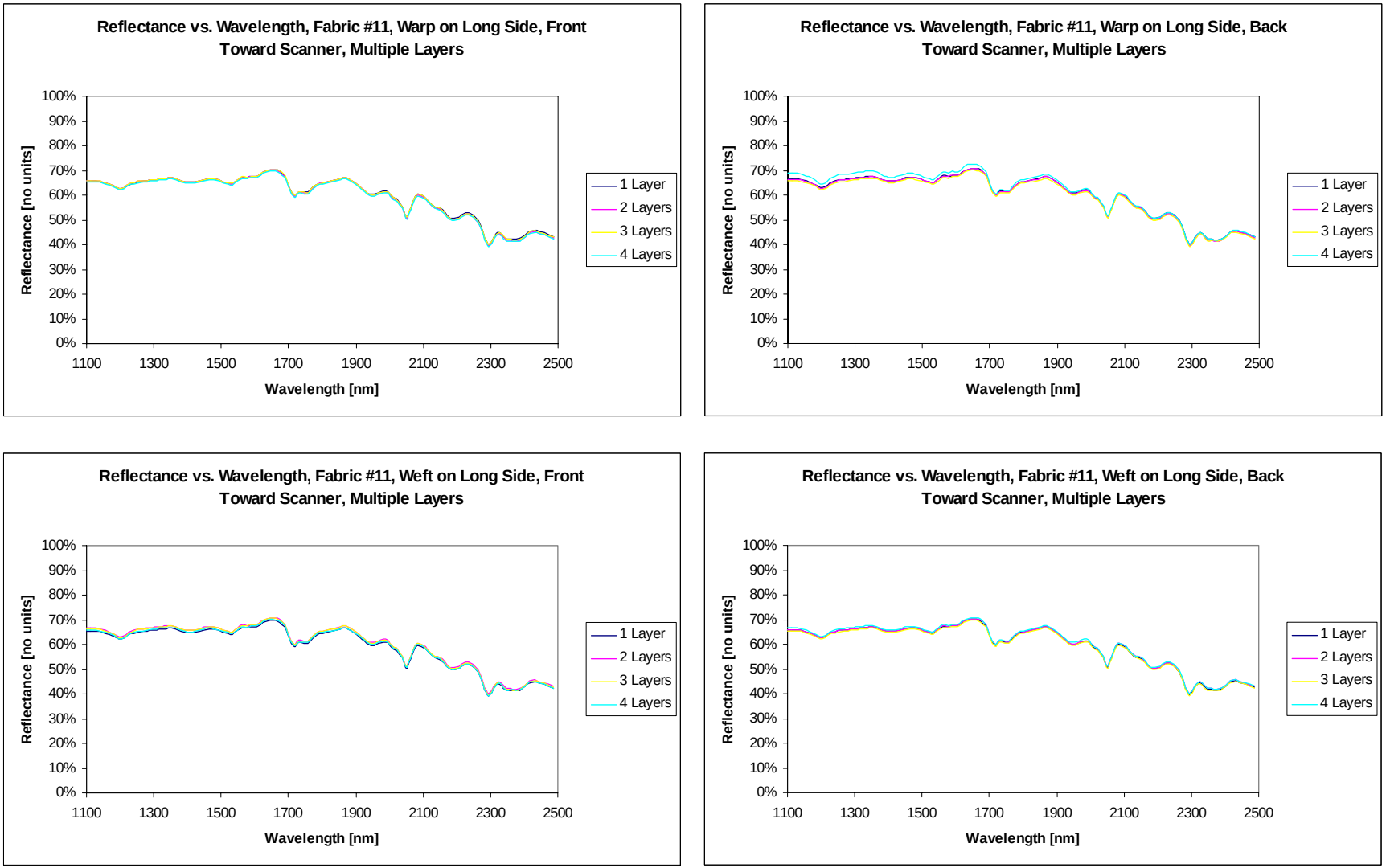

Figure A-11 Multiple Layer And Front vs. Back Comparisons For Fabric #11

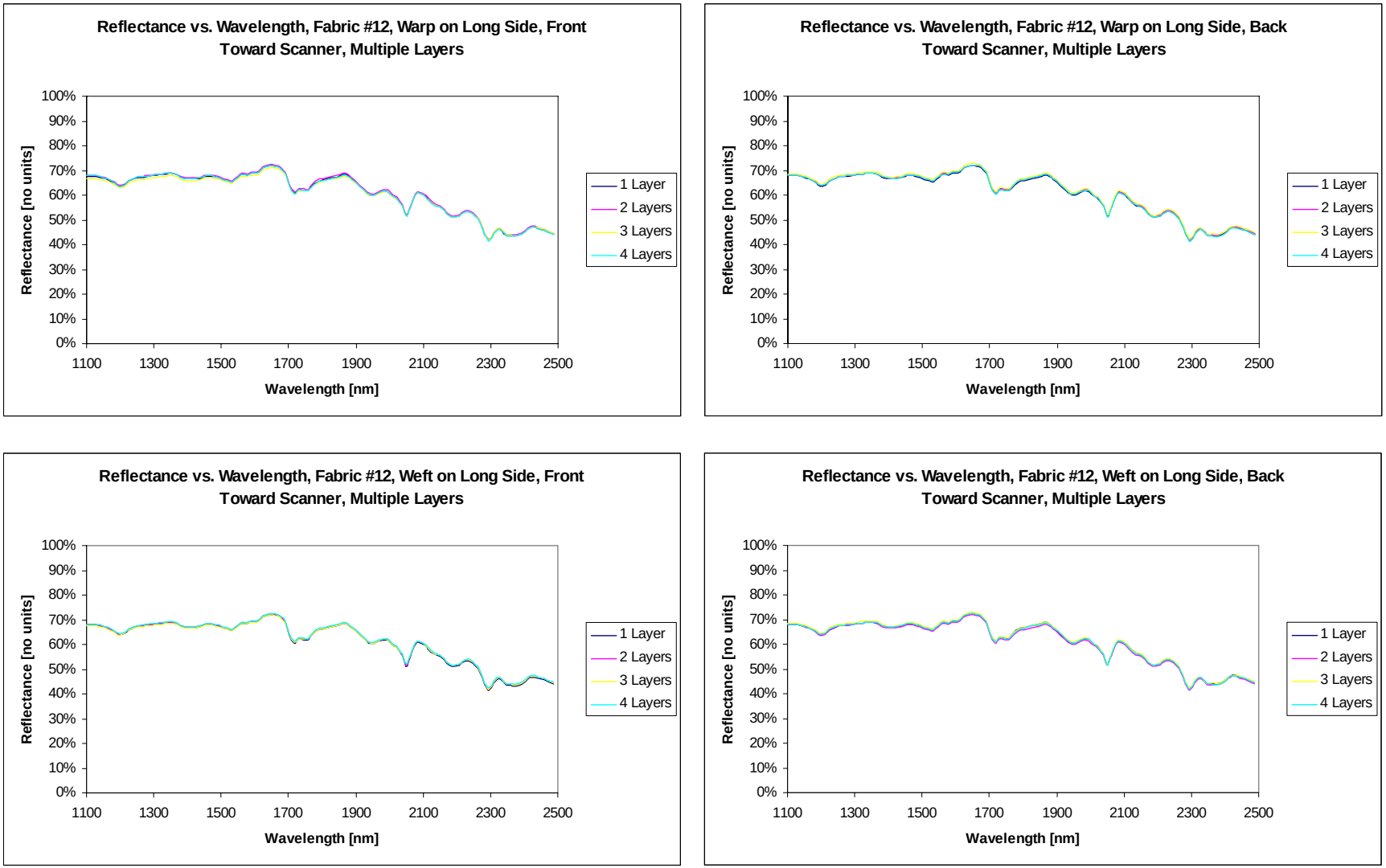

Figure A-12 Multiple Layer And Front vs. Back Comparisons For Fabric #12

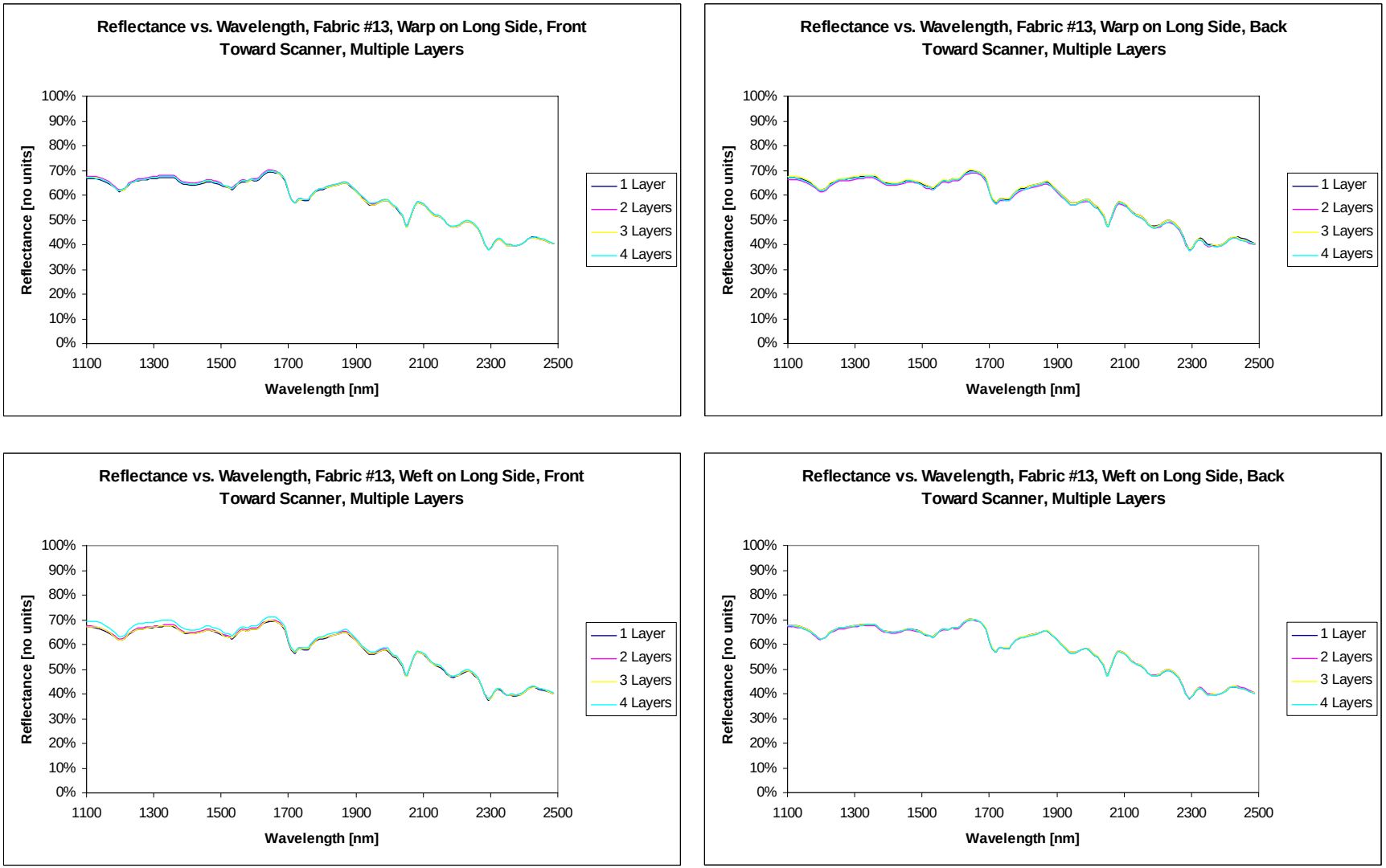

Figure A-13 Multiple Layer And Front vs. Back Comparisons For Fabric #13

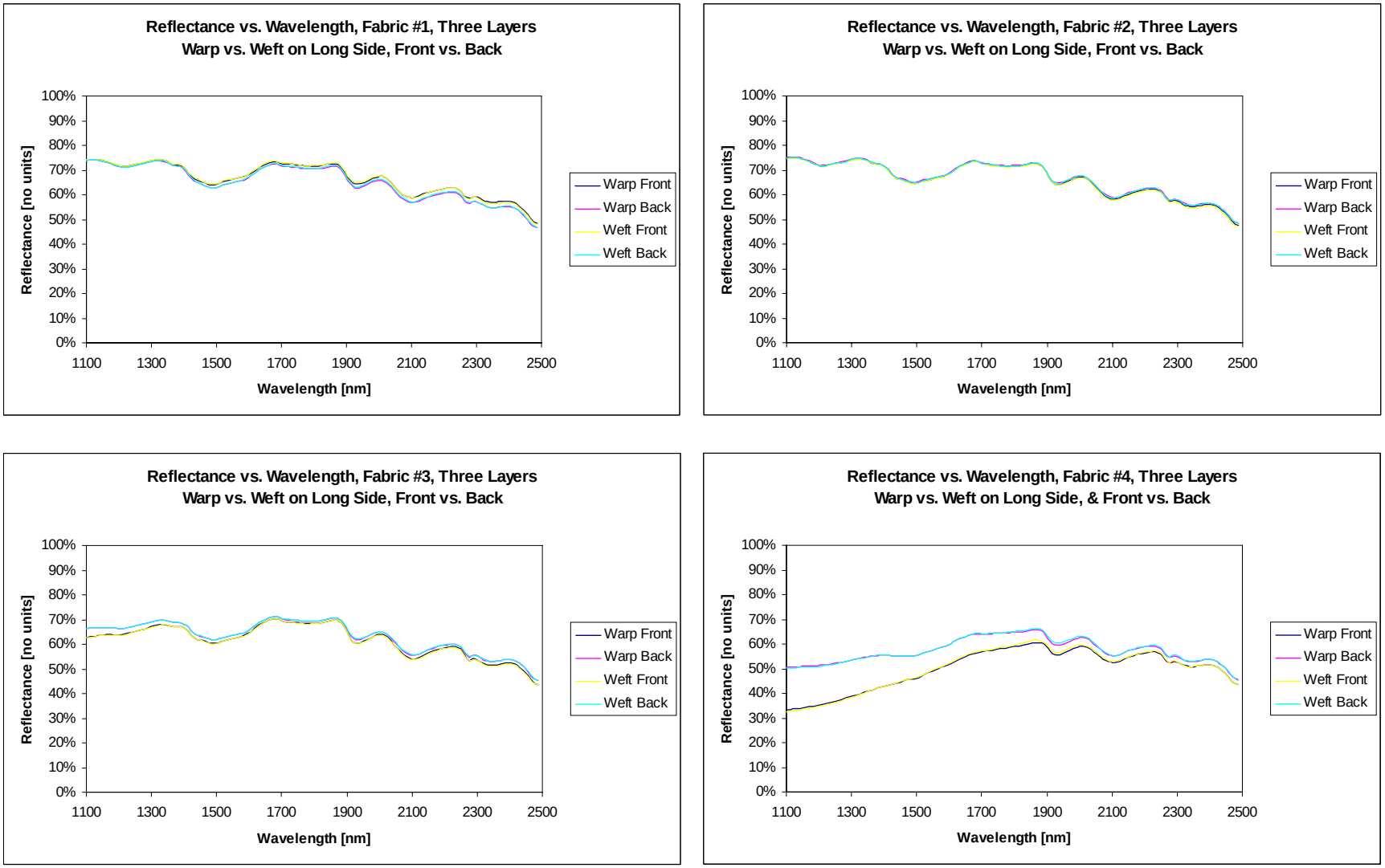

Figure A-14 Comparison Of Warp vs. Weft On Long Side and Front vs. Back For Fabrics #1-4, Three Layers

Figure A-15 Comparison Of Warp vs. Weft On Long Side and Front vs. Back For Fabrics #5-8, Three Layers

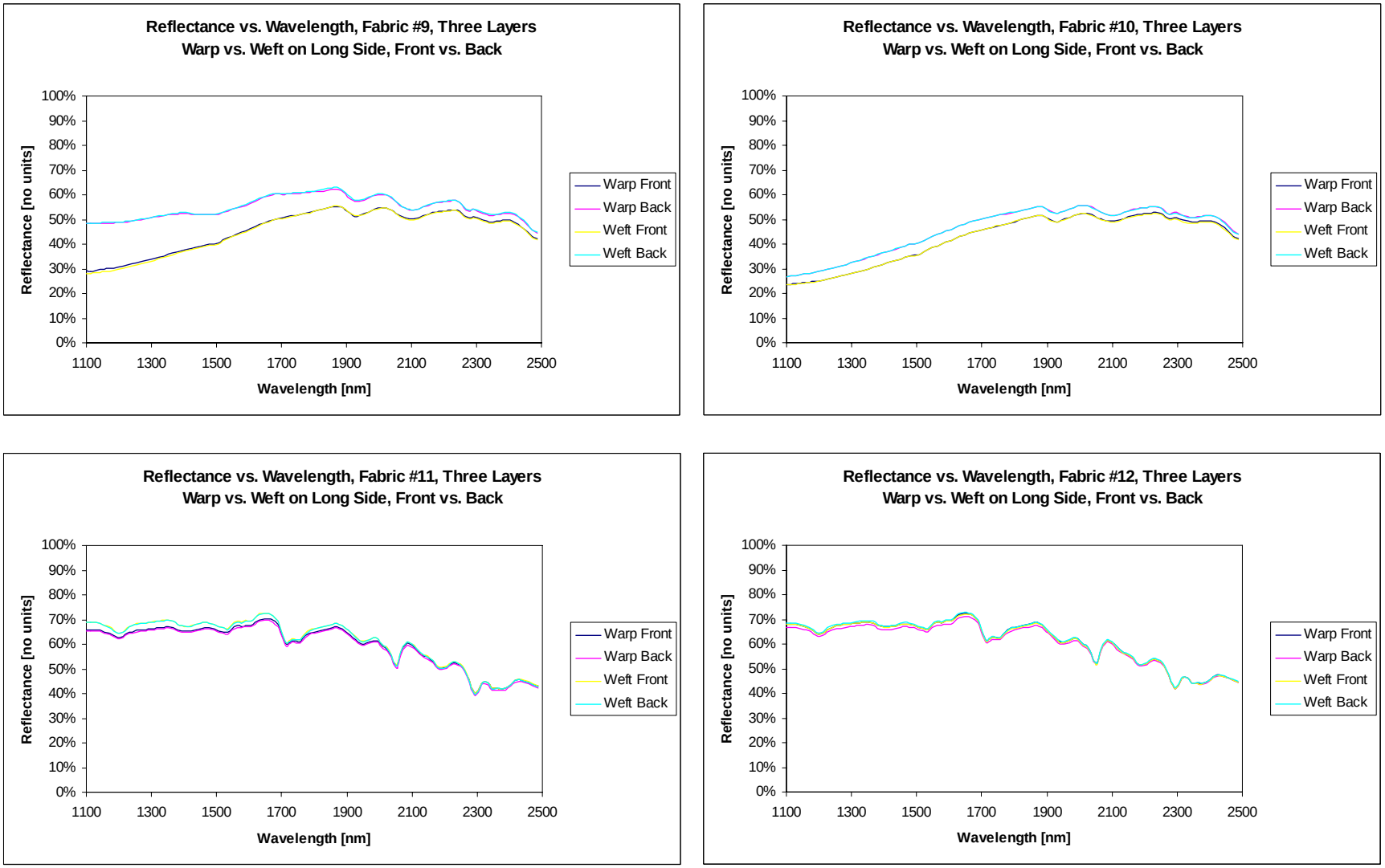

Figure A-16 Comparison Of Warp vs. Weft On Long Side and Front vs. Back For Fabrics #9-12, Three Layers

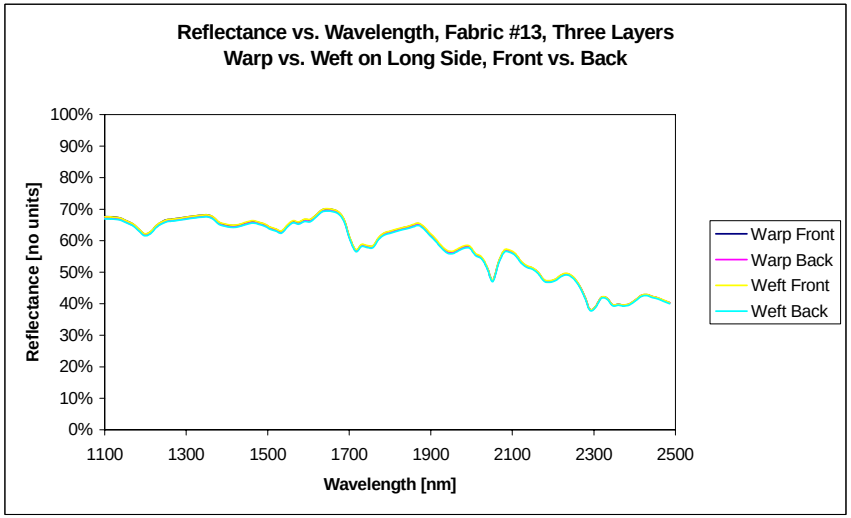

Figure A-17 Comparison Of Warp vs. Weft On Long Side and Front vs. Back For Fabric #13, Three Layers

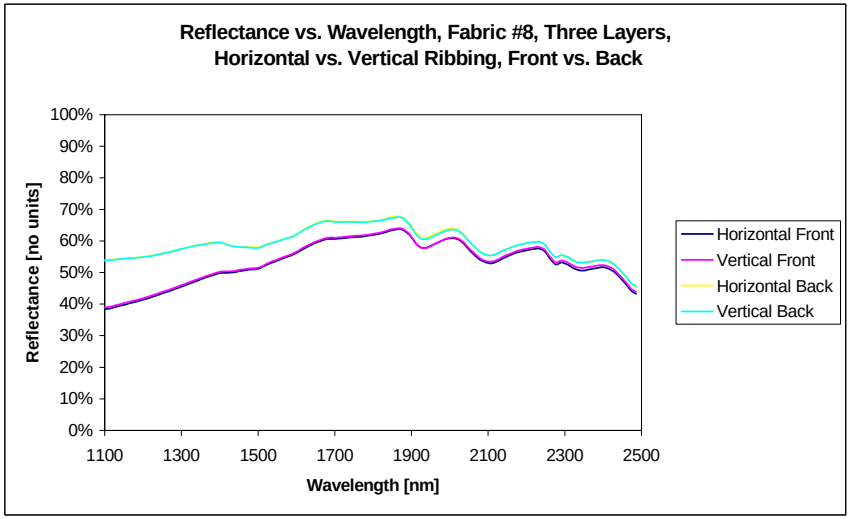

Figure A-18 Comparison Of Horizontal vs. Vertical Ribbing and Front vs. Back For Fabric #8, Three Layers

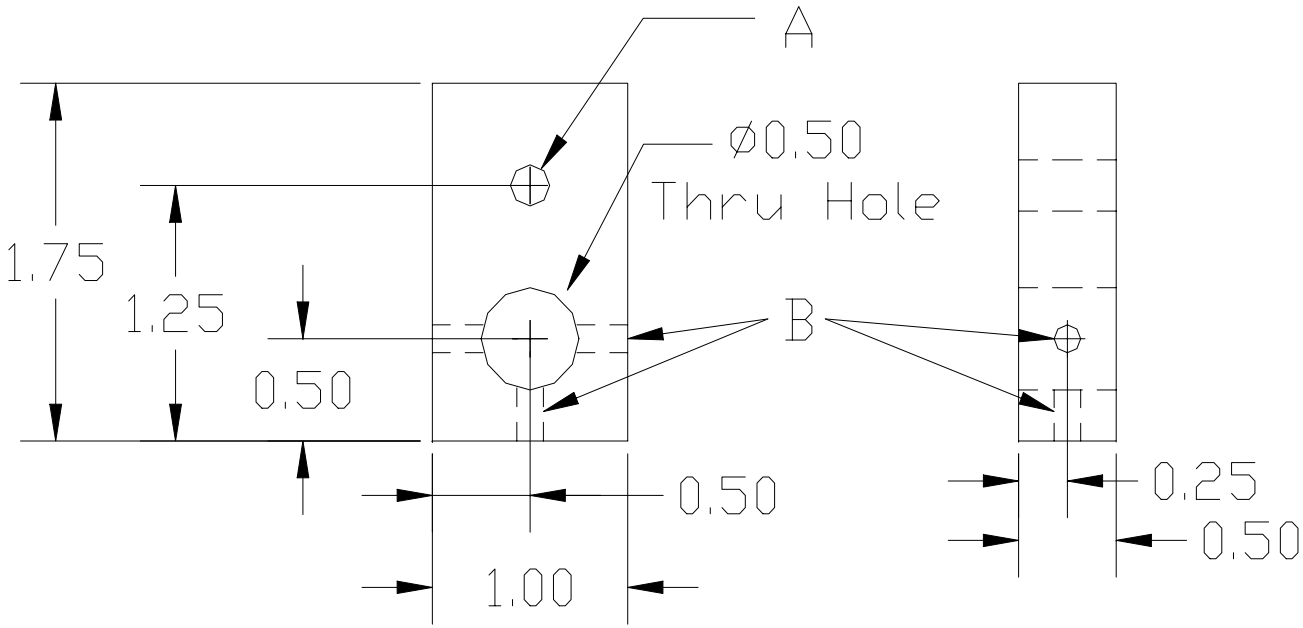

Note A: 1/4-20 Thru-Tap Replaced With 1/4-20 Stud
With 2-56 Thru-Tap In Center (0.5, 1.25)

Note B: 8-32 Taps Thru To ½″ Thru Hole (x3)

Figure A-19 AutoCAD Drawing Of Laser Diode Bracket

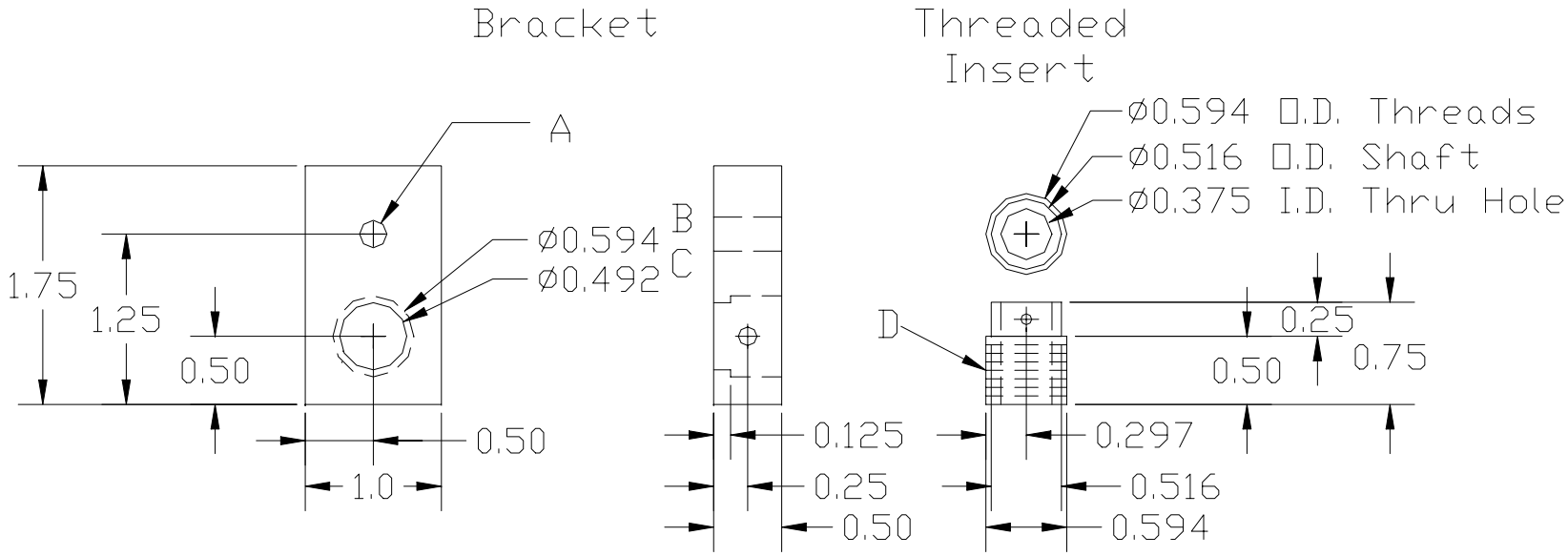

Note A: 1/4-20 Thru-Tap Replaced With 1/4-20 Stud With 2-56 Thru-Tap In Center (0.5, 1.25)

Note B: 0.594″ Diam. With 32 Pitch Thread, ⅜″ Deep, From Back

Note C: 0.492″ Diam. Thru Hole

Note D: 0.594″ O.D. Threads, 32 Pitch

Figure A-20 AutoCAD Drawing Of Photodiode Bracket

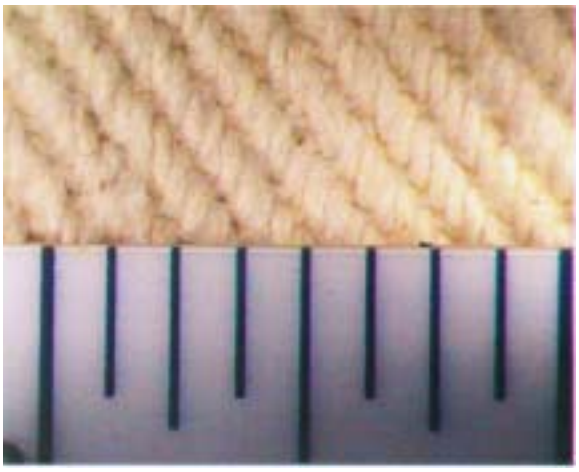

(a) Fabric #2, Tan Denim,
Front Side,
Warp Perpendicular to
Millimeter Scale

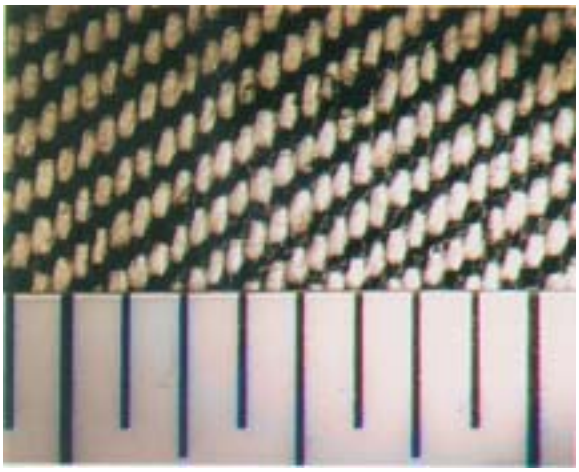

(b) Fabric #4, Dark Green/White
Denim, Back Side,
Weft Perpendicular to
Millimeter Scale

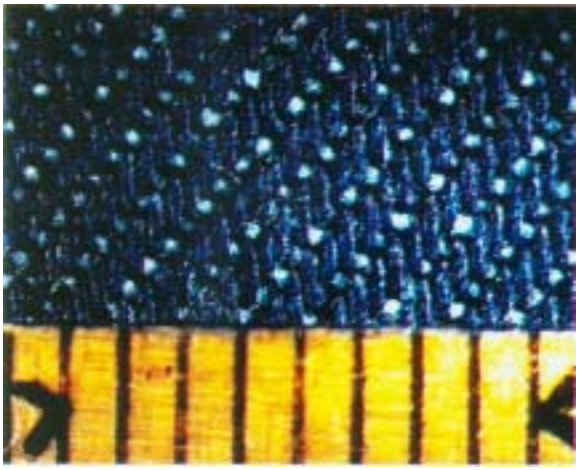

(c) Fabric #7, Blue/White Denim
Front Side,
Warp Perpendicular to
Millimeter Scale

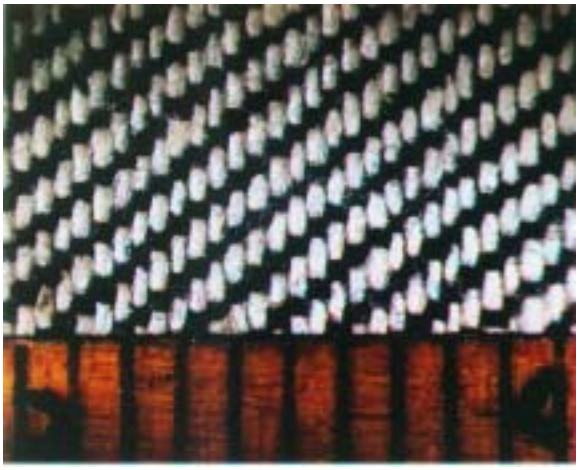

(d) Fabric #9, Black/White Denim
Back Side,
Weft Perpendicular to
Millimeter Scale

Figure A-21 Additional Example Images of Test Fabrics For Yarn Counts